FINE FOCUS

AN INTERNATIONAL MICROBIOLOGY JOURNAL FOR UNDERGRADUATE RESEARCH

VOLUME 10 | 2024

Tenth Anniversary Issue

FINE FOCUS

AN INTERNATIONAL MICROBIOLOGY JOURNAL FOR UNDERGRADUATE RESEARCH

We publish original research by undergraduate students in microbiology. This includes works in all microbiological specialties and microbiology education.

We are a web and print journal dedicated to showcasing the research of undergraduate students, internationally, in all fields of microbiology. *Fine Focus* is managed entirely by undergraduate students from production to print.

Cover Art

Original watercolor piece painted by Sharon Par Mawi Cung depicting an endospore stain of *Bacillus* spp. isolated from dairy farm specimens in 2021 that demonstrate antibiotic production against several ESKAPE pathogens. These bacteria are part of an ongoing investigation led by Managing Editor Dr. John McKillip to identify novel antibiotics to address the MDR bacteria crisis: https://open.spotify.com/episode/0lP0GMnt434bpafDUU1v1K?go=1&sp_cid=0c1a46c08ff032cbfd1b-27c820180374&utm_source=embed_player_p&utm_medium=desktop&nd=1

Fine Focus gratefully acknowledges the generous assistance of Katie Bohnert, Open Access Publishing and Web Hosting Specialist, Ball State University Libraries, for digital layout of this 10th Anniversary Issue of our journal, without whom volume 10 would not have come to fruition.

ISBN (Online): 2837-4282
ISBN (Print): 2381-0637

VOLUME 10 | SPRING 2024

Tenth Anniversary Issue

Contents

Objective Lens: Cora Wilson as a pioneer in education in rural Kentucky & beyond

John L. McKillip, *Fine Focus* Managing Editor

During the first 30 years of the 20th Century, many scholars agree that Cora Wilson Stewart was the most widely known authority of adult literacy in the world. By establishing the Moonlight Schools in Rowan County Kentucky in 1911, she rose to prominence as a well-regarded advocate for promoting literacy and adult education. Stewart frequently held viewpoints which ran counter to the mindset of educators in the 1920s and 1930s. Wilson was ahead of her time in many aspects of promoting literacy in an era largely before adult education was widely recognized (Fig. 1).

Wilson is remembered for being an eloquent and colorful speaker, and grew up believing that furthering one's education would open opportunities beyond the traditional molds that shaped rural Appalachia over 100 years ago (1). Cora Wilson moved beyond a series of failed marriages and domestic abuse to devote most of her time to public affairs, eventually adopting adult literacy as her primary mission. As the daughter of a physician and schoolteacher, Wilson would frequently go along on rounds with her father and help read or interpret medical advice, documents, and other communications to adult patients and families who could not read or write. Eventually earning her teaching credentials from Morehead (KY) Normal School (later Morehead State University), Wilson later was the first woman to be elected as President of the Kentucky Education Association, an advocacy group dedicated, then and now, to improved funding for schools, safety measures, smaller class sizes, and empowerment of employees and parents (2).

Shortly thereafter, Stewart, as a superintendent for Rowan County Schools, created the first Moonlight School in September 1911 (Figs. 2-4). Adults would attend Wilson's classes in the evenings, after children were home and chores were completed, and only on moonlit nights, to

Fine Focus, 10(1), 2-5. doi: 10.33043/FF.10.1.2-5.

be guided to and from the school safely. Wilson asked teachers to volunteer to teach in the evenings as the program grew. In 1914, Stewart successfully urged the Kentucky Governor to create a state illiteracy commission, and expand the Moonlight Schools statewide, with the goal of eliminating illiteracy by 1920. Regional communities held competitions, and various women's groups became involved to further the cause. After a few years, Wilson established the Moonlight School Institute, the first of its kind in America. Eventually, over 1,600 students were enrolled, 350 of whom had learned to read and write. Wilson also saw that similar schools be established to serve Black students, and by 1915, fifteen Moonlight Schools served these adults (3). Along this progressive path, Stewart published numerous books specifically for adults who had limited or no literacy, to encourage them to read, as well as one entitled *The Soldier's First Book*, aimed at military recruits for World War I.

Figure 1

Cora Stewart Wilson (1875-1958) in a photograph from January 1916, from Press Reference Book of Prominent Kentuckians, 1916, p. 224 (royalty-free image).

Alabama and Mississippi began Moonlight Schools shortly after the Wilson Schools in Kentucky became successful. By 1916, eighteen states had Moonlight Schools. Stewart went on to be Chairperson of the Illiteracy Commission of the National Education Association. Wilson was a pioneer and tireless advocate for education of underserved her entire adult life, and doubtless left a legacy which still remains underappreciated today. Another similar journey is included in this, our tenth anniversary issue of *Fine Focus*; that of Parisa (page 6), an international STEM scholar who writes about her first tenure-track faculty position at an HBCU, and the necessary cross-cultural literacy to be explored and appreciated when navigating challenges in a unique but also rewarding academic climate. In many ways, Parisa's journey draws many parallels to that of Cora Wilson Stewart – combining empathy and passion with determination and vision to achieve lifelong learning.

Figures 2, 3, & 4

The Original Cora Wilson Steward Moonlight School located near the campus of Morehead State University in Kentucky, USA. Photo credits: David Nickell, Hillsboro, KY.

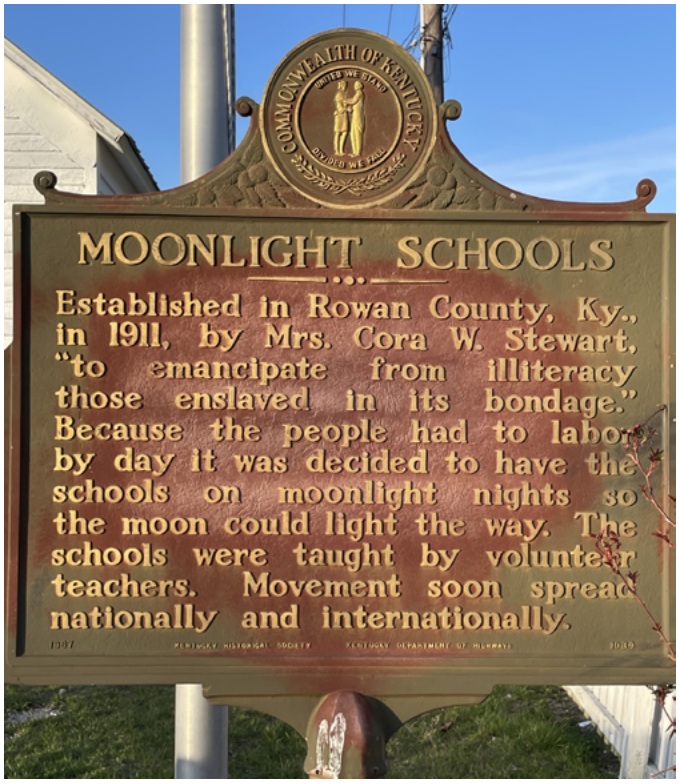

References

1. Nelms, Willie. Cora Wilson Stewart: Crusader against Illiteracy. McFarland & Co, 1997. Print.
2. Kentucky Education Association: https://www.kea.org/about_kea.uspx accessed 3.4.2024
3. https://nkaa.uky.edu/nkaa/items/show/2669 accessed 3.3.2024

Parisa Ebrahimbabaie's Academic Sojourn at Bethune-Cookman University: Unraveling the Complexities

Parisa Ebrahimbabie

Parisa Ebrahimbabaie's academic tenure at Bethune-Cookman University (B-CU) unfolds as a captivating narrative intricately woven with challenges stemming from her international background as a woman from Iran. This exploration of her experiences at the Historical Black University (HBCU) delves into the complexities of identity, cultural adjustments, and the unique dynamics of an academic environment rich in historical significance.

Adapting to B-CU requires more than adjusting to the physical surroundings; it involves a deep understanding of various facets of the local culture, including communication dynamics, social nuances, and aligning academic expectations with prevailing norms. This cultural transition demands a significant reassessment of approaches to teaching, research collaboration, and interpersonal relationships for a seamless integration into the academic and cultural environment at B-CU.

Fine Focus, 10(1), 6-8. doi: FF.10.1.6-8

Navigating the pervasive stereotypes linked to her nationality and gender poses a persistent challenge for Parisa. Overcoming preconceptions requires a delicate blend of assertiveness and cultural education to foster a more accurate understanding of her identity.

The intersection of Parisa's Iranian identity introduces challenges within the academic sphere, requiring a continuous negotiation of her identity within a landscape not always attuned to the complexity of her experiences. This intersectionality weaves into her daily interactions, shaping her role and experiences within the academic community.

Building authentic connections with colleagues and students at B-CU becomes a multifaceted challenge for Parisa. Overcoming cultural barriers and establishing professional rapport within the context of an HBCU necessitate an awareness of cultural diversity and an appreciation for the historical foundations shaping relationships in this distinctive academic community.

The unique setting of an HBCU exposes Parisa to an environment steeped in historical significance and cultural traditions. Navigating this context requires more than academic understanding; it demands a deep immersion into the institution's ethos. Grasping and appreciating the historical commitment to the African American community becomes fundamental to her role as an academic contributor.

Engaging with the predominantly African American local community at B-CU presents challenges connected to cultural sensitivity. Navigating community engagement demands dedication to academic outreach and a keen awareness of diverse perspectives within the community. Despite challenges, Parisa is very happy working at Bethune-Cookman University as an assistant professor, appreciating the positive and enriching academic environment.

Achieving a harmonious equilibrium between her diverse cultural identity and institutional expectations remains a continuous negotiation. Striking this delicate balance involves leveraging the strengths of her Iranian heritage while aligning with the cultural fabric of the HBCU. This intricate dance of identity within the academic realm is central to her ongoing experience.

Gender dynamics, evident within the institution and broader cultural context, significantly influence Parisa's professional journey. Navigating gender-related challenges, advocating for equity, and fostering an inclusive environment are integral components of her academic role.

Establishing a professional network within the academic sphere poses distinctive challenges. Cultural differences and potential biases add complexity to networking dynamics, necessitating active participation in opportunities to overcome barriers and forge meaningful connections within the university community.

Access to leadership positions for women, particularly from underrepresented backgrounds, poses nuanced challenges. Navigating the path to leadership roles demands professional acumen and a proactive approach to contribute meaningfully to

decision-making processes within the academic landscape.

Accessing research funding, laboratories, and resources presents Parisa with a multifaceted challenge. Adapting to constraints and identifying alternative avenues to pursue research goals becomes a crucial aspect of her academic journey. This adaptive resilience characterizes her approach to academic research within the distinctive institutional context.

Diverse levels of institutional support for diversity and inclusion at B-CU add complexity to Parisa's academic experience. Advocating for initiatives that advance diversity and actively participating in creating an inclusive environment are essential components of her role, requiring a nuanced understanding of institutional dynamics.

In conclusion, Parisa's academic journey at Bethune-Cookman University has been marked by diverse challenges extending beyond traditional academic boundaries. This narrative unravels the complexities inherent in her experience, shedding light on the multifaceted nature of her identity intersectionality within the unique landscape of an HBCU. As she continues navigating this intricate journey, her story stands as a testament to the resilience and adaptability required to thrive in the dynamic and diverse academic environments shaping the modern educational landscape. Importantly, she emphasizes her happiness and appreciation for the positive and enriching academic environment at Bethune-Cookman University.

Borrelia burgdorferi: The Deer Tick's Dark Secret

Andrew J. Gaetano

Elizabeth S. Danka

St. Norbert College, Division of Natural Sciences, De Pere, WI

Abstract

Since its recent discovery in the late 1970s, Lyme Disease (LD) has been a growing public health concern, especially in the United States where it accounts for the majority of vector-borne infections each year. The causative agent, *Borrelia burgdorferi*, is transmitted to humans through the bite of an infected *Ixodes* tick. This pathogen uses many unique mechanisms to both shield itself from the host immune response and cause disease. Clinically, LD presents in successive phases, with each increasing in severity as the bacterial cells migrate to new tissues and organ systems. On the epidemiological and ecological fronts, limitations in reporting, ecological changes, and a lack of public support hinder accurate surveillance and enhance the spread of the disease. The goal of this literature review is to increase public knowledge of *B. burgdorferi*, its vector, and the disease it causes, along with suggesting preventative measures to protect individuals who reside in high-risk areas. A collective and coordinated public health effort represents our greatest chance of restraining the LD-causing pathogen.

Keywords: *Borrelia burgdorferi*, *Ixodes scapularis*, Lyme Disease, Spirochete, Vector-borne infection
Manuscript received: 28 Feb 2023; accepted 13 July 2023

Fine Focus, 10(1), 9-37. doi: 10.33043/FF.10.1.9-37.

Discovery of the Causative Agent of Lyme Disease

In 1976, the Connecticut State Department of Health reported an outbreak of an unusual form of arthritis near Lyme, Connecticut (37). The affected individuals experienced recurrent bouts of pain and swelling in large synovial joints (such as the knee) without prior injury. Other clinical presentations included flu-like symptoms and unusual cutaneous lesions called erythema migrans (EM), which had first been described by the German physician Alfred Buchwald in 1883 (75). Although a causative agent had not yet been discovered, this unique combination of signs and symptoms was termed Lyme Disease (LD) (37). Most patients with the disease lived in heavily wooded areas away from the centers of towns, and the onset of their symptoms was often in the summer and early fall. The spatial and temporal distribution of cases hinted that the disease was likely transmitted through an insect vector, but the State Department of Health did not have any additional information. It would take six more years to identify the LD-causing pathogen.

In 1982, Wilhelm "Willy" Burgdorfer isolated a spirochete from *Ixodes scapularis*, the black-legged deer tick (7). This microorganism was soon shown to be responsible for the unique disease in Lyme, Connecticut. When ticks harboring this pathogen fed on New Zealand White rabbits, long-lasting EM-like lesions developed. Indirect immunofluorescence also confirmed that the rabbits produced antibodies specific to these spirochetes. A causal relationship between the newly discovered spirochete and LD in humans was established when the serum of clinically diagnosed patients revealed antibodies specific to the pathogen, which was subsequently named *Borrelia burgdorferi*. Despite its recent characterization, the earliest confirmed case of LD occurred in the 5,300-year-old Similaun Iceman ("ÖTZI") found preserved frozen in the Italian Alps (31). Arthritis was observed upon clinical examination, and DNA sequencing of samples from the Iceman confirmed the presence of *B. burgdorferi*.

While a great deal of work has focused on characterizing the pathogen, many challenges exist on the clinical and epidemiological fronts. Diagnosis and treatment of LD is complicated by *B. burgdorferi's* wide array of virulence strategies that allow it to infect multiple organ systems, lie dormant for long periods of time, and resist and suppress the host immune response (20, 47, 48). Additionally, the clinical manifestations can vary widely, which further heightens the challenge for clinicians to make a timely and accurate diagnosis. While a vaccine represents the most effective preventative measure, there are not any currently available on the market.

Due to limitations in disease surveillance, the reported number of LD cases in the United States is thought to be significantly lower than the Centers for Disease Control and Prevention's (CDC) annual estimate (34). Despite this, LD represents more than 80% of vector-borne illnesses making it the most common vector-borne disease in the country (3). Making matters worse, the home range of *B. burgdorferi's* vector and its reservoirs are expanding as the ecological landscape continues to change

(73). Approximately 90 million Americans live in states deemed "high risk" by the CDC, and even this high value is likely an underestimate of the total number of individuals at risk (13). Disease prevention depends on increasing public knowledge and awareness of *B. burgdorferi* and its disease-causing ability, *Ixodes* genus ticks and their life cycle, LD and its clinical manifestations, and of available precautionary measures for individuals in high-risk areas.

Introduction to *B. burgdorferi*

B. burgdorferi is a Gram-negative bacterium with an inner and outer membrane. Unlike most gram-negative organisms, *B. burgdorferi* lacks lipopolysaccharides (LPS) in the outer membrane and instead displays other immunogenic glycolipids (70). The spirochete bores through host tissues using internal periplasmic flagella that confer swimming motility and flat-wave morphology (32). While this flat-wave structure dominates, other pleomorphic forms exist under certain environmental conditions (see "Pleomorphic forms" and Figure 6) (44).

The *B. burgdorferi* genome consists of a single 910,725 base pair linear chromosome with 853 open reading frames whose products are involved in the basic processes of DNA replication, transcription, translation, solute transport, and energy metabolism (23). Due to a lack of biosynthetic genes, the spirochete is an obligate parasite and depends on an arthropod or mammalian host for survival. Aside from hemolysins and drug efflux pumps, *B. burgdorferi* lacks common virulence factors and instead relies on dynamic gene regulation to evade and suppress the host immune response (3).

As an obligate parasite, *B. burgdorferi* can be difficult to maintain in common laboratory cultures that do not closely mimic the host environment (1). To overcome this challenge, optimized Barbour-Stoenner-Kelly (BSK) media that contains 6% rabbit serum and a collagen matrix is used to support the growth of *B. burgdorferi* (62). *In vitro* cultivation consists of a two-step process whereby a rapidly growing starter culture is used to initiate the growth of a long-term culture with a high bacterial yield. While *in vivo* studies most accurately represent the conditions that *B. burgdorferi* naturally encounters, the ability to work with isolated, parasitic bacteria in the laboratory increases the feasibility of research.

Lyme Disease

The unique virulence and immune evasion strategies of *B. burgdorferi* manifest clinically in humans as a complex, multi-stage disease. In this section of the review, the life cycle of the arthropod vector, transmission to the mammalian host, and clinical manifestations of LD will be described.

1. Vector life cycle

Vectors are organisms, often insects, that harbor and transmit pathogens to other hosts. Within the *Ixodes* genus, black-legged deer ticks (*Ixodes scapularis*) are the main vectors that transmit *B. burgdorferi* to reservoirs such as mice and hosts such as humans. These reservoirs vary in their degree of competency to transmit *B. burgdorferi* back into an uninfected arthropod vector.

Ixodes ticks have a complex, two-year, four-stage life cycle, which consists of egg, larva,

nymph, and adult forms (Figure 1) (19). In the spring, adult female ticks at the end of their life cycle lay eggs that hatch into six-legged larvae within about 60 days. The females lay the eggs on grasses where the larvae will be exposed to mammals like deer and mice after hatching. To progress to the next stage of the life cycle, the larvae require a first blood meal which often comes from the reservoir-competent, white-footed mouse, but may also come from other small animals such as chipmunks, shrews, squirrels, and birds.

After larvae feed in the late summer to early fall, they molt into eight-legged nymphs that remain inactive during the winter months. In the spring, the nymphs take a second blood meal which allows them to develop into adults in the summer.

As adults, a third feeding, often from the reservoir-incompetent white-tailed deer (*Odocoileus virginianus*), is required to reproduce. After feeding, adult male and female ticks copulate on the deer, and females lay their eggs the following spring to complete the life cycle.

2. Route of transmission

For humans to develop LD, a tick harboring *B. burgdorferi* must bite the human and take a blood meal (7). The tick's first feeding as a larva is unable to cause infection because the bacteria cannot be passed down in eggs and the arthropod can only acquire the spirochete through feeding (19). Therefore, larvae must take a blood meal from an infected, reservoir-competent organism to obtain the pathogen before transmission to humans is possible. If this first blood meal contains *B. burgdorferi*, the pathogen will colonize the tick midgut and the bacterial cells lose their motility. A secondary feeding during the nymph stage is required

Figure 1

The Ixodes genus tick life cycle.

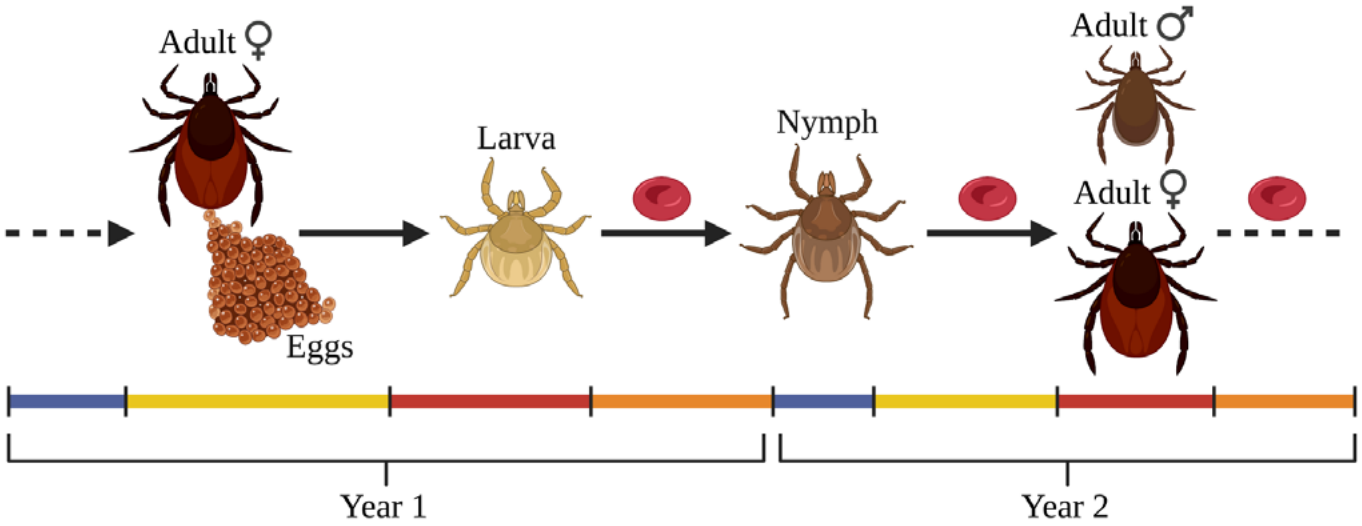

Note. A red blood cell indicates that a blood meal is required to progress to the following stage. The blue, yellow, red, and orange bars represent winter, spring, summer, and fall, respectively. Timeline is based on reference 19.

for *B. burgdorferi* to replicate, restore motility, and migrate to the tick's salivary glands where it becomes primed for transmission. Thus, nymphs represent the earliest stage of the tick life cycle where *B. burgdorferi* transmission resulting in LD in humans is possible.

To locate a host, ticks use a maneuver called questing where they climb to the top of grasses and other small plants, extend their front legs, and latch on to a passing animal (Figure 2B) (18). After finding a host, the tick migrates to a suitable location to take a blood meal. For humans, one study determined the distribution of tick attachment to be 9% head-neck, 5% arm, 24% stomach/groin, 7% back, 18% chest/shoulder, 25% leg/foot, and 12% hip (Figure 2A) (25).

After a tick begins feeding, transmission of *B. burgdorferi* is not immediate. There is a positive correlation between the duration of vector attachment and the probability of *B. burgdorferi* colonization and disease (57). In a murine study exploring this relationship, infection was established in 7% of mice after 36 hours, 25% after 42 hours, and 75% after 48 hours. This

Figure 2

Tick questing behavior leads to attachment to hosts.

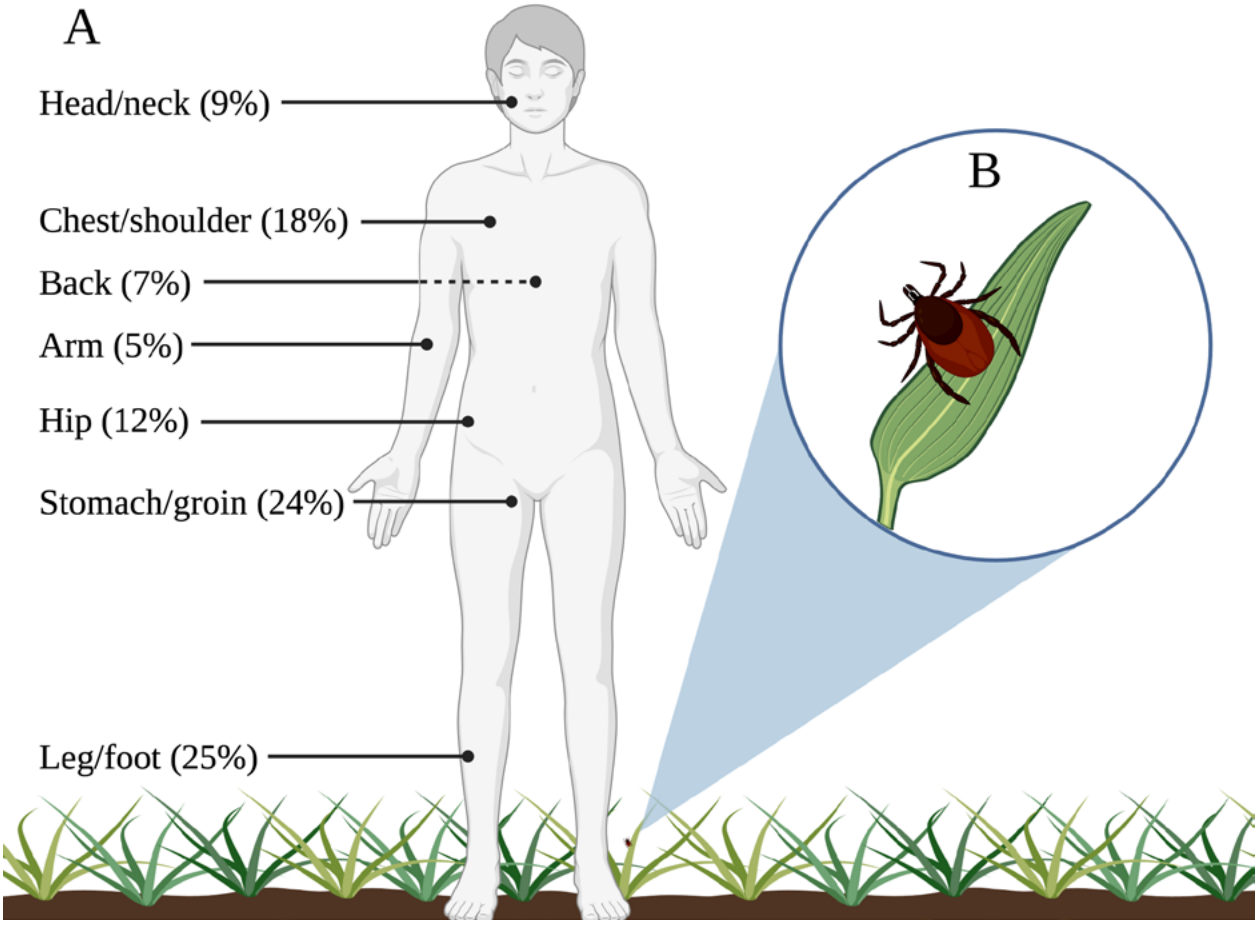

Note. Distribution of tick attachment sites on humans (A) and representation of the tick questing behavior that is used to seize a suitable host for a blood meal (B) (18, 25).

time-dependent transmission demonstrates the importance of rapid tick removal after attachment as a preventative measure against LD.

While there is no evidence that human-to-human transmission of *B. burgdorferi* is possible, there are many published cases of gestational LD with negative outcomes such as miscarriage, death following birth, and congenital abnormalities (72). However, a systematic review of these published cases concluded that most reports contained blinding issues, had missing or limited information on the mother's clinical symptoms, or used diagnostic methods that are no longer considered reliable. Therefore, additional research using reliable methods is necessary to determine the effects of gestational LD and the consequences it may have on women in their childbearing years.

3. Disease progression

LD progresses in three distinct phases termed early localized, early disseminated, and late disseminated infection (48). The basic signs, symptoms, and commonly affected tissues corresponding to each phase are presented in Figure 3, and each phase is described in depth below.

The first clinical manifestation of early localized *B. burgdorferi* infection is usually a slowly expanding cutaneous rash called erythema migrans (EM) (48). EM presents 7-14 days after exposure at the site of tick attachment in 70-90% of cases. The rash begins as a small red papule that takes on a bullseye appearance as it expands to an average diameter of 15 centimeters. EM is usually asymptomatic, but other flu-like symptoms such as headache, fatigue, malaise, and fever may occur. Early localized LD usually lasts for a few days to a month.

Early disseminated infection usually occurs three weeks to several months after the onset of primary EM, and it typically lasts 3-10 weeks (48). During this phase, *B. burgdorferi*

Figure 3

LD signs, symptoms, and commonly affected tissues.

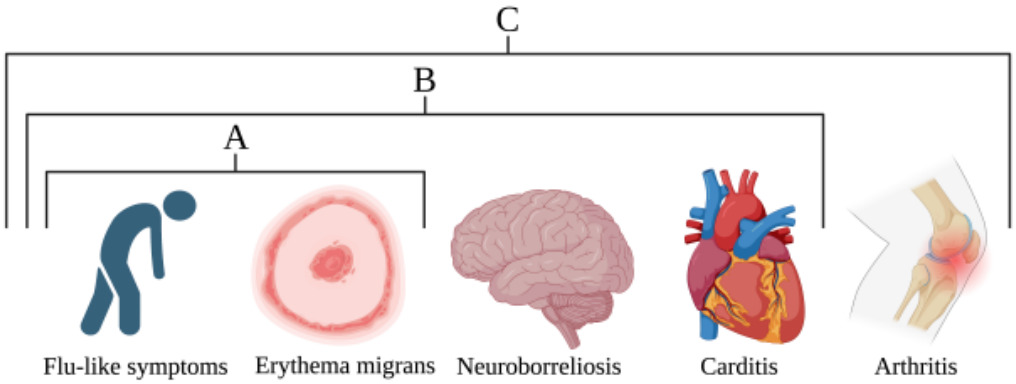

Note. Lyme disease progresses through three distinct stages: early localized (A), early disseminated (B), and late disseminated infection (C) (48). Each stage is characterized by different signs and symptoms that reflect the spread of the pathogen from the initial site of infection.

disseminates to the central nervous system (CNS), the cardiovascular system, and other cutaneous regions which leads to secondary EM away from the initial site. CNS involvement, termed Lyme neuroborreliosis, occurs in about 15% of untreated cases (22). Colonization of the nervous system can occur through penetration of the blood-brain barrier, migration from the peripheral nervous system, or movement through the cerebrospinal fluid. Common signs of neurologic involvement include bilateral cranial nerve palsies of the face, meningitis, and encephalitis. Cognitive impairment, psychiatric disturbances, and even seizures have been observed in patients with early disseminated LD (41). Cardiac involvement, termed Lyme carditis, typically occurs a few weeks to several months after EM onset in about 4-10% of untreated cases (21). Signs of Lyme carditis include prolonged PR interval, atrioventricular (AV) block, myocarditis, intraventricular conduction disturbances, bundle branch block, and congestive heart failure (50). Patients presenting with Lyme carditis may require electrocardiogram (ECG) monitoring and temporary or permanent pacemakers for AV block (74). General flu-like symptoms also accompany the early disseminated phase of infection (48).

Late disseminated infection, also called chronic LD, occurs months to years after the onset of primary EM and can last many years if untreated (48). Late-stage disease is marked by chronic, intermittent arthritis which occurs in about 80% of untreated individuals, along with continued neurologic, cardiac, and cutaneous manifestations (76, 30). Lyme-associated arthritis results from acute swelling and erythema in the joints, most commonly the knee (5). Excessive inflammation, infection-induced autoimmunity, and failure to down-regulate the inflammatory response are factors that contribute to chronic LD.

Virulence of *B. burgdorferi* in Hosts

Bacterial pathogens utilize several methods to spread through and damage host tissues. *B. burgdorferi* is no exception, and in this section of the review a few of the many disease-causing characteristics of this spirochete will be discussed.

1. Plasmid-derived virulence

In addition to the single, linear chromosome, the *B. burgdorferi* genome contains at least 17 linear and circular plasmids (lp and cp, respectively) (23). While some of these extrachromosomal DNA molecules have demonstrated critical roles in disease progression, others remain uncharacterized.

A cell's plasmid profile is its unique collection of plasmids. Long-term *in vitro* cultivation of *B. burgdorferi* results in concurrent changes to both plasmid profile and murine infectivity (64). Over time, the total number of plasmids within each cell decreases, which coincides with a drop in virulence. The degree to which the virulence of *B. burgdorferi* depends on its plasmid profile was expanded upon in a study that examined the infective phenotypes of a collection of clonal mutants, each with a different combination of plasmids (60). High-infectivity was observed in the presence of both linear plasmid 25 (lp25) and 28-1 (lp28-1), intermediate-infectivity was observed in the presence of lp25 and the absence of lp28-1, and

low-infectivity was observed in the absence of lp25 independent of lp28-1 (Table 1).

While some *B. burgdorferi* plasmids have been linked to highly infective phenotypes, others take on different roles (60). For example, cp26 is required to cause disease, but its presence does not affect the degree of infectivity. Other plasmids such as cp9 and lp21 are not associated with infectivity at all. Further characterization of *B. burgdorferi* plasmids linked to infectivity will lead to a greater understanding of the organism's requirements for infection and disease.

2. Temperature-dependent gene regulation

B. burgdorferi relies on both an arthropod vector and a mammalian host for survival. Upon transmission from vector to host, the spirochete experiences a temperature change from 23˚C to 37˚C. This change activates genetic regulatory mechanisms that allow *B. burgdorferi* to adapt to its surrounding environment and successfully establish a mammalian infection (65).

Outer surface proteins (Osp) are immunogenic lipoproteins found on the cell surface of *B. burgdorferi*. OspC, a known antiphagocytic factor, is required to establish a mammalian infection (8). In unfed ticks at 23˚C, *B. burgdorferi* predominantly expresses *ospA* (65). After the tick takes a 37˚C mammalian blood meal, the spirochete's *osp* expression profile changes to *ospC*. This was confirmed by examining *B. burgdorferi*-infected murine serum which contained antibodies specific to OspC. One explanation for this temperature-dependent gene regulation relies on the topology of the *ospC*-containing cp26 plasmid. At 23˚C, the plasmid is in a supercoiled state which blocks the transcriptional machinery from accessing the *ospC* locus. *In vitro* work demonstrated that upon exposure to warm (37˚C) mammalian serum the supercoiling of cp26 is reversed permitting expression of *ospC*.

Another explanation for the temperature-dependent regulation of *ospC* involves small regulatory RNAs (sRNA) (40). RpoS is an alternative sigma factor involved in the initia-

Table 1

B. burgdorferi *infectivity as it relates to linear and circular plasmid profile.*

	Infectivity-associated		**Not infectivity-associated**		**Always present**
Infective phenotype*, #	lp25	lp28-1	cp9	lp21	cp26
High	+	+	+/-	+/-	+
Intermediate	+	-	+/-	+/-	+
Low	-	+/-	+/-	+/-	+

Note. * + plasmid must be present for the given infective phenotype, - plasmid must be absent for the given phenotype, +/- plasmid does not affect infective phenotype
#Data from reference 60

tion of *ospC* transcription. Expression of *rpoS* is regulated by DsrAAB, a temperature-sensitive sRNA. At 23˚C, the *rpoS* transcript contains a secondary stem-loop structure that occludes the ribosome binding site (RBS) preventing translation of the sigma factor. Also at 23˚C, DsrAAB exhibits secondary structure which prevents interactions between the sRNA and the *rpoS* transcript that are necessary for high levels of gene expression (Figure 4A). At 37˚C, DsrAAB loses its secondary structure which allows it to post-transcriptionally regulate the *rpoS* transcript. This results in loss of the *rpoS* stem-loop structure, RBS availability, and active translation of RpoS sigma factors (Figure 4B). The high level of RpoS expression at 37˚C greatly enhances the expression of *ospC*, which helps facilitate transmission of *B. burgdorferi* from the arthropod vector to the mammalian host.

Since the discovery of this molecular thermometer, over 1000 other *B. burgdorferi*-sRNAs have been identified, many of which demonstrate temperature-sensitivity (59). These molecules likely contribute to genetic regulatory mechanisms that promote *B. burgdorferi* transmission by allowing the pathogen to adapt to changing environmental conditions.

3. Motility

B. burgdorferi possesses periplasmic bundles

Figure 4

Temperature-dependent expression of ospC.

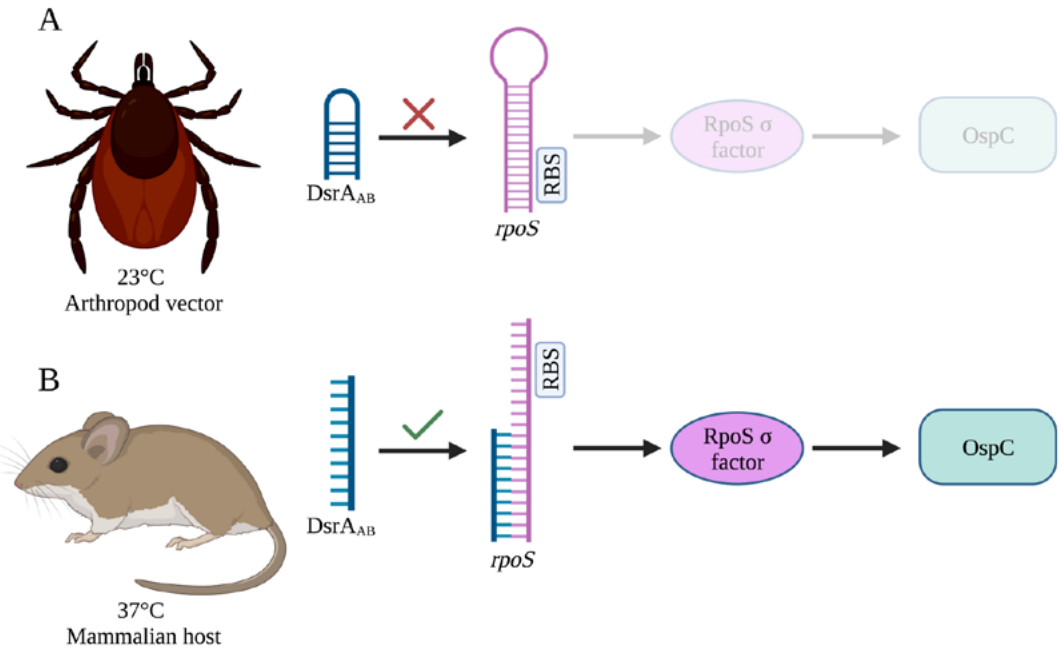

Note. A temperature shift accompanies the transmission of *B. burgdorferi* from the arthropod vector to the mammalian host (40). At 23˚C in the unfed tick, secondary structure of the sRNA DsrAAB prevents translation of the *rpoS* transcript, resulting in low levels of *ospC* expression (A). At 37˚C in the mammalian host, DsrAAB secondary structure is reversed, allowing for the production of *RpoS* and *OspC* (B).

of flagella that originate from basal bodies at its terminal ends (32). These structures confer flat-wave morphology and corkscrew swimming motility, which allow the spirochete to move both forward and backward as it bores through host tissues. This unique ability is integral to pathogenicity because it allows *B. burgdorferi* to disseminate throughout the human body, which results in the wide range of clinical manifestations associated with LD.

The *flaB* and *fliG* genes are required for flagellar functioning (68). The *flaB* gene encodes the major flagellar filament protein FlaB. *flaB* mutants are nonmotile, have a straight, bacillus morphology rather than the classic flat-wave morphology, and exhibit decreased viability in both the mammalian host and arthropod vector. The *fliG* gene encodes the C-ring at the base of the flagellar basal body, which is important for rotational torque generation. Inactivation of *fliG* results in reduced motility and infectivity despite proper assembly of the flagellar filament (38, 39). These results indicate that periplasmic flagella of *B. burgdorferi* play an important role in transmission and infectivity.

4. Chemotaxis

Some microorganisms use chemotaxis to migrate toward a chemoattractant or away from a chemorepellent in the environment. *B. burgdorferi* utilizes chemotaxis to colonize arthropod vectors and to infect mammalian hosts.

Figure 5

Salp12 salivary protein serves as a chemoattractant for B. burgdorferi.

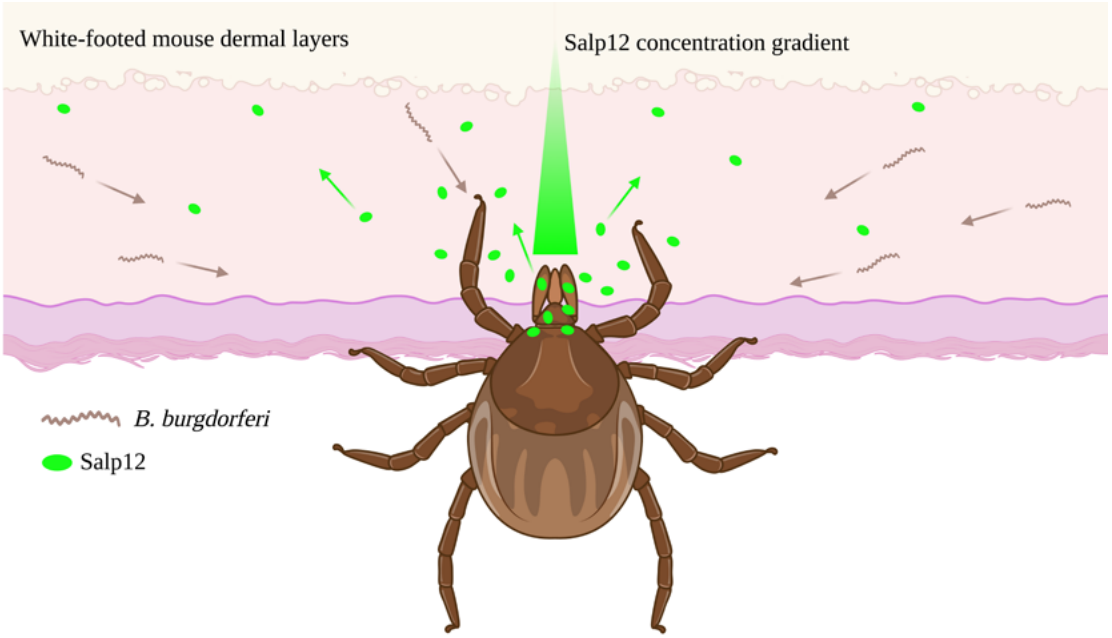

Note. Attachment of the *I. scapularis* tick to a host allows for the release of Salp12 salivary protein into the host (46). *B. burgdorferi* swims up the Salp12 concentration gradient to encounter the tick. This process promotes colonization of the tick midgut, which will allow *B. burgdorferi* to be transmitted to the next mammal that the tick feeds on.

The Salp12 salivary protein of the *Ixodes scapularis* tick serves as a chemoattractant for the bacterial cells that helps them colonize the arthropod vector (46). When uninfected ticks take a blood meal from an infected reservoir such as the white-footed mouse (*Peromyscus leucopus*), Salp12 diffuses into the host, attracting resident *B. burgdorferi* cells (Figure 5). This allows the bacteria to enter and colonize the arthropod midgut. Knockdown of *salp12* results in a significant reduction of *B. burgdorferi* colonization of the tick, which demonstrates the importance of chemotaxis for transmission of the pathogen to its vector.

To colonize the mammalian host, a chemotactic response that involves the *B. burgdorferi cheA2* gene is required (69). This gene encodes the histidine kinase of a two-component regulatory system that controls the directional rotation of *B. burgdorferi* flagella. Mutations in *cheA2* result in unidirectional movement and failure to be attracted into the mammalian host upon tick attachment. Interestingly, while *cheA2* mutants are unable to establish an infection in mammals, they retain the ability to colonize ticks. Together, these studies show the key role that chemotaxis plays during transmission of *B. burgdorferi* to the human host.

Innate Immune Evasion

The innate immune system is a nonspecific, noninducible line of defense that protects fungi, animals, and plants against a broad range of pathogens. *B. burgdorferi* uses many methods to evade this first line of defense.

1. Complement inactivation

The complement cascade is a tightly regulated pathway of sequentially activated proteins used to identify and eliminate pathogens through opsonization, phagocytosis, and formation of the membrane attack complex (MAC). *B. burgdorferi* expresses several Osps that disrupt this pathway including the surface lipoprotein BBK32, which binds and inactivates the C1 protease complex (2). This is the initiating component of the complement cascade, and its inactivation prevents all downstream steps. BBK32 mutants exhibit decreased virulence, which demonstrates the importance of complement inactivation for successful infection. Other Osps involved in complement disruption such as OspA, OspC, and CspA function by converting the blood protein plasminogen to plasmin, which is a known inhibitor of the cascade (24, 27, 55).

2. Antimicrobial peptide resistance

Antimicrobial proteins and peptides (AMPs) are produced by the host immune system to defend against pathogenic bacteria. Lactoferrin is an AMP that inhibits microbial growth by scavenging free iron, which is a cofactor required by most bacteria (9). *B. burgdorferi* avoids the effects of lactoferrin by using a manganese cofactor for biological redox reactions instead of iron (2). Cathelicidin is another AMP produced by many mammalian cells. While this molecule usually functions by interacting with cell surface components to disrupt microbial membrane integrity, it exhibits limited binding to the *B. burgdorferi* outer membrane (63). Additionally, the *B. burgdorferi* BBA57 surface protein has demonstrated the ability to downregulate the expression of some AMPs such as bactericidal/permeability-increasing protein (BPI), further promoting its virulence in hosts (6).

3. Phagocyte interference

The host immune response relies on phagocytic macrophages and dendritic cells to engulf and destroy foreign matter. While phagocytes effectively clear *B. burgdorferi* when exposed to purified bacterial cells *in vitro*, the pathogen can successfully evade these effects *in vivo* (16). This is likely due to the upregulation of the anti-inflammatory cytokine IL-10 in phagocytes upon *B. burgdorferi* engulfment. Normally, IL-10 functions to dampen the host immune response after pathogen clearance to prevent endogenous tissue damage. *B. burgdorferi*-induced premature overproduction of IL-10 inhibits the production of proinflammatory immune factors that are critical to the host's defense. Macrophages deficient in the ability to produce IL-10 generate greater levels of proinflammatory cytokines during *B. burgdorferi* infection, which promote phagocytic events that aid in removal of the pathogen (16). These findings demonstrate the important role that reprogramming the host immune response plays during *B. burgdorferi* infection.

4. Pleomorphic forms

B. burgdorferi shows pleomorphism, which is the ability to alter cellular morphology. This is often used by organisms to survive in extreme environments. In addition to the dominant flat-wave morphology, *B. burgdorferi* has been observed in other forms including blebs, round bodies (RB), and biofilm-like (BFL) aggregates (Figure 6) (44).

At 37˚C, nearly all *B. burgdorferi* cells are found in their dominant flat-wave or spirochetal form. Environmental stress signals such as extreme pH, high temperatures, and high levels of reactive oxygen species (ROS) result in a conversion of flat-wave cells to other forms such as RBs, which have reduced metabolic requirements (47). Subsequent removal of *B. burgdorferi* from these unfavorable conditions causes a reversion back to the dominant

Figure 6

B. burgdorferi *cells can be found in four distinct morphologies.*

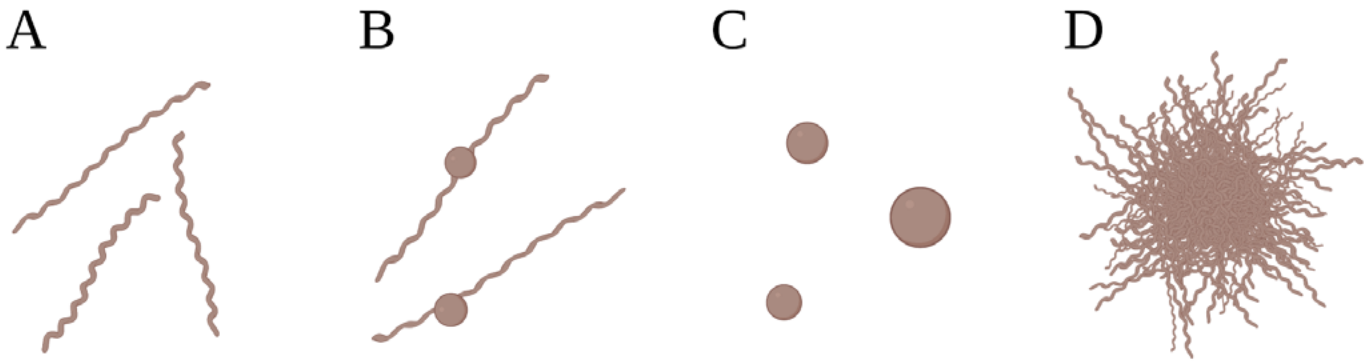

Note. Schematic representation of *B. burgdorferi* pleomorphic forms based on images obtained from differential interference contrast (DIC) microscopy (44). Flat-wave spirochetes (A), blebs (B), round bodies (RB; C), and biofilm-like aggregates (BFL; D) are not drawn to scale.

flat-wave morphology. Additionally, low levels of BFL aggregates are thought to exist in all environmental conditions where, like biofilms, they promote attachment to host tissues and resist phagocytosis (44). These findings support the idea that *B. burgdorferi* enhances its survival by altering its morphology as environmental conditions change.

The human body contains many microenvironments where *B. burgdorferi* may exist in different pleomorphic forms. To more successfully diagnose and treat LD, it will be important to continue exploring the physiological niches where each morphology dominates. This will guide the pharmacological development of novel treatments that more precisely and accurately target each distinct morphology of *B. burgdorferi*.

Adaptive Immune Evasion

Unlike the nonspecific innate immune system, the adaptive immune system defends against specific pathogens using antibodies and immune cells produced in response to a past exposure. *B. burgdorferi* disrupts the normal functioning of the adaptive immune system in many ways, three of which will be described in this review.

1. Germinal center disruption

During an infection, antigen-presenting cells (APC) display segments of immunogenic proteins from a phagocytosed pathogen on the major histocompatibility complex class II (MHC II) molecules on their cell surface. Next, these APCs present the antigens to B- and T-lymphocytes in secondary lymphoid tissues such as the spleen and lymph nodes. In these tissues, germinal centers form, and it is within these structures that antibody-producing plasma cells and B-lymphocytes develop to confer long-term immunity. During a *B. burgdorferi* infection, the host immune system generates structurally defective, short-lived germinal centers that are unable to generate high quantities of antibody-producing immune cells (20). This leaves the host immunosuppressed and allows *B. burgdorferi* to cause further infection.

2. Antibody class switching

Several classes of immunoglobulins (Igs) exist, each with a unique function in the host immune response. During an infection, the host's ability to shift production from one Ig class to another is useful in targeting pathogenic microorganisms located in multiple tissue types. Upon *B. burgdorferi* infection, pentameric IgM molecules are produced in high quantities, while monomeric IgG production is suppressed (28). IgG is the major circulating Ig found in the blood, and downregulating its production results in a less effective immune response. This is yet another way that *B. burgdorferi* manipulates the host immune response to further propagate an infection.

3. Antigenic variation

B. burgdorferi modifies its immunogenic cell surface proteins in a process called antigenic variation, which promotes evasion from the host's adaptive immune response (15, 79). For example, the immunoreactive VlsE surface lipoprotein encoded on lp28-1 undergoes frequent modification (Figure 7). Upstream of the *vlsE* locus are 15 silent *vls* cassettes that randomly recombine into the expressed region

Figure 7

vls *cassette recombination leads to highly varied VlsE proteins.*

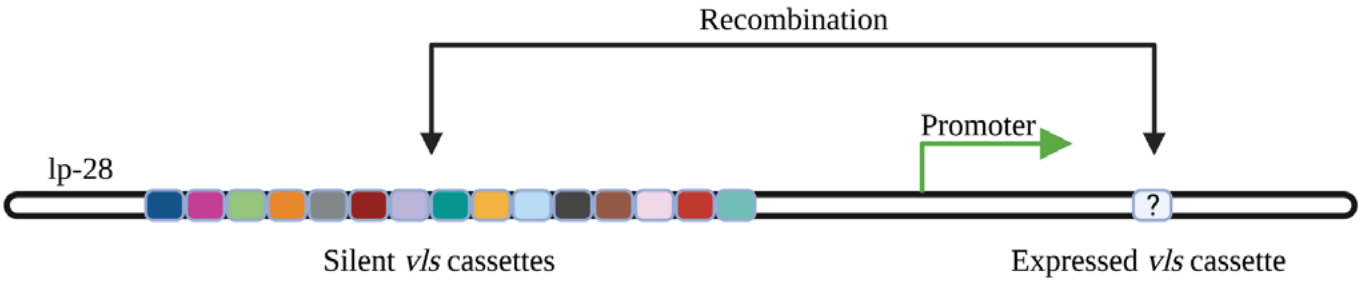

Note. Antigenic variation of the *B. burgdorferi* immunogenic VlsE surface lipoprotein encoded on lp28-1 is accomplished through recombination events between the upstream, silent *vls* cassettes and the downstream expressed region (15). This allows the pathogen to continuously modify the structure of the expressed antigen, which provides a mechanism of immune evasion.

of the gene during *B. burgdorferi* infection. This results in a mosaic VlsE with an estimated 10^{40} possible variants. Continuous modification of the structure of this surface lipoprotein prevents previously generated immune factors from functioning properly.

Incidence and Reporting of Lyme Disease

Understanding the epidemiology of vector-borne diseases such as LD is critical for disease prevention. The incidence rate and geographic distribution of infections provides health officials with pertinent information that can be used to organize public health efforts in high-risk areas. This section of the review will focus on LD surveillance, limitations in reporting, and ecological challenges that exacerbate the spread of disease.

1. CDC case definition

The CDC has published clinical guidelines that define a LD diagnosis (12). The 2022 case definition requires specific clinical and laboratory criteria to be met. Clinically, a patient must present at least one early or late-stage manifestation including EM, arthritis in one or more joints, nervous system abnormalities (lymphocytic meningitis, facial palsy, or unexplainable encephalomyelitis), or cardiovascular involvement (atrioventricular conduction defects). The laboratory criteria include at least one of the following: isolation of *B. burgdorferi* in culture, detection of *B. burgdorferi* by polymerase chain reaction (PCR), detection of *B. burgdorferi* antigens by immunohistochemical assay, or a positive two-tier serology test.

2. Surveillance data

Since its discovery, LD has been recognized throughout the world, particularly in Europe and Asia, and outside of the Northeast or New England region of the United States (67). Although surveillance in other countries is difficult, there are an estimated 85,000 cases annually in Europe, with the majority occurring in Germany, Austria, Slovenia, and Sweden.

In the US, LD is the most common vector-borne disease affecting an estimated 476,000 people annually from 2010-2018 (33, 34, 52). Most cases present in just a few states, with the highest incidences being reported in the Northeast, Mid-Atlantic, and upper Midwest regions (Figure 8) (67). According to the CDC, most cases occur in the summer months from June to August, which coincides with nymphal scavenging (13).

In the Northeast, there have been drastic spikes in disease occurrence, particularly in Maine where the incidence quadrupled between the years 2005 and 2015 (67). Northern expansion of LD is occurring, and this trend is expected to persist as the suitable habitat for ticks continues to expand (54).

In the Midwest, cases are on the rise with the majority concentrated in Wisconsin, Minne-

Figure 8

3-year (2018-2020) average LD incidence by state.

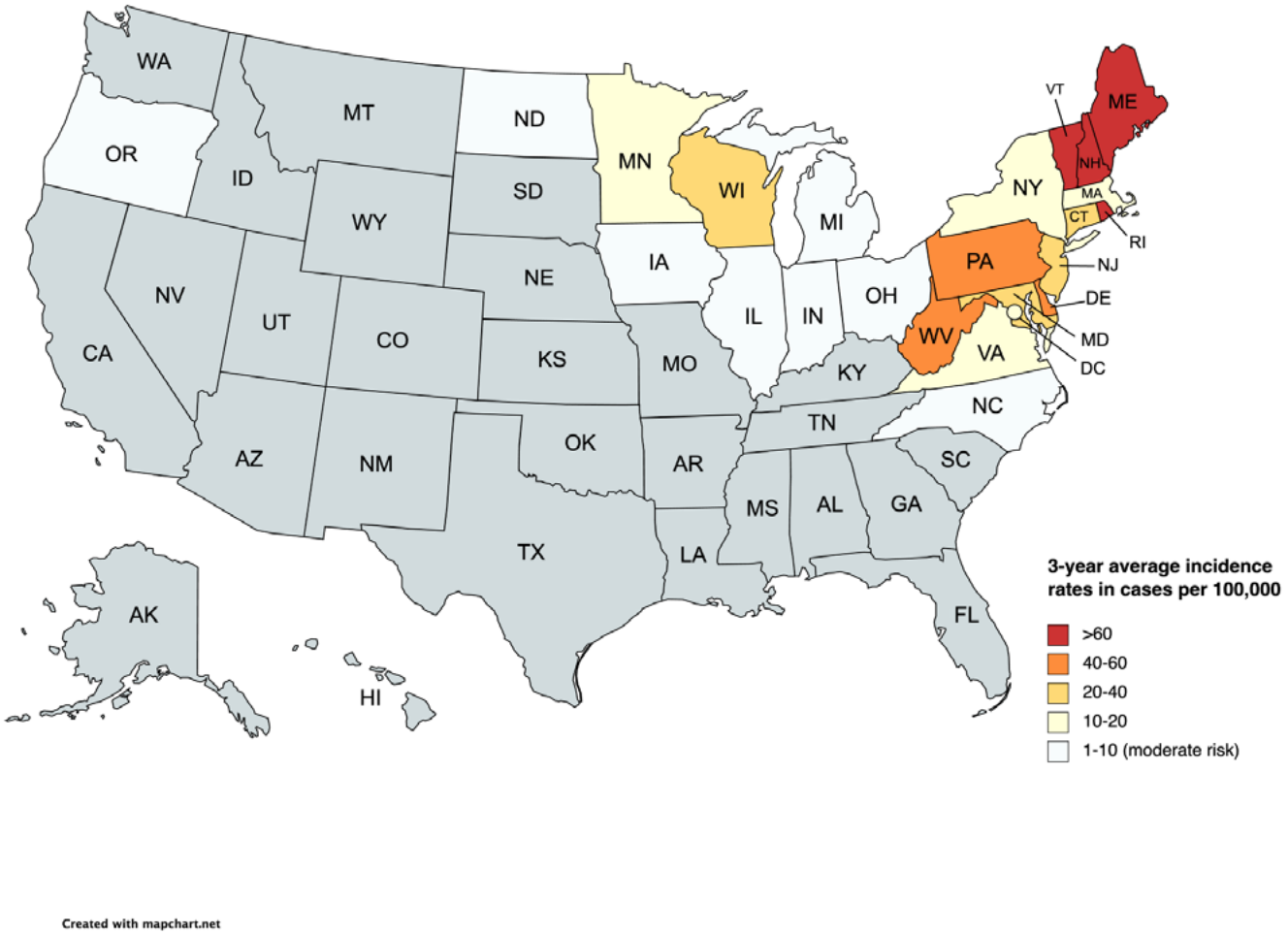

Note. The CDC considers a state "high risk" if it has greater than 10 confirmed cases of LD per 100,000 persons for three reporting years. In this review, states with 1-10 cases per 100,000 persons are considered to have moderate risk. This figure is based on data reported in reference 13.

sota, and northern Illinois (67). According to the CDC, Wisconsin had the fourth highest incidence of LD in 2019 behind Pennsylvania, New York, and New Jersey (13). Past models predicted further spread of *Ixodes* ticks throughout the Midwest into northern Michigan, the Ohio River Valley, and northwest Minnesota, which has indeed been observed in recent years (26).

In the Southeast, LD incidence is relatively low despite vectors being well established in areas such as coastal Florida, South Carolina, North Carolina, and Georgia (67). In this region, *Ixodes affinis* and *I. minor* ticks harbor *B. burgdorferi*, but these species lack the questing ability of *I. scapularis* and rarely feed on humans (4). Reported north to south gene flow of *I. scapularis* raises the possibility of altered southeastern tick behavior to that of the questing northern ticks, which could lead to a greater incidence of LD in this region in the future (78).

3. Limitations in reporting

LD has been a nationally reportable disease since 1991 (10). This means that physicians are required to report cases to state and local health departments who relay this information to the CDC. Due to the disease's recent characterization, the CDC points out limitations in surveillance that prevent the accurate estimation of LD incidence. These include both under-reporting in high incidence areas and over-reporting in low incidence areas due to clinical misclassification, inconsistencies in the funding and practices of health departments from one state to the next, and the collection of LD data based on area of residence rather than the location of exposure. The latter leads to the misinterpretation of surveillance data for tourists who account for a significant proportion of cases. Furthermore, the LD case definition has undergone five modifications since deemed nationally reportable in 1991, which makes it more difficult for clinicians to stay current with reporting guidelines. Due to these limitations, the CDC estimates that the actual number of annual LD cases is about 10 times greater than what is reported.

The recent COVID-19 pandemic has also greatly affected the reporting of many diseases including LD (36). While surveys indicated that Americans spent more time outdoors in 2020 than in 2019 putting them at greater risk for LD, the CDC reported about half the number of confirmed cases (13). One group of researchers successfully predicted this discrepancy before the CDC published their 2020 incidence data (43). Their study looked at the online traffic of the CDC's tick removal website as an indirect quantifier of tick encounters (14). In 2020, the most recent year with published LD data, there were 25% more online visits than in 2019 suggesting that more individuals found themselves at risk for developing LD. Conversely, emergency department visits for tick bites and the frequency of LD diagnostic testing were significantly reduced in 2020. This was likely due to health officials and clinicians being preoccupied during the initial spread of SARS-CoV-2 in the spring and early summer of 2020, which coincided with the peak seasons for tick bites. On top of this, many patients delayed or avoided seeking out healthcare for more minor affiliations, due to fear of contracting COVID-19 or contributing to overburdened healthcare systems (36). This

sudden change in LD reporting was not consistent with long-term, epidemiological trends, which suggests that the COVID-19 pandemic significantly affected reporting. An organized public health effort is needed to address this discrepancy in LD reporting and restore a high standard of surveillance.

4. Climate and ecological challenges

After the colonial period in North America, deforestation, agricultural expansion, and urbanization drastically altered the landscape, which primed the area for LD spread (73). One way this has occurred is through shifts in predator community dynamics (35). Coyotes have replaced populations of both large and small predators such as wolves, bears, and foxes. The reduction in the number of foxes, which are more efficient predators of small mammals than coyotes, has decreased the amount of predation faced by *B. burgdorferi's* main reservoir, the white-footed mouse. This has allowed the white-footed mouse to expand its home range, which has broadened the potential area of *B. burgdorferi* transmission to humans. Additionally, the reduction of large predator populations along with vast agricultural expansion has allowed deer populations to flourish, increasing the reproductive range of LD vectors.

The gradual increase in the temperature of the Earth's atmosphere also plays a key role in host/reservoir expansion. Models used to study these effects suggest dramatic expansions of *Ixodes* tick populations, which will broaden the range of *B. burgdorferi* (56). Over the next four decades, the geographic distribution of the white-footed mouse is predicted to expand northward by about 300 kilometers (61). If this manifests, it will have significant effects on the distribution of LD.

Disease Treatment and Prevention

Complete eradication of *B. burgdorferi* is implausible given its many hosts, reservoirs, and vectors. Rather, proper treatment of affected individuals and public health efforts to increase awareness of preventative measures in high-risk areas represent our best strategy to minimize the incidence of LD.

1. Treatment

Early localized infection is often treated with oral antibiotics such as doxycycline, amoxicillin, cefuroxime, or azithromycin (76). Pregnant women and children under the age of eight should avoid the use of doxycycline due to its adverse effects on bone development (29).

Early disseminated infection is treated based on the affected tissues. Patients with Lyme carditis or severe Lyme neuroborreliosis often receive intravenously administered ceftriaxone or cefotaxime, followed by one of the oral antibiotic regimens used to treat early localized infections (77). When only mild nervous system involvement such as isolated facial nerve palsy presents, oral antibiotic treatment usually suffices (76).

Treatment for late disseminated, chronic LD also depends on the presented signs and symptoms. If arthritis occurs without neurologic involvement, oral antibiotics are usually administered. If cardiac or neurologic involvement persists from the early disseminated phase of infection, intravenous antibiotic treatment may be necessary (76).

Prophylactic antibiotics are often prescribed in cases of suspected *B. burgdorferi* exposure after a tick bite. In a randomized clinical trial with patients that had removed an *Ixodes* genus tick within 72 hours, a single dose of doxycycline was 87% effective at preventing EM (49). This demonstrates the importance of immediate medical attention after a possible *B. burgdorferi* exposure to prevent long-term LD.

2. Vector-focused approach

While the elimination of *Ixodes* genus ticks is highly unlikely due to their vast, expanding range, local measures can be taken to greatly reduce the chances of human-tick interactions. One such method involves the use of carbaryl, an insecticide that is also lethal to arachnids, which has proven extremely effective at eliminating tick populations (66). Unfortunately, this is a broad-spectrum insecticide that also kills moths, beetles, cockroaches, ants, and mosquitoes, which could have negative ecological effects (51). This downside of the use of carbaryl should be weighed against the positive impact of treating outdoor public gathering spaces and private landscapes to limit *B. burgdorferi* exposures (Figure 9A).

Permethrin is another insecticide that can be used against ticks, which poses little to no ecological threat since it is applied to clothing rather than broadly to the environment. Permethrin-based treatment of clothes and shoes has proven effective at preventing tick bites, killing ticks upon attachment, and preventing the transmission of pathogens such as *B.*

Figure 9

LD preventative measures.

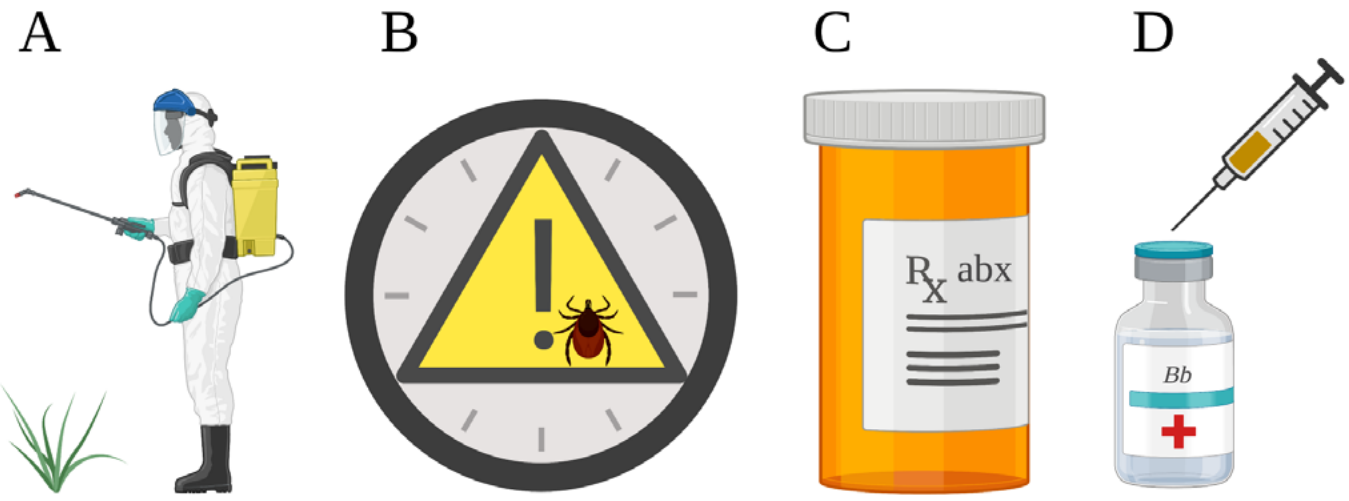

Note. The common methods for preventing LD include targeting reservoirs and vectors as well as best practices for humans who may have encountered ticks. These measures include the treatment of landscapes with insecticides (A), frequent self-examination and prompt removal of attached ticks (B), immediate medical intervention after exposure (C), and vaccine development (D) (17, 49, 57, 66).

burgdorferi (45). In a controlled study of the effectiveness of permethrin-treated outdoor gear, individuals wearing treated clothing received 3.36 times less tick bites than those wearing untreated clothing. Additionally, of the ticks attached to subjects, 97.6% were alive upon removal from individuals wearing untreated clothing, while only 22.6% of ticks were alive upon removal from those wearing permethrin-treated clothing. Outdoor gear can be purchased pre-treated with permethrin, or the insecticide can be applied at home carefully following the CDC's recommendations which include wearing protective gloves, reading the directions before application, allowing clothing to dry before use, and avoiding direct exposure to skin (11).

Other behavioral preventative measures should be taken to minimize the chances of acquiring LD. Frequent self-examination for ticks during and after outdoor activities in high-risk areas is critical (Figure 9B). As previously mentioned, there is a positive, nonlinear relationship between the duration of tick attachment and LD outcomes (57). Therefore, prompt removal of ticks and immediate prophylactic antibiotic treatment significantly decreases the chances of *B. burgdorferi* transmission (Figure 9C). Additionally, tucking pant legs into socks and covering bare skin in the outdoors are good strategies to prevent tick bites. Insect repellents that contain N, N-diethyl-meta-toluamide, commonly known as DEET, may also be helpful, but the effectiveness and duration of efficacy are inconsistent compared to other insecticides like permethrin (45).

3. Reservoir-focused approach

Small rodent reservoirs such as the white-footed mouse play a critical role in transmission of *B. burgdorferi* to its arthropod vector. While culling reservoir populations has been proposed, this would likely have negative ecological consequences. Instead, researchers have turned to the treatment of reservoirs to reduce populations of ticks and therefore the LD-causing spirochete (42). This has been attempted through the dispersal of permethrin-treated cotton in tick-infected areas, which is used by mice as nesting material. While this strategy significantly reduced *B. burgdorferi* transmission, additional research and development is needed to optimize the efficacy of this reservoir-focused treatment.

4. Vaccination efforts

While vector- or reservoir-focused approaches may be beneficial, immunization represents the most effective method of disease prevention (Figure 9D). In 1998, the United States Food and Drug Administration (FDA) approved a recombinant *B. burgdorferi* OspA vaccine called LYMErix (58). This vaccine functions by inducing the production of antibodies that target and eliminate *B. burgdorferi* as it enters the body during a tick bite. Less than four years after becoming available to the public, LYMErix was removed from the market due to low sales, anti-vaccine backlash, safety concerns, and class-action lawsuits. Although the FDA investigated the safety concerns and concluded there was a lack of evidence for the claims, the vaccine has not been available to the public since early 2002 (53).

Currently, companies such as Valneva are developing new LD vaccines designed to specifically protect individuals against North American and European strains of *B. burgdorferi* (17). These VLA15 protein subunit vaccines use the immunoreactive C-terminus of the OspA protein to induce protective immunity. They have proven effective in murine models and are currently undergoing human clinical trials. Wide-spread public acceptance of these vaccines in development represents our greatest potential defense against LD.

Additionally, researchers have begun to explore wildlife vaccination as an approach to LD prevention (71). OspA-based oral bait vaccines for reservoir populations of white-footed mice have demonstrated the ability to reduce the risk of LD in preliminary studies. These vaccines elicit an immune response that protects these animals from infection and reduces transmission of the pathogen to its arthropod vector. Decreasing the number of *B. burgdorferi*-harboring vectors in the environment will reduce the chances of human infection. Once the efficacy of wildlife vaccination is optimized, this may represent a successful long-term strategy to disease prevention.

Conclusion

B. burgdorferi, the causative agent of LD, is a highly complex parasite that uses an arthropod vector for transmission to mammalian hosts. The high rate of infection achieved by this spirochete is mainly derived from its unique ability to both evade and disrupt various aspects of the host immune response as it disseminates throughout the body. Clinically, LD has a variable presentation which makes it difficult for physicians to diagnose and treat their patients.

In the United States, LD is a major public health concern, especially in the upper Midwest and Northeast regions. Surveillance limitations, a lack of public awareness, and failed vaccination efforts in the past represent some of the major challenges to disease prevention. Enhancing the general public's understanding of the risks associated with outdoor activities and providing individuals in high-risk areas with everyday preventative measures can decrease the incidence of LD in the short-term. In the long-term, widespread acceptance of novel vaccines is likely our most promising solution.

While LD presents several clinical and epidemiological challenges, a collective and coordinated public health effort represents our greatest chance of controlling the deer tick's dark secret.

Glossary of Abbreviations

AMP: antimicrobial protein/peptide

BFL: biofilm-like (aggregates)

BSK: Barbour-Stoenner-Kelly media

CDC: Centers for Disease Control and Prevention

cp: circular plasmid

EM: erythema migrans

FDA: United States Food and Drug Administration

Ig: immunoglobulin

lp: linear plasmid

LD: Lyme Disease

LYMErix: OspA Lyme Disease vaccine

Osp: outer surface protein

RB: round bodies

sRNA: small regulatory RNA

References

1. Ahmed N. 2014. Cultivation of parasites. *Tropical Parasitology*. 4(2): 80-89. doi:10.4103/2229-5070.138534. Url: https://www.ncbi.nlm.nih.gov/pmc/articles/PMC4166808/

2. Anderson C, and Brissette C. 2021. The Brilliance of *Borrelia:* Mechanisms of Host Immune Evasion by Lyme Disease-Causing Spirochetes. *Pathogens*. 10(3): 281. doi:10.3390/pathogens10030281. Url: https://www.mdpi.com/2076-0817/10/3/281

3. Ante V, Farris L, Saputra E, Hall A, O'Bier N, Chavez A, Marconi R, Lybecker M, Hyde J. 2021. The *Borrelia burgdorferi* Adenylate Cyclase, CyaB, Is Important for Virulence Factor Production and Mammalian Infection. *Frontiers in Microbiology*. 25(12): 676192. doi:https://doi.org/10.3389/fmicb.2021.676192. Url: https://www.frontiersin.org/articles/10.3389/fmicb.2021.676192/full

4. Arsnoe I, Hickling G, Ginsberg H, McElreath R, Tsao J. 2015. Different Populations of Blacklegged Tick Nymphs Exhibit Differences in Questing Behavior That Have Implications for Human Lyme Disease Risk. *PLOS ONE*. 10(5): e0127450. doi:https://doi.org/10.1371/journal.pone.0127450. Url: https://journals.plos.org/plosone/article?id=10.1371/journal.pone.0127450

5. Arvikar S, Steer A. 2015. Diagnosis and Treatment of Lyme Arthritis. *Infectious Disease Clinics of North America*. 29(2): 269-280. doi:10.1016/j.idc.2015.02.004. Url: https://www.ncbi.nlm.nih.gov/pmc/articles/PMC4443866/

6. Bernard Q, Smith A, Yang X, Koci J, Foor S, Cramer S, Zhuang X, Dwyer J, Lin Y, Mongodin E, Marques A, Leong J, Anguita J, Pal U. 2018. Plasticity in early immune evasion strategies of a bacterial pathogen. *PNAS*. 115(16): E3788-E3797. doi:https://doi.org/10.1073/pnas.1718595115. Url: https://www.pnas.org/doi/full/10.1073/pnas.1718595115

7. Burgdorfer W, Barbour A, Hayes S, Benach J, Grunwaldt E, Davis J. 1982. Lyme Disease-A Tick-Borne Spirochetosis? *Science*. 216: 1317-1319. doi:10.1126/science.7043737. Url: https://escholarship.org/content/qt9vj3t37b/qt9vj3t37b_noSplash_13d2b56576d2ac55d60a1dd32ddc3074.pdf

8. Carrasco S, Troxell B, Yang Y, Brandt S, Li H, Sandusky G, Condon K, Serezani C, Yang X. 2015. Outer Surface Protein OspC Is an Antiphagocytic Factor That Protects *Borrelia burgdorferi* from Phagocytosis by Macrophages. *Infection and Immunity*. 83(12): 4848-4860. doi:https://doi.org/10.1128/IAI.01215-15. Url: https://journals.asm.org/doi/10.1128/IAI.01215-15

9. Cavestro G, Ingegnoli A, Aragona G, Lori V, Mantovani N, Altavilla N, Dal Bo N, Pilotto A, Bertele A, Franze A, Di Mario F, Borghi L. 2002. *Acta Biomedica*. 73(5-6): 71-3. Url: https://pubmed.ncbi.nlm.nih.gov/12643075/#:~:text=Lactoferrin%20is%20an%20iron%20binding,ions%20available%20for%20microorganism%27s%20metabolism

10. Centers for Disease Control and Prevention (CDC). Last reviewed November 15, 2022. Lyme Disease: Surveillance explained and available data. Accessed March 18, 2022. Url: https://www.cdc.gov/lyme/stats/survfaq.html#:~:text=Limitations%20of%20surveillance%20data&text=Not%20every%20case%20of%20Lyme,occur%20in%20low%20incidence%20areas.

11. Centers for Disease Control and Prevention (CDC). Last reviewed February 5, 2020. CDC-TV: What You Need to Know about Permethrin-transcript. Accessed January 7, 2023. Url: https://www.cdc.gov/cdctv/injuryviolenceandsafety/permethrin-transcript.html

12. Centers for Disease Control and Prevention (CDC): Division of Health Informatics and Surveillance. Last reviewed August 30, 2021. Lyme Disease (*Borrelia burgdorferi*) 2022 Case Definition. Accessed March 17, 2022. Url: https://ndc.services.cdc.gov/case-definitions/lyme-disease-2022/

13. Centers for Disease Control and Prevention (CDC), National Center for Emerging and Zoonotic Infectious Disease (NCEZID), Division of Vector-Borne Diseases (DVBD). Last reviewed August 29, 2022. Lyme Disease: Data and surveillance. Accessed March 18, 2022. Url: https://www.cdc.gov/lyme/datasurveillance/index.html?CDC_AA_refVal=https%3A%2F%2Fwww.cdc.gov%2Flyme%2Fstats%2Findex.html

14. Centers for Disease Control and Prevention (CDC), National Center for Emerging and Zoonotic Infectious Disease (NCEZID), Division of Vector-Borne Diseases (DVBD). Last reviewed May 13, 2022. Ticks: Removing a tick. Accessed January 10, 2023. Url: https://www.cdc.gov/ticks/removing_a_tick.html

15. Chaconas G, Castellanos M, Verbey T. 2020. Changing of the guard: How the Lyme disease spirochete subverts the host immune response. *Journal of Biological Chemistry.* 295(2): 301-313. doi:https://doi.org/10.1074/jbc.REV119.008583. Url: https://www.jbc.org/article/S0021-9258(17)48327-X/fulltext

16. Chung Y, Zhang N, Wooten R. 2013. *Borrelia burgdorferi* Elicited-IL-10 Suppresses the Production of Inflammatory Mediators, Phagocytosis, and Expression of Co-Stimulatory Receptors by Murine Macrophages and/or Dendritic Cells. *PLOS ONE.* 8(12): e84980. doi:https://doi.org/10.1371/journal.pone.0084980. Url: https://journals.plos.org/plosone/article?id=10.1371/journal.pone.0084980

17. Comstedt P, Schuler W, Meinke A, Lundberg U. 2017. The novel Lyme borreliosis vaccine VLA15 shows broad protection against *Borrelia* species expressing six different OspA serotypes. *PLOS ONE.* doi:https://doi.org/10.1371/journal.pone.0184357. Url: https://journals.plos.org/plosone/article/file?id=10.1371/journal.pone.0184357&type=printable

18. Cook M. 2014. Lyme borreliosis: a review of data on transmission time after tick attachment. *International Journal of General Medicine*. 8: 1-8. doi:10.2147/IJGM.S73791. Url: https://www.dovepress.com/lyme-borreliosis-a-review-of-data-on-transmission-time-after-tick-atta-peer-reviewed-fulltext-article-IJGM

19. Diuk-Wasser M, Vannier E, Krause P. 2016. Coinfection by Ixodes Tick-Borne Pathogens: Ecological, Epidemiological, and Clinical Consequences. *Trends in Parasitology*. 32(1): 30-42. doi:https://doi.org/10.1016/j.pt.2015.09.008. Url: https://www.cell.com/trends/parasitology/fulltext/S1471-4922(15)00210-X?_returnURL=https%3A%2F%2Flinkinghub.elsevier.com%2Fretrieve%2Fpii%2FS147149221500210X%3Fshowall%3Dtrue

20. Elsner R, Hastey C, Olsen K, Baumgarth N. 2015. Suppression of Long-Lived Humoral Immunity Following *Borrelia burgdorferi* Infection. *PLOS PATHOGENS*. 11(7): e1004976. doi:https://doi.org/10.1371/journal.ppat.1004976. Url: https://journals.plos.org/plospathogens/article?id=10.1371/journal.ppat.1004976

21. Fish A, Pride Y, Pinto D. 2008 Lyme Carditis. *Infectious Disease Clinics of North America*. 22:275-288. Url: https://www.cdc.gov/lyme/resources/fish2008-508.pdf

22. Ford L, Tufts D. 2021. Lyme Neuroborreliosis: Mechanisms of *B. burgdorferi* Infection of the Nervous System. *Brain Sciences*. 11(6): 789. doi:10.3390/brainsci11060789. Url: https://www.mdpi.com/2076-3425/11/6/789

23. Fraser C, Casjens S, Huang W, Sutton G, Clayton R, Lathigra R, White O, Ketchum K, Dodson R, Hickey E, Gwinn M, Dougherty B, Tomb J, Fleischmann R, Richardson D, Peterson J, Kerlavage A, Quachenbush J, Salzburg S, Hanson M, Vugt R, Palmer N, Adams M, Gocayne J, Weidman J, Utterback T, Watthey L, McDonald L, Artiach P, Bowman C, Garland S, Fujii C, Cotton M, Horst K, Roberts K, Hatch B, Smith H, Venter J. 1997. Genomic sequence of a Lyme disease spirochaete, *Borrelia burgdorferi*. *Nature*. 390: 580-586. doi:https://doi.org/10.1038/37551. Url: https://www.nature.com/articles/37551

24. Fuchs H, Wallich R, Simon M, Kramer M. 1994. The outer surface protein A of the spirochete *Borrelia burgdorferi* is a plasmin(ogen) receptor. *Proc. Natl. Acad. Sci. USA*. 91:12594–12598. doi:10.1073/pnas.91.26.12594. Url: https://www.pnas.org/doi/epdf/10.1073/pnas.91.26.12594

25. Gunduz A, Turkmen S, Turedi S, Nuhoglu I, Topbas M. 2008. Tick Attachment Sites. *Wilderness and Environmental Medicine*. 19(1):4-6. doi:https://doi.org/10.1580/06-WEME-BR-067.1. Url: https://www.wemjournal.org/article/S1080-6032(08)70142-X/fulltext

26. Hahn M, Jarnevich C, Monaghan A, Eisen R. 2016. Modeling the Geographic Distribution of Ixodes scapularis and Ixodes pacificus in the Contiguous United States. *Journal of Medical Entomology*. 53(5): 1176-1191. doi:https://doi.org/10.1093/jme/tjw076. Url: https://academic.oup.com/jme/article/53/5/1176/1751790

27. Hallstrom R, Haupt K, Kraiczy P, Hortschansky P, Wallich C, Zipfel P. 2010. Complement Regulator—Acquiring Surface Protein 1 of *Borrelia burgdorferi* Binds to Human Bone Morphogenetic Protein 2, Several Extracellular Matrix Proteins, and Plasminogen. *The Journal of Infectious Disease*. 202(3):490-498. doi:https://doi.org/10.1086/653825. Url: https://academic.oup.com/jid/article/202/3/490/831946

28. Hastey C, Elsner R, Barthold S, Baumgarth N. 2012. Delays and Diversions Mark the Development of B Cell Responses to *Borrelia burgdorferi* Infection. *The Journal of Immunology*. 188:5612-5622. doi:https://doi.org/10.4049/jimmunol.1103735. Url: https://journals.aai.org/jimmunol/article/188/11/5612/86779/Delays-and-Diversions-Mark-the-Development-of-B

29. Holmes N, Charles P. 2009. Safety and Efficacy Review of Doxycycline. *SAGE Journals- Clinical medicine Insights: Therapeutics*. doi:https://doi.org/10.4137/CMT.S2035. Url: https://journals.sagepub.com/doi/10.4137/CMT.S2035

30. Hu L, Steere A, Hall K. 2023. Patient education: Lyme disease symptoms and diagnosis (Beyond the Basics). *UpToDate*. Url: https://www.uptodate.com/contents/lyme-disease-symptoms-and-diagnosis-beyond-the-basics/print

31. Kean W, Tocchio S, Kean M, Rainsford K. 2012. The musculoskeletal abnormalities of the Similaun Iceman ("ÖTZI"): clues to chronic pain and possible treatments. *Inflammopharmacology*. 21: 11-20. doi:10.1007/s10787-012-0153-5. Url: https://link.springer.com/article/10.1007/s10787-012-0153-5

32. Kudryashev M, Cyrklaff M, Baumeister W, Simon M, Wallich R, Frischknecht F. 2009. Comparative cryo-electron tomography of pathogenic Lyme disease spirochetes. *Molecular Microbiology*. 71(6): 1415-1434. doi:https://doi.org/10.1111/j.1365-2958.2009.06613.x. Url: https://onlinelibrary.wiley.com/doi/10.1111/j.1365-2958.2009.06613.x

33. Kugeler K, Jordan R, Schulze T, Griffith K, Mead P. 2015. Will Culling White-Tailed Deer Prevent Lyme Disease? *Zoonoses and Public Health*. 63(5): 337-345. doi:https://doi.org/10.1111/zph.12245. Url: https://www.ncbi.nlm.nih.gov/pmc/articles/PMC4912954/

34. Kugeler K, Schwartz A, Delorey M, Mead P, Hinckley A. 2021. Estimating the Frequency of Lyme Disease Diagnoses, United States, 2010-2018. *Emerging Infectious Diseases*. 27(2): 616-619. doi:10.3201/eid2702.202731. Url: https://www.ncbi.nlm.nih.gov/pmc/articles/PMC7853543/

35. Levi T, Kilpatrick A, Mangel M, Wilmers C. 2012. Deer, predators, and the emergence of Lyme disease. *PNAS*. 109(27). doi:https://doi.org/10.1073/pnas.1204536109. Url: https://www.pnas.org/doi/full/10.1073/pnas.1204536109

36. Lindquist S, Goldoft M. 2021. Impact of a Pandemic on Disease Reporting. *epiTRENDS*. 26(1). Url: https://doh.wa.gov/sites/default/files/legacy/Documents/5100//420-002-epitrends2021-01.pdf

37. Lloyd D. 1976. Circular Letter #12-32 To: Directors of Health (Lyme Disease PSA). State of Connecticut: State Department of Health. Hartford, Connecticut, 06115. Url: https://portal.ct.gov/-/media/Departments-and-Agencies/DPH/dph/infectious_diseases/lyme/1976circularletterpdf.pdf

38. Lloyd S, Tang H, Wang X, Hillings S, Blair D. 1995. Torque Generation in the Flagellar motion of *Escherichia coli*: Evidence of a Direct Role for FliG but Not for FliM or FliN. *Journal of Bacteriology*. 178(1): 223-231. doi:https://doi.org/10.1128/jb.178.1.223-231.1996. Url: https://journals.asm.org/doi/epdf/10.1128/jb.178.1.223-231.1996

39. Lowder B, Duyvesteyn M, Blair D. 2005. FliG Subunit Arrangement in the Flagellar Rotor Probes by Targeted Cross-Linking. *Journal of Bacteriology*. 187(16): 5640-5647. doi:10.1128/JB.187.16.5640-5647.2005. Url: https://journals.asm.org/doi/10.1128/JB.187.16.5640-5647.2005

40. Lybecker M, Samuels D. 2007. Temperature-induced regulation of RpoS by a small RNA in *Borrelia burgdorferi. Molecular Microbiology*. 64(4) 1075-1089. doi:https://doi.org/10.1111/j.1365-2958.2007.05716.x. Url: https://onlinelibrary.wiley.com/doi/10.1111/j.1365-2958.2007.05716.x

41. Markeljevic J, Sarac H, Rados M. 2011. Tremor, seizures and psychosis as presenting symptoms in a patient with chronic lyme neuroborreliosis (LNB). *Collegium Antropologicum*. Suppl 1:313-8. Url: https://pubmed.ncbi.nlm.nih.gov/21648354/

42. Mather T, Ribeiro J, Spielman A. 1987. Lyme disease and babesiosis: acaricide focused on potentially infected ticks. *The American Journal of Tropical Medicine and Hygiene*. 36(3): 609-614. doi:10.4269/ajtmh.1987.36.609. Url: https://pubmed.ncbi.nlm.nih.gov/3555140/

43. McCormick D, Kugeler K, Marx G, Jayanthi P, Dietz S, Mead, P, Hinckley A. 2021. Effects of COVID-19 Pandemic on Reported Lyme Disease, United States, 2020. *Emerging Infectious Diseases*. 27(10): 2715-2717. Doi: 10.3201/eid2710.210903. Url: https://www.ncbi.nlm.nih.gov/pmc/articles/PMC8462321/#:~:text=Despite%20ongoing%20exposure%2C%20Lyme%20disease,changes%20in%20healthcare%2Dseeking%20behavior.

44. Merilainen L, Herranen A, Schwarzbach A, Gilbert L. 2015. Morphological and biochemical features of *Borrelia burgdorferi* pleomorphic forms. *Microbiology*. 161(Pt 3): 516–527. doi:10.1099/mic.0.000027. Url: https://www.microbiologyresearch.org/content/journal/micro/10.1099/mic.0.000027

45. Miller N, Rainone E, Dyer M, Gonzales M, Mather T. 2011. Tick Bite Protection With permethrin-Treated Summer-Weight Clothing. *Journal of Medical Entomology*. 48(2): 327-333. Doi: https://doi.org/10.1603/ME10158. Url: https://academic.oup.com/jme/article/48/2/327/893233?login=false

46. Murfin K, Kleinbard R, Aydin M, Salazar S, Fikrig E. 2019. *Borrelia burgdorferi* chemotaxis toward tick protein Salp12 contributes to acquisition. *Ticks and Tick-borne Diseases.* 10(5):1124-1134. doi:https://doi.org/10.1016/j.ttbdis.2019.06.002. Url: https://www.sciencedirect.com/science/article/abs/pii/S1877959X19300950?via%3Dihub

47. Murgia R, Cinco M. 2004. Induction of cystic forms by different stress conditions in *Borrelia burgdorferi. Journal of Pathology, Microbiology and Immunology*. 112(1):57-62. doi:10.1111/j.1600-0463.2004.apm1120110.x. Url: https://pubmed.ncbi.nlm.nih.gov/14961976/

48. Murray T, Shapiro E. 2012. Lyme Disease. *Clinics in Laboratory Medicine*. 30(1):311-328. doi:10.1016/j.cll.2010.01.003. Url: https://www.ncbi.nlm.nih.gov/pmc/articles/PMC3652387/

49. Nadelman R, Nowakowski J, Fish D, Falco R, Freeman K, McKenna D, Welch P, Marcus R, Aguero-Rosenfeld M, Dennis D, Wormser G, Tick Bite Study Group. 2001. Prophylaxis with Single-Dose Doxycycline for the Prevention of lyme Disease after an *Ixodes scapularis* Tick Bite. *New England Journal of Medicine*. 345: 79-84. doi:10.1056/NEJM200107123450201. Url: https://pubmed.ncbi.nlm.nih.gov/11450675/

50. Nagi K, Joshi R, Thakur R. 1996. Cardiac Manifestations of Lyme Disease: a review. *Canadian Journal of Cardiology*. 12(5): 503-506. PMID: 8640597. Url: https://europepmc.org/article/med/8640597

51. National Pesticide Information Center (NPIC). Last reviewed 2003. Carbaryl: General Fact Sheet. Accessed January 9, 2023. Url: http://npic.orst.edu/factsheets/carbgen.pdf

52. Nelson, Christina A. et al. September 2015. Incidence of Clinician-Diagnosed Lyme Disease, United States, 2005-2010. *Emerging Infectious Diseases.* 21(9): 1625-1631. doi:10.3201/eid2109.150417

53. Nigrovic L, Thompson K. 2007. The Lyme vaccine: a cautionary tale. *Epidemiology & Infection*. 135(1): 1-8. Doi: 10.1017/S0950268806007096. Url: https://www.ncbi.nlm.nih.gov/pmc/articles/PMC2870557/

54. Ogden N, Barker I, Francis C, Heagy A, Lindsay L, Hobson K. 2015. How far north are migrant birds transporting the tick *Ixodes scapularis* in Canada? Insights from stable hydrogen isotope analyses of feathers. *Ticks and Tick-borne Diseases.* 6(6): 715-720. doi:https://doi.org/10.1016/j.ttbdis.2015.06.004. Url: https://www.sciencedirect.com/science/article/abs/pii/S1877959X15001119?via%3Dihub

55. Onder O, Humphrey P, McOmber B, Korobova F, Francella N, Greenbaum D, Brisson D. 2012. OspC Is a Potent Plasminogen Receptor on the Surface of *Borrelia burgdorferi*. *Journal of Biological Chemistry (Cell Biology).* 287(20):16860-16868. doi:https://doi.org/10.1074/jbc.M111.290775. Url: https://www.jbc.org/article/S0021-9258(20)60819-5/fulltext

56. Ostfeld R, Brunner J. 2015. Climate change and Ixodes tick-borne disease of humans. *The Royal Society Publishing; Philosophical Transactions B*. 370:20140051. doi:https://doi.org/10.1098/rstb.2014.0051. Url: https://royalsocietypublishing.org/doi/10.1098/rstb.2014.0051

57. Piesman J. 1993. Dynamics of *Borrelia burgdorferi* transmission by nymphal Ixodes dammini ticks. *Journal of Infectious Disease*. 167(5):1082-5. doi:10.1093/infdis/167.5.1082. Url: https://pubmed.ncbi.nlm.nih.gov/8486940/

58. Poland G. 2001. Prevention of Lyme Disease: A Review of the Evidence. *Mayo Clinic Proceedings*. 76(7): 713-724. doi:https://doi.org/10.4065/76.7.713. Url: https://www.mayoclinicproceedings.org/article/S0025-6196(11)65002-7/fulltext

59. Popitsch N, Bilusic I, Rescheneder P, Schroeder R, Lybecker M. 2017. Temperature-dependent sRNA transcriptome of the Lyme disease spirochete. *BMC Genomics*. 18: 28. Doi: 10.1186/s12864-016-3398-3. Url: https://www.ncbi.nlm.nih.gov/pmc/articles/PMC5216591/

60. Purser J, Norris S. 2000. Correlation between plasmid content and infectivity in *Borrelia burgdorferi*. PNAS. 97(25): 13865-13870. doi:https://doi.org/10.1073/pnas.97.25.13865. Url: https://www.pnas.org/doi/full/10.1073/pnas.97.25.13865

61. Roy-Dufresne E, Logan T, Simon J, Chmura G, Millien V. 2013. Poleward Expansion of the White-Footed Mouse under Climate Change: Implications for Spread of Lyme Disease. PLOS ONE. 8(11): e80724. doi:https://doi.org/10.1371/journal.pone.0080724. Url: https://journals.plos.org/plosone/article?id=10.1371/journal.pone.0080724

62. Sapi E, Pabbati N, Datar A, Davies E, Rattelle A, Kuo B. 2013. Improved Culture Conditions for the Growth and Detection of Borrelia from Human Serum. International Journal of Medical Sciences. 10(4): 362-376. doi: 10.7150/ijms.5698. Url: https://www.ncbi.nlm.nih.gov/pmc/articles/PMC3590594/pdf/ijmsv10p0362.pdf

63. Sarkar A, Tilly K, Stewart P, Bestor A, Battisti J, Rosa P. 2009. *Borrelia burgdorferi* Resistance to a Major Skin Antimicrobial Peptide Is Independent of Outer Surface Lipoprotein Content. Antimicrobial Agents and Chemotherapy. 53(10): 4490-4494. doi:10.1128/AAC.00558-09. Url: https://www.ncbi.nlm.nih.gov/pmc/articles/PMC2764146/

64. Schwan T, Burgdorfer W, Garon C. 1988. Changes in infectivity and plasmid profile of the Lyme disease spirochete, *Borrelia burgdorferi*, as a result of in vitro cultivation. Infection and Immunology. 56(8): 1831–1836. doi:10.1128/iai.56.8.1831-1836.1988. Url: https://journals.asm.org/doi/epdf/10.1128/iai.56.8.1831-1836.1988

65. Schwan T, Piesman J, Golde W, Dolan M, Rosa P. 1995. Induction of an outer surface protein on *Borrelia burgdorferi* during tick feeding. PNAS. 92: 2909-2913. doi:10.1073/pnas.92.7.2909. Url: https://www.pnas.org/doi/epdf/10.1073/pnas.92.7.2909

66. Stafford K. 1991. Effectiveness of Carbaryl Applications for the Control of Ixodes dammini Nymphs in an Endemic Residential Area. Journal of Medical Entomology. 28(1): 32-36. doi:https://doi.org/10.1093/jmedent/28.1.32. Url: https://academic.oup.com/jme/article-abstract/28/1/32/2220853?redirectedFrom=fulltext

67. Stone B, Tourand Y, Brissette C. 2017. Brave New Worlds: The Expanding Universe of Lyme Disease. Vector Borne and Zoonotic Diseases. 17(9): 619-629. doi:10.1089/vbz.2017.2127. Url: https://www.ncbi.nlm.nih.gov/pmc/articles/PMC5576071/

68. Sultan S, Manne A, Stewart P, Bestor A, Rosa P, Charon N, Motaleb M. 2013. Motility Is Crucial for the Infectious Life Cycle of *Borrelia burgdorferi*. Infection and Immunology. 81(6): 2012-2021. doi:https://doi.org/10.1128/IAI.01228-12. Url: https://journals.asm.org/doi/10.1128/IAI.01228-12

69. Sze C, Zhang K, Kariu T, Pal U, Li C. 2012. *Borrelia burgdorferi* Needs Chemotaxis To Establish Infection in Mammals and To Accomplish Its Enzootic Cycle. American Society for Microbiology. 80(7): 2485-2492. doi:https://doi.org/10.1128/IAI.00145-12. Url: https://journals.asm.org/doi/10.1128/IAI.00145-12

70. Takayama K, Rothenberg R, Barbour A. 1987. Absence of lipopolysaccharide in the Lyme disease spirochete, *Borrelia burgdorferi*. Infection and Immunity. 55(9): 2311-2313. doi:https://doi.org/10.1128/iai.55.9.2311-2313.1987. Url: https://journals.asm.org/doi/epdf/10.1128/iai.55.9.2311-2313.1987

71. Voordouw M, Tupper H, Onder O, Devevey G, Graves C, Kemps B, Brisson D. 2013. Reductions in Human Lyme Disease Risk Due to the Effects of Oral Vaccination on Tick-to-Mouse and Mouse-To-Tick Transmission. Vector Borne and Zoonotic Diseases. 13(4): 203-214. Doi: 10.1089/vbz.2012.1003. Url: https://www.ncbi.nlm.nih.gov/pmc/articles/PMC3610442/

72. Waddell L, Greig J, Lindsay L, Hinckley A, Ogden N. 2018. A systematic review on the impact of gestational Lyme disease in humans on fetus and newborn. PLOS ONE. 13(11) e0207067. doi:10.1371/journal.pone.0207067. Url: https://journals.plos.org/plosone/article?id=10.1371/journal.pone.0207067

73. Walter K, Carpi G, Caccone A, Diuk-Wasser M. 2017. Genomic insights into the ancient spread of Lyme disease across North America. Nature: ecology and evolution. 1569-1576 doi:10.1038/s41559-017-0282-8. Url: https://www.nature.com/articles/s41559-017-0282-8

74. Wang C, Chacko S, Abdollah H, Baranchuk A. 2018. Treating Lyme carditis high-degree AV block using a temporary-permanent pacemaker. Annals of Noninvasive Electrocardiology. 224(3): e12599. doi:10.1111/anec.12599. Url: https://onlinelibrary.wiley.com/doi/epdf/10.1111/anec.12599

75. Weber K, Burgdorfer W, Schierz G. 1993. Aspects of Lyme Borreliosis: The Historical Road to the Discovery of *Borrelia burgdorferi*. Germany: Springer Berlin, Heidelberg. Url: https://link.springer.com/chapter/10.1007/978-3-642-77614-4_2

76. Wright W, Riedel D, Talwani R, Gillian B. 2012. Diagnosis and Management of Lyme Disease. American Family Physician. 85(11): 1086-1093. doi:https://www.aafp.org/afp/2012/0601/afp20120601p1086.pdf. Url: https://pubmed.ncbi.nlm.nih.gov/22962880/

77. Yeung C, Baranchuk A. 2019. Diagnosis and Treatment of Lyme Carditis: JACC Review Topic of the Week. Journal of the American College of Cardiology. 74(21): 2709-2711. doi:https://doi.org/10.1016/j.jacc.2018.11.035. Url: https://www.sciencedirect.com/science/article/pii/S0735109718394427?via%3Dihub

78. Zee J, Piesman J, Hojgaard A, Black W. 2015. Nuclear Markers Reveal Predominantly North to South Gene Flow in Ixodes scapularis, the Tick Vector of the Lyme Disease Spirochete. PLOS ONE. 10(11): e0139630. doi:https://doi.org/10.1371/journal.pone.0139630. Url: https://journals.plos.org/plosone/article?id=10.1371/journal.pone.0139630

79. Zhang J, Norris S. 1998. Genetic Variation of the *Borrelia burgdorferi* Gene vlsE Involves Cassette-Specific, Segmental Gene Conversion. Infection and Immunology. 66(8): 3698–3704. doi:10.1128/IAI.66.8.3698-3704.1998. Url: https://journals.asm.org/doi/10.1128/IAI.66.8.3698-3704.1998

Daily Case Trends of COVID-19: A Comparative Analysis of Indiana and Washington State

Lillia G. Marble

John L. McKillip

Department of Biology, Ball State University, Muncie, IN 47306

Abstract

The COVID-19 pandemic has caused immense and immeasurable disruption to billions of lives worldwide, and the strain on healthcare workers and facilities will undoubtedly be seen for years to come. Many factors impact the incidence and prevalence of COVID-19 in states, such as policies and legislation, funding, partisanship of the statehouse, vaccination rates, and rurality. The purpose of this paper is to analyze the differences in the daily positive cases between Indiana and Washington State and examine the respective ways each state tried to mitigate the morbidity and mortality of the virus. Indiana and Washington State were chosen as the states have similar populations in different geographical locations in the country and varying responses to the pandemic. Data was obtained from the respective state health departments over a period of two and a half years from March 2020 to December 2022. Independent t-tests were used for the analysis of the data between Indiana and Washington. Overall, Indiana had a higher daily positive case rate when compared to Washington. Indiana had a lower vaccination rate and had more hospitalizations and deaths compared to Washington and the US population as a whole. The difference in the findings of each state could be attributed to the partisanship of the state and the ways in which partisanship influences the enacting of legislation and policies intended to mitigate disease, as well as public health funding allocated by the state.

Keywords: COVID-19, statistical analysis, Indiana, public health, Washington

Manuscript received 11 December 2023; accepted 21 April 2024

Fine Focus, 10(1), 38-57. doi: 10.33043/FF.10.1.38-57

Introduction & History

The COVID-19 pandemic is a global health crisis caused by the novel coronavirus SARS-CoV-2. The virus, which causes a pneumonia-like illness in humans, was first identified in Wuhan, China in December 2019 originating from a "wet market" in which infected live animals were sold for food, becoming zoonotic when it started infecting humans. This viral illness started quickly spreading throughout China and other surrounding countries. In January 2020, the World Health Organization (WHO) declared this outbreak of the novel coronavirus a public health emergency, and by March 2020, the WHO declared it a worldwide pandemic, at which point there were more than 118,000 cases in 114 countries and more than 4,000 documented deaths globally (9).

The first case of the novel coronavirus in the United States was reported on January 20th, 2020, in Seattle, Washington after family-related travel to Wuhan, China (9). By April 10th, 2020, the United States had become a global hotspot for the SARS-CoV-2 virus, with more than 500,000 cases since January (9). As the only industrialized country without universal healthcare and equitable access to care, the United States was especially susceptible to a high rate of spread, quickly surpassing China to become the epicenter of cases in the world early in the pandemic (18).

Two weeks prior to the Trump Administration's issuance of a nationwide emergency, Governor Jay Inslee of Washington State issued a statewide emergency on February 29th, 2020, making it the first state to implement public health interventions to slow the spread of the virus (12). By the end of March 2020, many state and local governments had issued similar statewide emergencies and implemented various public health measures to slow the spread of this novel virus, one of these states being Indiana who declared a statewide public health emergency on March 6th, 2020. These public health measures included lockdowns/travel restrictions, social distancing, and face covering mandates, recommended by the World Health Organization (WHO) and Centers for Disease Control and Prevention (CDC) based on evidence-based practices for mitigating airborne or droplet transmitted diseases. Various states implemented much stricter mitigation measures, while other states were much laxer in the policies they implemented.

Since early 2020, the pandemic has had a profound impact on the global economy and healthcare systems. The hospitals and healthcare systems in many countries – including the United States – were overwhelmed, underprepared, and vastly understaffed for the influx of patients admitted with this virus. Shortages of personal protective equipment and medical supplies became the norm after the pandemic caused severe disruptions in the global supply chain. Vaccines were developed and approved for emergency use in record time, with the first vaccine doses administered to healthcare workers and first responders in December 2020. While vaccines have been effective in reducing the severity of illness and hospitalizations, new variants of the virus have emerged, and the pandemic continues to pose a significant public health threat. The purpose of this paper is to compare disease

morbidity and mortality between two states of similar populations – Indiana and Washington State – with varying degrees of public health policy and mitigation strategies. The two states are relatively similar in population (IN: 6.7 million; WA: 7.6 million) (37) and have a few similar demographics; they both have the same median age of 37.8 years, they have a similar female population percentage (IN: 50.4%; WA: 49.6%), and similar high school education levels (IN: 89.8%; WA: 91.9%) (35,36). Although these are a handful of the similarities between Indiana and Washington, there are some major differences; for example, Indiana is located in the Midwest region of the United States, while Washington is located in the Pacific Northwest. These states also differ historically in their political outlooks. In the 2020 Presidential election, 57% of voting-eligible residents in Indiana voted Republican, while only 38% of voting-eligible Washington residents voted Republican – compared to 41% and 58% voting Democrat, respectively (45,46). Historically, Indiana has been Republican-led since 2004, and Washington has been Democrat-led since 1988. Analyzing two states in differing parts of the country with varying political views yet otherwise similar demographics allows for a diverse set of data to compare.

Daily testing data from Indiana and Washington State was collected and analyzed comparatively using independent samples t-tests. Several sets of data were compared: each year of 2020, 2021, and 2022, respectively; the Delta variant wave in mid-2021; the Omicron variant wave from December 2021 to January 2022; the 2020-2021 winter/respiratory season; the 2021-2022 winter/respiratory season; and the entirety of the data from March 2020 to December 2022.

The COVID-19 Delta and Omicron variant waves were compared as they were the two largest COVID-19 waves in the dataset and the most transmissible variants in the dataset, resulting in higher incidences (7,11,13, 20). The winter/respiratory seasons were also compared as respiratory illnesses tend to increase in the winter months in the peak influenza season from December to March.

The difference in policies implemented by each state as well as the partisanship of the state ultimately played a major role in determining the course and outcome of the pandemic by impacting the incidences of cases. The differences in data could be attributed to a variety of factors including vaccination rates, public health initiatives & legislation, funding, and access to healthcare facilities.

Materials & Methods

Study Design

The COVID-19 incidences in Indiana and Washington State were compared using daily positive cases reported to each state's respective department of health. The daily positive cases were collected for each state (Appendix A) and analyzed using independent T-tests on SPSS. To control for differences in population, each daily data point was divided by each state's population (IN: 6.7 million; WA: 7.6 million), as reported by the 2020 Census Bureau (37) to standardize the values per 100,000 people. The statistical analyses were as follows: all time (March 2020 – December 2022); 2020

calendar year; 2021 calendar year; 2022 calendar year; Delta variant wave (July-September 2021); Omicron variant wave (November 2021-January 2022); 2020-2021 Winter/Respiratory Season; and 2021-2022 Winter/Respiratory Season. Other values such as vaccination rates, death rates, and hospitalization rates were also collected and compared.

Statistical Analyses

To analyze the statistical differences between the case rates of Washington and Indiana, independent T-tests were used. To control for differences in population, the daily case counts were divided by their respective state's population, as reported by the 2020 US Census Bureau. Independent T-tests were used to compare different data sets from the pandemic. The daily positive COVID-19 case rates for the two states were compared from the period of March 2020 to December 2022 using independent t-tests. Analysis was also done on the individual years of 2020, 2021, and 2022 using independent t-tests, respectively. The Delta variant wave and the Omicron variant wave were also compared using independent t-tests as they were the two largest COVID-19 variant waves in the dataset. In addition, the COVID-19 cases during the yearly flu/respiratory season from October to May – with peaks from December to March – was also analyzed using independent T-tests as respiratory illnesses tends to increase in the winter months.

The daily case values were the primary comparative analysis between Indiana and Washington, but other values were collected and compared as well. These values obtained from the State Departments of Health included hospitalization numbers, death counts, and vaccination rates. Hospitalization and death rates were calculated by dividing the total counts of hospitalizations and deaths from COVID-19 in the state by the total number of COVID-19 cases. The hospitalization and death counts were divided by the population of each respective state to get the standardized value per 100,000 people.

Standard deviation was analyzed for each independent t-test performed and included in the subsequent data tables. Standard error was also used in the graphs indicated by the error bars on each column. Standard error was used in the graphs due to the sheer size of the data and because it does not follow a normal bell-curve distribution.

Results

The general trend, after controlling for population, showed that Indiana had a higher COVID-19 incidence with a p value of <0.001. Indiana continued to have a higher incidence in all analyses, albeit not all results were statistically significant. The exceptions from the statistically significant p value are the daily case rates from the 2021-2022 respiratory/flu season (IN>WA, $p = 0.134$) and the 2022 calendar year (IN>WA, $p = 0.419$) (see Tables 1 & 3).

When compared to the total US data for hospitalization and death rates, Indiana had higher rates (7.64% and 1.28%, respectively) and Washington had lower rates (4.23% and 0.81%, respectively) than the US average (5.84% and 1.08% respectively) (Table 5). Similarly, for both the primary series and the updated booster, Indiana had lower vaccination rates (57.1% and 10.4%, respectively) and Washington had

higher vaccination rates (76.1% and 24.5%, respectively) than the total US vaccination rate (69.3% and 16.3%, respectively) (Table 4).

Rurality was defined using the Federal Office of Management and Budget's definition of a rural county which classifies a county as rural if the largest urban area in that county is less than 50,000 people (39). Using this definition, Indiana had a greater percentage of rural counties and a greater percentage of populates (78.3% & 34%, respectively) in those counties than the US average (65.2% & 14%, respectively), while Washington had a lower percentage of rural counties and a lower percentage of populates (51.3% & 9.3%, respectively) compared to the US average (Table 6).

The mean and standard error are graphed for each of the tables below. In addition, the maximum and minimum values for each month (March 2020 – December 2022) were graphed for each state (Figures 2 & 3). Public health funding data is also included for each state (Table 7).

Case Rates

Table 1

Daily case rates standardized per 100,000 people

Daily COVID-19 Case Rates (per 100,000)				
Time	**State**	**Mean**	**SD**	***p* value**
All Time (Mar 2020 – Dec 2022)	Indiana	29.13	37.69	< 0.001
	Washington	20.25	32.16	
2020 (Mar 2020 – Dec 2020)	Indiana	25.94	31.36	< 0.001
	Washington	10.46	11.32	
2021 (Jan 2021 – Dec 2021)	Indiana	30.67	26.53	< 0.001
	Washington	19.48	17.98	
2022 (Jan 2022 – Dec 2022)	Indiana	30.21	49.91	0.419
	Washington	29.47	48.62	

Note. The mean and standard deviation for each state in each analysis is listed, with the corresponding *p* values of each analysis.

Figure 1

Mean daily cases per 100,000 people and standard error of Indiana and Washington State for the years of 2020, 2021, 2022, and March 2020-December 2022.

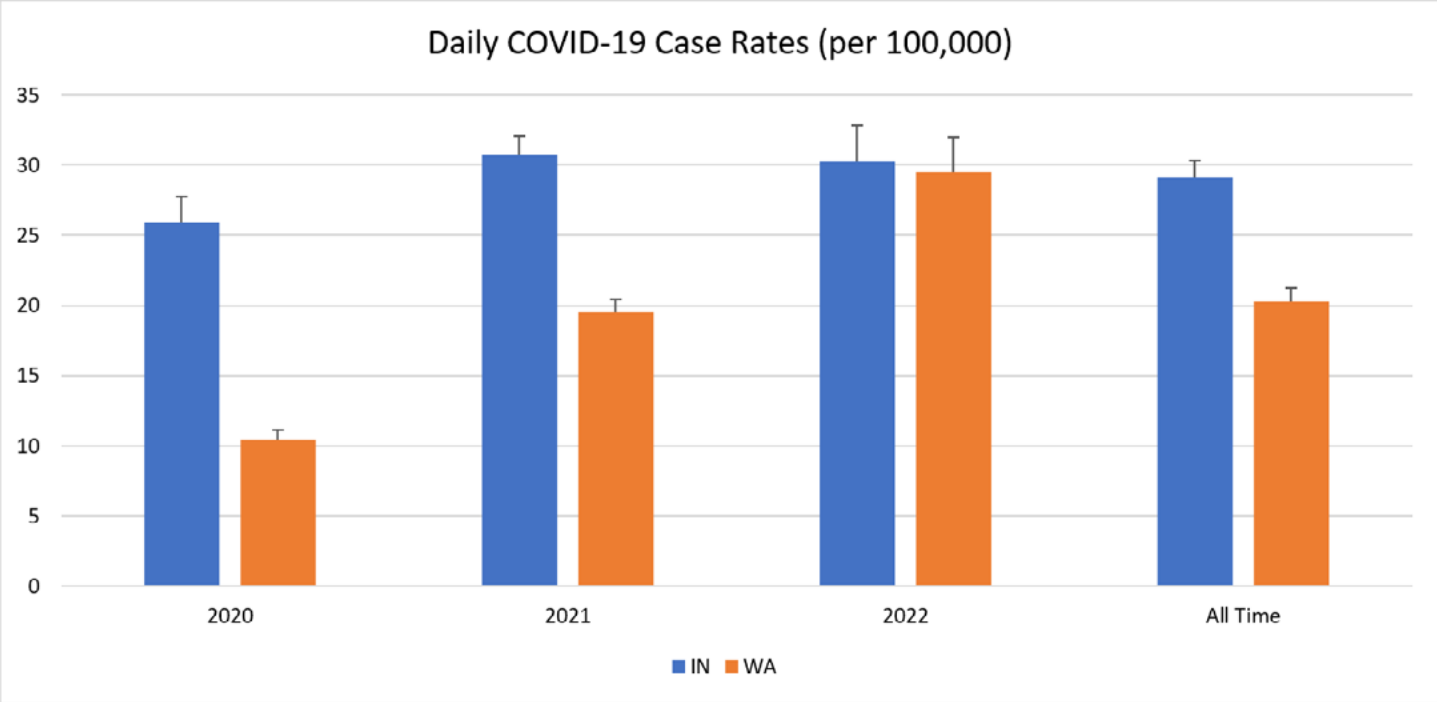

Note. The numerical results of the statistical analysis can be found in Table 1.

Table 2

Daily case rates standardized per 100,000 for each of the Delta and Omicron variant waves.

COVID-19 Variant Waves Case Rates (per 100,000)				
Time	**State**	**Mean**	**SD**	***p* value**
Delta (July 2021 – Sept 2021)	Indiana	37.96	19.34	< 0.001
	Washington	28.55	11.05	
Omicron (Dec 2021 – Feb 2022)	Indiana	102.08	73.01	0.048
	Washington	82.52	81.56	

Note. The mean, standard deviation, and p values are listed for each state in each of the analyses.

Figure 4

Mean daily cases and standard error for the Omicron and Delta variant waves standardized per 100,000 people.

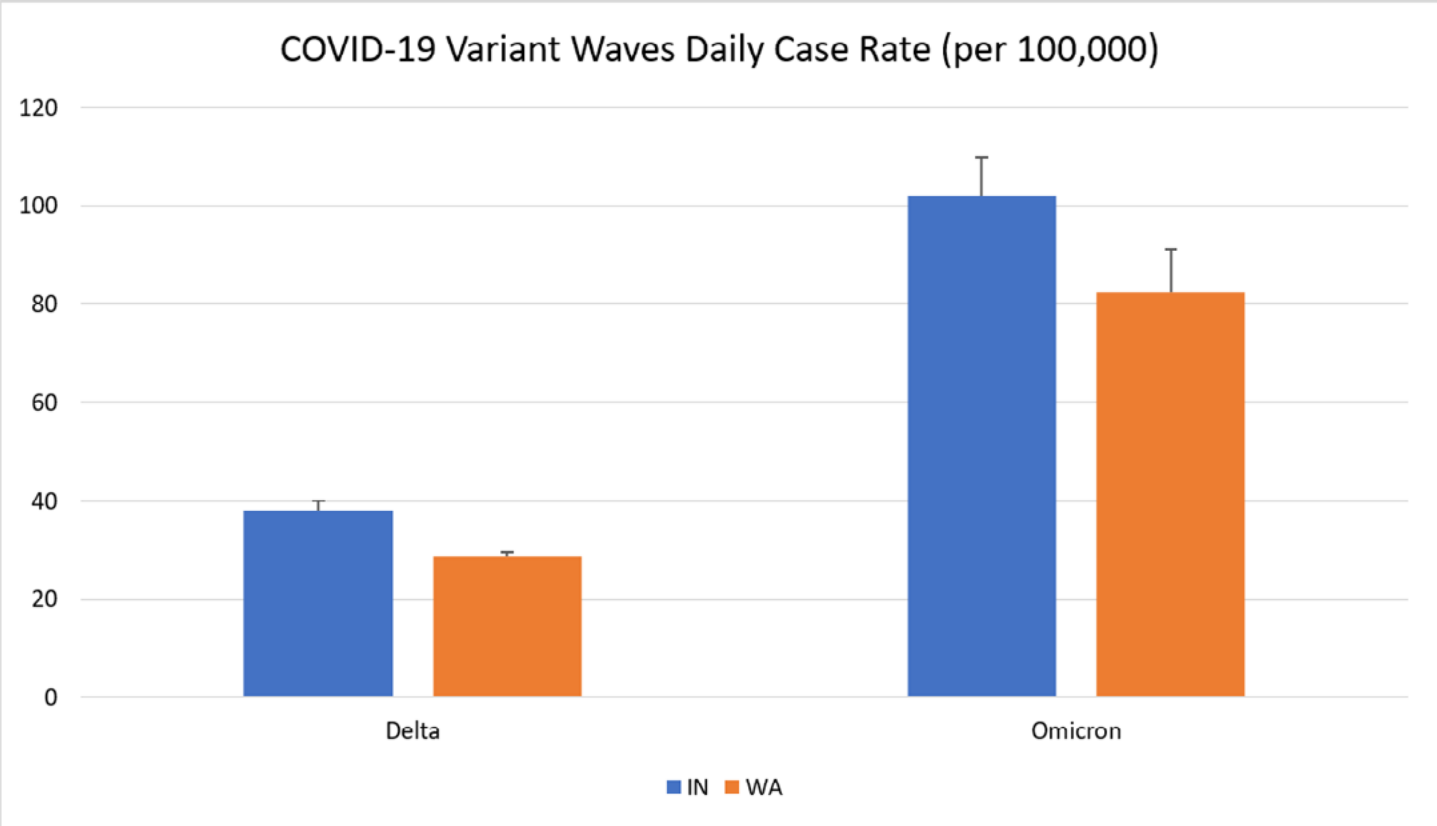

Note. Numerical results are shown in Table 2.

Table 3

Results from comparative analysis of daily cases for each of the winter/respiratory seasons standardized per 100,000 people

Winter/Respiratory Season Daily COVID-19 Case Rates (per 100,000)				
Time Period	**State**	**Mean**	**SD**	***p* value**
Flu Season 2021 (Dec 2020 – Mar 2021)	Indiana	43.04	33.57	< 0.001
	Washington	18.49	12.29	
Flu Season 2022 (Dec 2021 – Mar 2022)	Indiana	73.15	77.58	0.134
	Washington	62.01	77.62	

Note. The mean, standard deviation, and the corresponding *p* values for each analysis are listed.

Figure 5

Mean daily cases and standard error per 100,000 people reported for Indiana and Washington for the 2021-2022 and 2022-2023 winter/respiratory seasons.

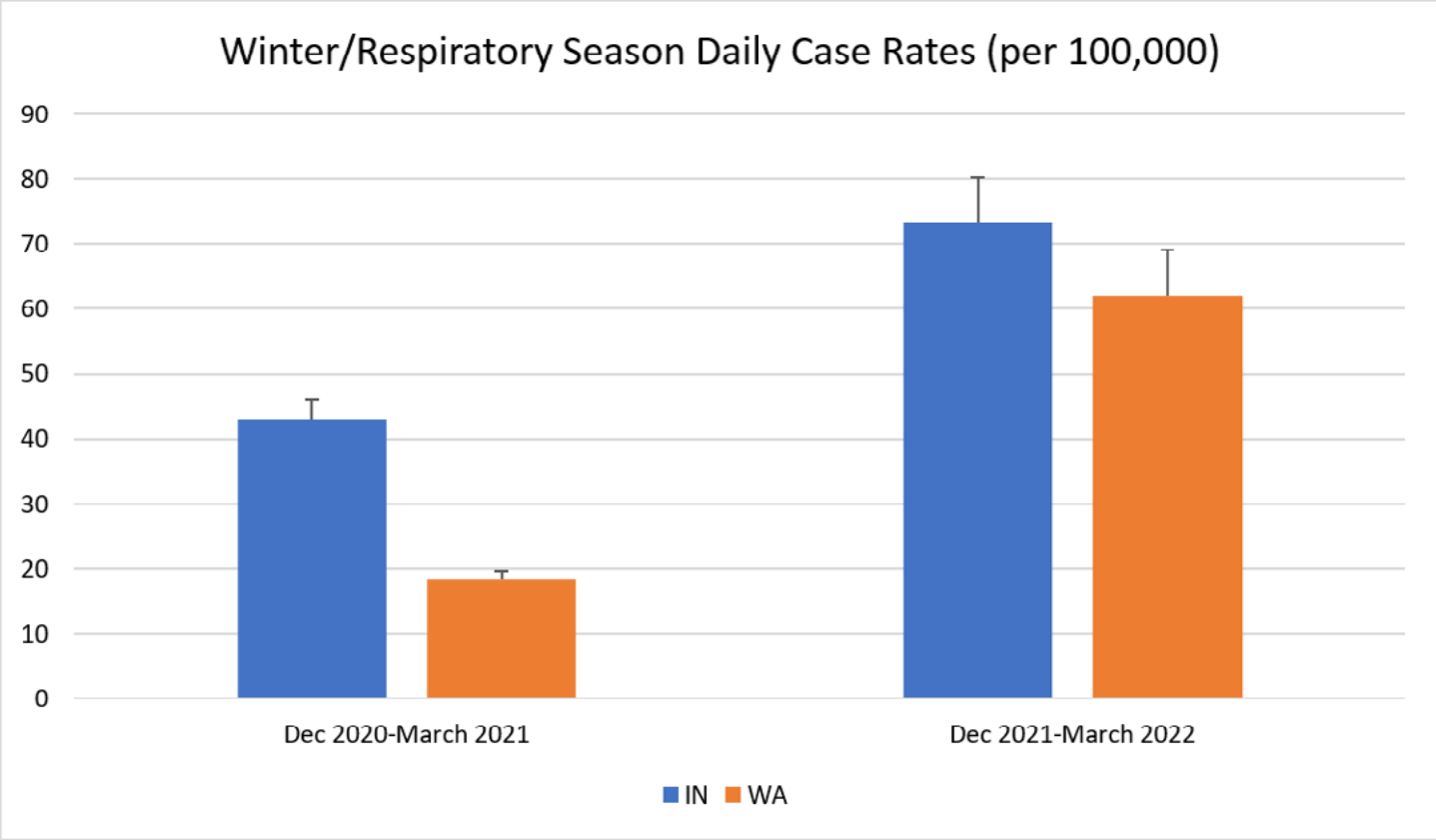

Note. Numerical results shown in Table 3.

Other Factors

Table 4

Vaccination rates for Indiana, Washington, and the total United States.

COVID-19 Vaccination Rates		
State	**Primary Series**	**Updated Booster**
Indiana	57.1%	10.4%
Washington	76.1%	24.5%
United States (total)	69.3%	16.3%

Note. Data is included for both the primary series and the updated booster. (10;17;43)

Table 5

Hospitalization and death rates and total hospitalizations and deaths from COVID-19 standardized per 100,000 people for Indiana, Washington, and the total United States.

COVID-19 Hospitalizations & Deaths		
State	**Hospitalization Rates**	**Hospitalizations (per 100,000)**
Indiana	7.64%	2391
Washington	4.23%	1070
United States (total)	5.84%	1860
State	**Death Rates**	**Deaths (per 100,00)**
Indiana	1.28%	388
Washington	0.81%	205
United States (total)	1.08%	337

Note. The hospitalization rates for each state were calculated by dividing the total number of COVID-19 hospitalizations by the total number of COVID-19 cases reported.

Table 6

Rural county data for Indiana, Washington, and the total United States

	Rural Counties	
State	**% of Rural Counties**	**% of Population in Rural Counties**
Indiana	78.3%	34%
Washington	51.3%	9.3%
United States (total)	65.2%	14%

Note. A rural county is defined using the Office of Management and Budget's definition of rural counties as an urban area less than 50,000 people (39). The percentage of rural counties was calculated by dividing the number of rural counties by the total number of counties. The percentage of population in rural counties was calculated by dividing number of inhabitants in the rural counties by the total state population.

Table 7

Public health funding data from Indiana and Washington state

	Public Health Funding		
State	**Funding per person (2019)**	**Funding per person (2021)**	**Public Health Ranking**
Indiana	$15	$15	40th
Washington	$46	$89	9th

Note. Data includes per person public health funding for 2019 and 2021 from State Health Compare (30 & 40).

Graphs

Figure 2

Maximum and minimum reported cases per 100,000 people per month from March 2020 to December 2022 in Indiana.

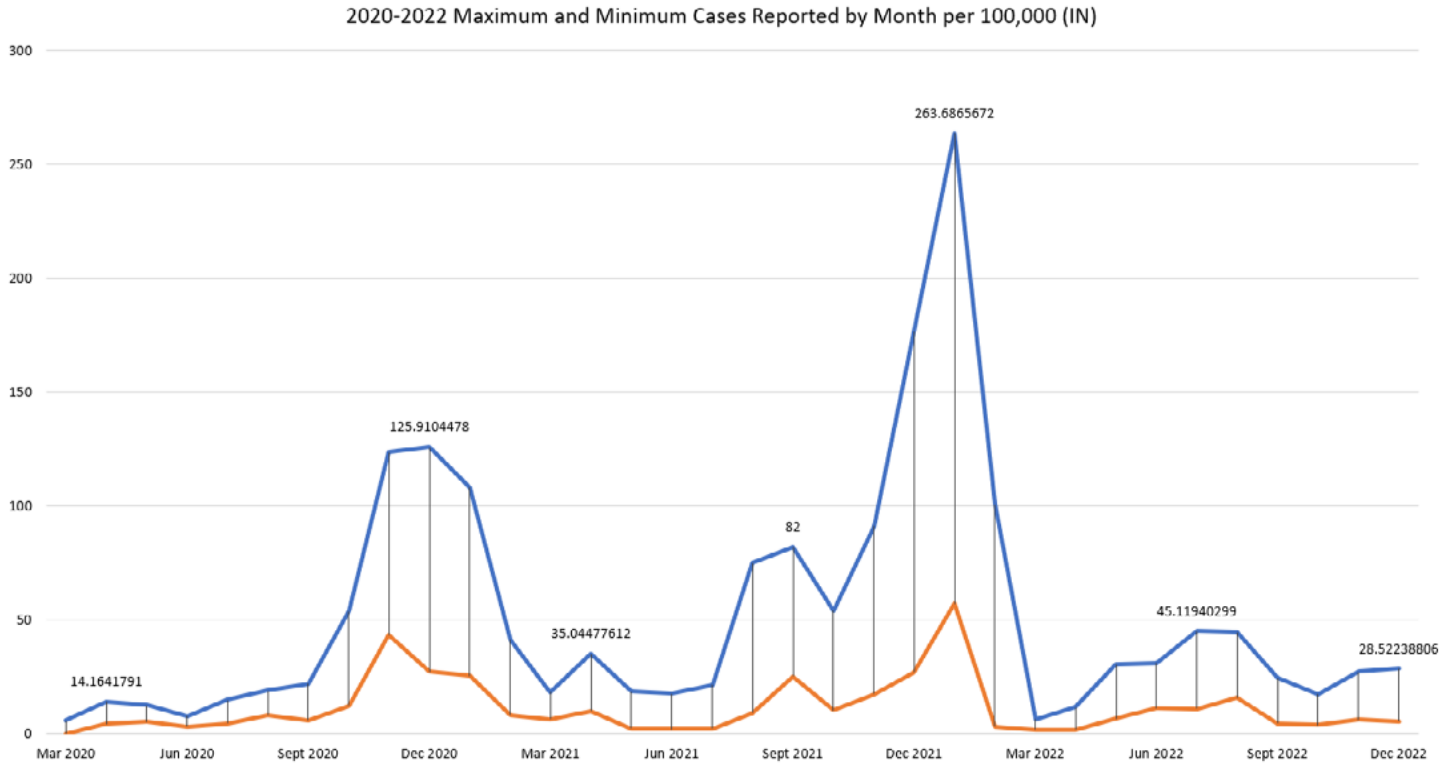

Discussion

The COVID-19 pandemic has had a severe impact on the global economy and on the lives of billions of people worldwide. The effects of this pandemic on healthcare systems and individuals will be seen for decades to come. A comparative analysis of daily cases from Indiana and Washington State and the effect of the implemented public health policies of each respective state were used to determine the best practices to mitigate disease for future public health emergencies. The mitigation strategies such as social distancing guidelines and face mask mandates implemented had a direct impact on the incidence and prevalence of COVID-19 cases. The implementation of such policies is crucial in reducing the spread of COVID-19 and mitigating the impact of the pandemic on society.

Health is multi-factorial, so it is difficult to pinpoint the exact cause of the differences in the cases between Indiana and Washington state; however, there are several factors that have been shown to impact the incidence and prevalence of disease which are directly applicable here. Tables 1, 2, and 3 demonstrate the general trend that Washington had a lower daily case incidence than Indiana, albeit insignificantly during the 2021-2022 winter/respiratory season (Table 3) and the 2022 calendar year (Table

Figure 3

Maximum and minimum reported cases per 100,000 people reported per month from January 2020 to December 2022 in Washington State

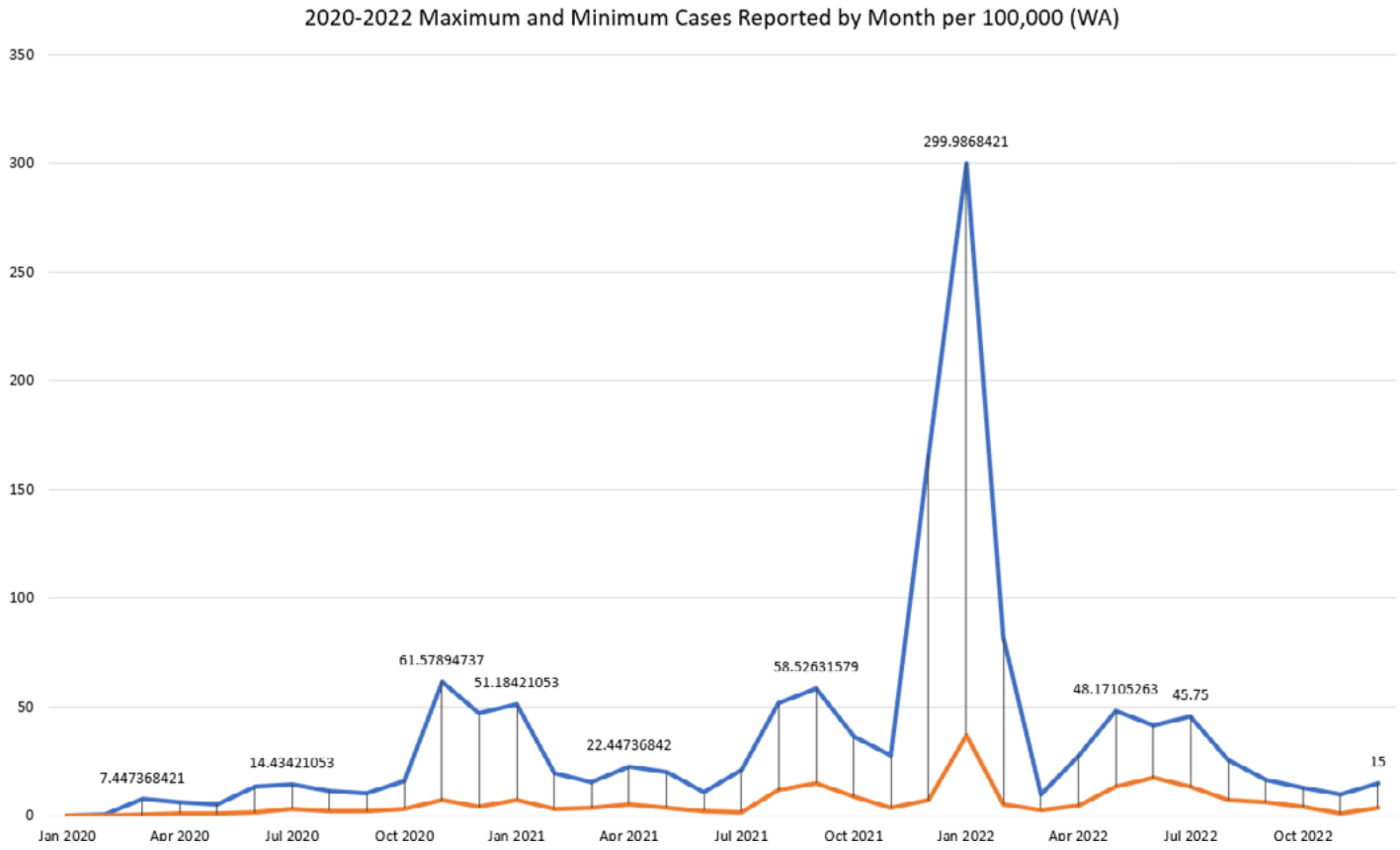

1). In addition to generally having a smaller daily case rate, Washington's peaks tended to have a shorter duration than Indiana's peaks during the different variant waves (Figure 4). The phrase "flattening the curve" was used in early 2020 to describe the intended effect of the mitigation strategies, and it is illustrated in the differences of the peaks (Figures 2 & 3). These states vary in the legislation and implementation of public health policies designed to mitigate the spread of disease; without such measures, morbidity and mortality would have likely been much higher.

The difference in the data could be largely attributed to the implementation of policies meant to reduce the transmission of disease (such as mask mandates and social distancing guidelines) and vaccination rates. Other factors contributing to the differences in data include public health funding which impacts access to healthcare (including testing sites), and education initiatives which combat the misinformation crisis. The combination of these factors ultimately helped dictate the course of the pandemic in each state.

Immunizations are used to prevent severe illness and death from infectious diseases, and the COVID-19 virus is no different. The first doses of the COVID-19 vaccine were administered to healthcare workers and first responders

in December 2020, with the general population receiving doses based on a roll-out schedule in early 2021. Washington had a primary series of vaccination rate of 76.1% (Table 4) and Indiana's primary series vaccination rate was 57.1% (Table 4). As vaccination prevents severe disease resulting in hospitalization or death, the hospitalization and death data was also analyzed (Table 5). In Washington, 4.23% of cases resulted in hospitalization and 0.81% of cases resulted in death, and 7.64% of cases in Indiana resulted in hospitalization and 1.28% of cases resulted in death (Table 4). Washington had 1070 hospitalizations per 100,000 people (Table 5) and Indiana had over twice that number with 2391 hospitalizations per 100,000 (Table 5). The higher rates of hospitalization and deaths are inversely correlated with vaccination rates; the greater percentage of the population that is vaccinated against the virus, the lower the hospitalization and death rates are.

Public health policies such as mask mandates, social distancing, and lockdowns were implemented to slow the spread of the virus. Although each individual policy is effective, the greatest outcome on the incidence and prevalence of cases was found to be a combination of such factors (23). In addition to the policies, the timing and duration of the policy implementation was also important – factors found to be notably influenced by political factors in the state, such as the partisanship of the state governor (1,2,5). Generally, Democratic governors tended to implement statewide mask mandates and stay-at-home orders sooner than their Republican counterparts, and they also tended to continue having these policies in place for a longer period (5). States which were quicker to implement policies and leave them in place for a longer duration saw a reduced incidence and prevalence in COVID-19 cases while states which were slower to implement policies and quicker to rescind them had the opposite effect (25). Washington tended to have a reduced incidence and prevalence of cases compared to Indiana (Table 1). Washington is Democratic-led and was the first state to implement any mitigation policies, and yet was one of the last states to rescind its mask mandate in 2022 (44) and had a smaller case incidence. Indiana is Republican-led and was one of the first states to rescind its mask mandate in early 2021 (21), less than one year after implementing it – a factor the higher daily case incidence can likely be attributed to.

Similarly, public health funding – which impacts the mitigation strategies implemented – is also influenced by partisanship of state government; Democratic-led states tend to allocate more funds toward public health and education, while Republican-led states tend to allocate funds away from public health (6). Public health funding is important in expanding access to healthcare facilities – including COVID-19 testing locations – but it is also critical in educating the public on various health topics and combatting misinformation. When misinformation is combatted through education initiatives, it leads to higher levels of vaccination and higher rates of adherence to mitigation strategies such as masking and social distancing (29). These concepts are demonstrated in each respective state; Washington has historically ranked high for public health, while Indiana has historically ranked low – according to the CDC,

Washington had a public health ranking of 9th in the country, while Indiana had a ranking of 40th (40). Furthermore, Washington's response to the pandemic included an 93% increase in state public health spending per person from 2019 to 2021 ($46/person and $89/person, respectively), while Indiana's state public health spending remained stagnant at $15 per person from 2019 to 2021 (30). These contrarieties in public health funding can be directly seen in the availability of COVID-19 testing sites statewide; Washington had over 1000 testing locations (43), while Indiana had 554 testing sites (16). The lack of accessibility of healthcare sites and testing facilities disproportionately affects rural areas – communities that historically tend to be underfunded, lack healthcare infrastructure, and have higher rates of poverty; these discrepancies which have been further highlighted by the COVID-19 pandemic (8). Rural counties have been shown to have higher rates of COVID-19 and lower vaccination rates – oftentimes due to misinformation and lack of education surrounding vaccines and public health (8). Indiana's low public health funding coupled with the state's rurality (Table 7) likely contribute to the higher incidence and illustrate the impact of accessibility of healthcare and education on case incidence and prevalence in a community.

While the general trend of data across the two states is that Indiana had a significantly higher daily case rate, the 2021-2022 winter/respiratory season (December 2021 – March 2022) (Table 3 & Figure 5), and the 2022 calendar year (Table 1 & Figure 1) are the exceptions with p values of 0.134 and 0.419, respectively. The commonality between these time frames is the peak of the Omicron variant wave, in which states were reporting cases of nearly 23,000 cases per day. The Omicron wave from early December 2021 to early February 2022 had the highest reported daily case counts throughout the course of the pandemic, with the mean (IN: 102.08; WA: 82.52, Table 2) being triple the mean of the Delta wave in mid-2021 (IN: 37.96; WA: 28.55, Table 2), and four times the mean of the entire dataset from March 2020 to December 2022 (IN: 29.13; WA: 20.25, Table 1). The number of cases reported during the nine-week long Omicron wave accounted for nearly thirty percent of all cases in the two-and-a-half-year duration of data, a significant percentage for such a short period of time. With the Omicron variant resulting in many asymptomatic infections, these numbers are probably vastly underreported as PCR tests were in short supply especially in states with limited testing; in addition, countless self-administered tests were not reported to the state health department.

The variation of the p values could be attributed to testing availability. Washington has about twice the amount of testing locations in comparison to Indiana, meaning that COVID tests are more available and accessible to everyone, including those in rural counties who may typically lack access to healthcare services (16, 43). During the peak of the Omicron wave, Washington state also increased access to testing due to the increased incidence and prevalence of cases, which ultimately led to higher reported cases during the wave and throughout the rest of 2022; Indiana presumably had similar case levels but due to lack of

testing accessibility, cases undoubtedly went untested, and therefore, unreported to the state. Increased access to testing sites allows individuals who are exposed to the virus or present with symptoms to be able to test without having to travel long distances.

In relation to this dataset, the omicron variant was the most transmissible variant, with an estimated basic reproduction number (R0) between 10 and 24 – almost triple that of the delta variant, which was estimated between 5 and 8 (11). The transmissibility of the omicron variant . The enhanced transmissibility and immune evasion cause rapid spread in communities; this sharp increase in cases is seen in Figures 2 and 3 which detail the highest and lowest reported daily cases of each month. In addition to its immune evasion properties, the omicron variant also causes more asymptomatic infections compared to other variants (11). Access to testing and healthcare facilities plays a critical role in catching these asymptomatic infections.

Despite the sociopolitical landscape of the state and the public perception of the disease, these policies – which are recommended by scientists and public health experts – should be implemented as soon as possible to curb new cases and prevent full-scale outbreaks, as well as mitigate the impact on society. The current trend of disseminating misinformation and rejecting evidence-based methods in government legislation is detrimental to the lives of countless individuals as well the effectiveness of mitigation strategies in future public health emergencies. If any lesson is to be learned from the death and disaster of the COVID-19 pandemic, it is that adequate public health funding and appropriate evidence-based policies implemented quickly are vital and essential to effectively reducing the morbidity and mortality of disease.

Author Correspondence

Correspondence concerning this article should be addressed to: Lillia G. Marble, lmarble@bsu.edu.

References

1. Adolph, C., Amano, K., Bang-Jensen, B., Fullman, N., & Wilkerson, J. (2021, April 1). Pandemic Politics: Timing State Level Social Distancing Responses to COVID-19. Journal of Health Politics, Policy and Law, 45(6), 997-1015. doi: 10.1215/03616878-8802162.

2. Adolph, C., Amano, K., Bang-Jensen, B., Fullman, N., Magistro, B., Reinke G., & Wilkerson, J. (2020, August 31). Governor partisanship explains the adoption of statewide mandates to wear face coverings. MedRxiv, 1-33.

3. Andrews, N., Stowe, J., Kirsebom, F., Toffa, S., Rickeard, T., Gallagher, E., Gower, C., Kall, M., Groves, N., O'Connell, A., Simons, D., Blomquist, P. B., Zaidi, A., Nash, S., Aziz, N. I. B. A., Thelwall, S., Dabrera, G., Myers, R., Amirthalingam, G., Gharbia, S., Barrett, J. C., Elson, R., Ladhani, S. N., Ferguson, N., Zambon, M., Campbell, C. N. Brown, K., Hopkins, S., Chand, M., Ramsay, M., Bernal, J. L. (2021, December 14). Effectiveness of COVID-19 vaccines against the Omicron (B.1.1.529) variant of concern. medRxiv, 2021.2012.2014.21267615. https://doi.org/10.1101/2021.12.14.21267615

4. Ao, D., Lan, T., He, X., Liu, J., Chen, L., B, D. T., Z, K., & W, X. (2022, March 16). SARS-CoV-2 Omicron variant: Immune escape and vaccine development. MedComm., 3(1), e126. https://doi.org/10.1002/mco2.126

5. Baccini, L., Brodeur, A. (2020, December 1). Explaining Governors' Response to the COVID-19 Pandemic in the Unites States. American Politics Research, 49(2), 215-220. doi: 10.1177/1532673X20973453.

6. Beland, L. & Oloomi, S. (2016, September 20). PARTY AFFILIATION AND PUBLIC-SPENDING: EVIDENCE FROM U.S. GOVERNORS. Economic Inquiry., 55(2), 982–995. https://doi.org/10.1111/ecin.12393

7. Burki, T. K. (2021, December 17). Omicron variant and booster COVID-19 vaccines. The Lancet Respiratory Medicine, 10(2). https://doi.org/10.1016/S2213-2600(21)00559-2

8. Capasso, A., Kim, S., Ali, A. H., Jones, A. M., DiClemente, R. J., & Tozan, Y. (2022, February 9). Socioeconomic predictors of COVID-19-related health disparities among United States workers: A structural equation modeling study. PLOS Global Public Health, 2(2). https://doi.org/10.1371/journal.pgph.0000117

9. Centers for Disease Control and Protection (2023, March 15). CDC Museum COVID-19 Timeline. David J. Spencer CDC Museum: In Association with the Smithsonian Institution. https://www.cdc.gov/museum/timeline/covid19.html#:~:text=January%2020%2C%20 2020,respond%20to%20the%20emerging%20outbreak.

10. Centers for Disease Control and Protection (2023). COVID-19 Vaccinations in the United States [Data Set]. CDC. https://covid.cdc.gov/covid-data-tracker/#vaccinations_vacc-people-fully-percent-total

11. Fan, Y., Li, X., Zhang, L., Wan, S., Zhang, L., & Zhou, F. (2022, April 28). SARS-CoV-2 Omicron variant: recent progress and future perspectives. Signal Transduction Target Therapy, 141. https://doi.org/10.1038/s41392-022-00997-x

12. Governor Jay Inslee. (2020, February 29). Inslee issues COVID-19 emergency proclamation. Retrieved April 5, 2023, from https://www.governor.wa.gov/news-media/inslee-issues-covid-19-emergency-proclamation

13. Guerra, F. M., Bolotin, S., Lim, G., Heffernan, J., Deeks, S. L., Li, Y., & Crowcroft, N. S. (2017, July 27). The basic reproduction number (R0) of measles: a systematic review. The Lancet. Infectious diseases, 17(12), e420–e428. https://doi.org/10.1016/S1473-3099(17)30307-9

14. Howard, J. (2022, February 11). While awaiting updated CDC guidance, here's the data states are using to lift COVID-19 restrictions. CNN Health. https://www.cnn.com/2022/02/11/health/covid-metrics-states-lifting-restrictions/index.html

15. Huang, J., Fisher, B. T., Tam, V., Wang, Z., Song, L., Shi, J., Rochelle, C. L., Wang, X., Morris, J. S., Coffin, S. E., & Rubin, D. M. (2022, February 16). The Effectiveness of Government Masking Mandates On COVID-19 County-Level Case Incidence Across The United States, 2020. Health Affairs, 41(3). https://doi.org/10.1377/hlthaff.2021.01072

16. Indiana Department of Health. (2023). Indiana COVID-19 Home Dashboard. https://www.coronavirus.in.gov/indiana-covid-19-dashboard-and-map/

17. Indiana Department of Health. (2023). Indiana COVID-19 Vaccination Dashboard. https://www.coronavirus.in.gov/vaccine/vaccine-dashboard/

18. Johns Hopkins Coronavirus Resource Center. Coronavirus COVID-19 global cases by the Center for Systems Science and Engineering. https://coronavirus.jhu.edu/map.html. Published 2020. Accessed October 1, 2023.

19. Karki, J. E. & Benmir, M. (2022, June 17). Chapter 9 – Some key concepts of mathematical epidemiology. Mathematical Analysis of Infectious Disease., 137-162. https://doi.org/10.1016/B978-0-32-390504-6.00014-0

20. Kim, D., Shinde, S., Lone, S., Ramasubba R. P., & Ghodake, G. (2021, November 23). COVID-19 Pandemic: Public Health Risk Assessment and Risk Mitigation Strategies. Journal of Personalized Medicine. 11. 1243. 10.3390/jpm11121243.

21. King, C. (2021, March 18). Our year of COVID: Key dates in Indiana's fight against the coronavirus. Indianapolis Star. https://www.indystar.com/in-depth/news/2021/03/18/indiana-covid-timeline-key-dates-states-fight-vs-pandemic/6813412002/

22. Kumar, A., Prasoon, P., Kumari, C., Pareek, V., Faiq, M. A., Narayan, R. K., Kulandhasamy, M., & Kant, K. (2020, October 21). SARS-CoV-2-specific virulence factors in COVID-19. Journal of Medical Virology, *93*(3), 1195-1836. https://doi.org/10.1002/jmv.26615

23. Li, K., Jarvis, S., & Minhas, F. (2021, July 1). Elementary effects analysis of factors controlling COVID-19 infections in computational simulation reveals the importance of social distancing and mask usage. Computers in Biology and Medicine, 134 doi:https://doi.org/10.1016/j.compbiomed.2021.104369

24. Mitchell, A., Jurkowitz, M., Oliphant, J. B., & Shearer, E. (2020, June 29). Americans rate CDC highly, Trump and his administration poorly on getting the facts right about COVID-19. Pew Research Center. https://www.pewresearch.org/journalism/2020/06/29/americans-rate-cdc-highly-trump-and-his-administration-poorly-on-getting-the-facts-right-about-covid-19/

25. Neelon, B., Mutiso, F., Mueller, N. T., Pearce, J. L., & Benjamin-Neelon, S. E. (2021, January 6). Associations between governor political affiliation and COVID-19 cases, deaths, and testing in the United States. medRxiv. https://doi.org/10.1101/2020.10.08.20209619

26. Petersen, E., Koopmans, M., Go, U., Hamer, D. H., Petrosillo, N., Castelli, F., Storgaard, M., Khalili, S. A., & Simonsen, L. (2020, July 3). Comparing SARS-CoV-2 with SARS-CoV and influenza pandemics. Lancet Infectious Disease., 20(9), e238-e244. https://doi.org/10.1016/S1473-3099(20)30484-9

27. Pew Research Center. (2020, August 27). Mask use increased in summer months. https://www.pewresearch.org/short-reads/2020/08/27/more-americans-say-they-are-regularly-wearing-masks-in-stores-and-other-businesses/ft_2020-08-27_maskwearing_01a/

28. Prior, C. (2014, August). Rural Indiana: A Demographic and Economic Overview. Indiana State University Rural-Urban Entrepreneurship Development Institute. https://www2.indstate.edu/news/pdf/2014-08_IN%20Rural_Counties_Economic_Overview.pdf

29. Roozenbeek, J., Schneider, C. R., Dryhurst, S., Kerr, J., Freeman, A. L. J., Recchia, G., van der Bles, A. M., van der Linden, S. (2020, July 6). Susceptibility to misinformation about COVID-19 around the world. R. Soc. Open Sci. 7: 201199. http://dx.doi.org/10.1098/rsos.201199

30. State Health Compare. (2021). Per person state public health funding map. https://statehealthcompare.shadac.org/map/117/per-person-state-public-health-funding#a/37/154

31. Substance Abuse & Mental Health Services Administration. (2023, January 4). 2021 National Survery on Drug Use and Health. https://www.samhsa.gov/data/report/2021-nsduh-detailed-tables

32. Thomas, L. (2021, February 22). An overview of spike protein antigen COVID-19 vaccine candidates. Medical News. https://www.news-medical.net/news/20210222/An-overview-of-spike-protein-antigen-COVID-19-vaccine-candidates.aspx

33. Trust for America's Health. (2022). State Profile: Indiana. https://www.tfah.org/state-details/indiana/

34. Trust for America's Health. (2022). State Profile: Washington. https://www.tfah.org/state-details/washington/

35. US Census Bureau. (2020). QuickFacts Indiana. https://www.census.gov/quickfacts/IN

36. US Census Bureau. (2020). QuickFacts Washington. https://www.census.gov/quickfacts/WA

37. US Census Bureau. (2020). 2020 Census Results. https://www.census.gov/programs-surveys/decennial-census/decade/2020/2020-census-results.html

38. US Department of Agriculture. (2007, September 4). Washington – Rural Definitions: State-Level Maps. https://www.ers.usda.gov/webdocs/DataFiles/53180/25602_WA.pdf?v=0

39. US Department of Health & Human Services. (2020, June 25). Defining Rural Population. https://www.hhs.gov/guidance/document/defining-rural-population#:~:text=Office%20of%20Management%20and%20Budget%20Definition&text=A%20Metro%20area%20contains%20a,(MSA)%20are%20considered%20rural.

40. US News & World Report. (2023). Best States 2023. https://www.usnews.com/news/best-states

41. Vanderpool, R. C., Gaysynsky, A., & Chou, W. S. (2020, October 1). Using a Global Pandemic as a Teachable Moment to Promote Vaccine Literacy and Build Resilience to Misinformation. https://doi.org/10.2105/AJPH.2020.305906

42. Wang, H. (2022, April 16). Estimating excess mortality due to the COVID-19 pandemic: a systematic analysis of COVID-19-related mortality, 2020-21. The Lancet, 399: 1513-36. https://doi.org/10.1016/S0140-6736(21)02796-3

43. Washington State Department of Health. (2023). COVID-19 Dashboard. https://doh.wa.gov/data-and-statistical-reports/diseases-and-chronic-conditions/communicable-disease-surveillance-data/respiratory-illness-data-dashboard

44. Washington State Department of Health. (2023, March 3). Masking requirements in healthcare, long-term case, and correctional facilities to end April 3. https://doh.wa.gov/newsroom/masking-requirements-healthcare-long-term-care-and-correctional-facilities-end-april-3#:~:text=OLYMPIA%20%2D%2D%20Effective%20April%203,people%20age%205%20and%20older.

45. 270 to Win. (2020). Indiana. https://www.270towin.com/states/Indiana

46. 270 to Win. (2020). Washington. https://www.270towin.com/states/Washington

Appendix

Indiana and Washington dataset available at https://doi.org/10.33043/FF.10.1.38-57

Positive effects of *Moringa oleifera* and *Moringa stenopetala* seed and leaf extracts against selected bacteria

Grace J. Miller[1]
Kaley Necessary[2]
Robert Burchell [2]
Yui Iwase[2]
Nicole L. Lautensack[2]
Blake Russell[2]
Erik G. Holder[2]
Emma E. Knee[2]
W. Matthew Sattley[2]
[1] **School of Natural and Applied Sciences, Taylor University, Upland, IN**
[2] **Division of Natural Sciences, Indiana Wesleyan University**

Keywords: *Moringa oleifera*, *Moringa stenopetala*, antibacterial, plant extract, disk diffusion test, minimum inhibitory concentration, medicinal plant

Manuscript received 19 February 2023; accepted 11 April 2023

Fine Focus, 10(1), 58-73. doi: 10.33043/FF.10.1.58-73.

Abstract

Moringa oleifera is hailed as the "miracle tree" for its impressive catalog of nutritional, medicinal, and water purification benefits. A (sub)tropical plant with a rapid growth rate (3–5 m in a single season), *Moringa* has proven beneficial in multiple ways in developing regions around the world. In addition to its high nutrient content and water clarifying properties, *Moringa* seed and leaf extracts have shown potential as natural antibacterial agents. Based on this, we anticipated that extracts from multiple species of *Moringa* would exhibit potentially useful antibacterial properties against a range of bacterial species. To explore this, both disk diffusion and minimum inhibitory concentration (MIC) culture techniques were employed to assess the inhibitory effects of seed and leaf extracts from *M. oleifera* and *M. stenopetala* against species of bacteria commonly used in research and teaching laboratories. Aqueous seed extracts from both *Moringa* species showed broad-spectrum activity but were especially effective at inhibiting the growth of Gram-positive bacteria, including species of *Staphylococcus*, *Streptococcus*, and *Bacillus*. *Moringa* leaf extracts also exhibited antibacterial activity, with ethanolic leaf extracts showing greater efficacy than aqueous leaf extracts in disk-diffusion assays. Temporary acidification (1 h at pH 2) of *Moringa* seed and leaf extracts had a detrimental effect on their antibacterial activity. MIC assays using *Moringa* leaf extracts also showed more pronounced inhibition of Gram-positive bacteria (MIC = 12.5% v/v) versus Gram-negative species (MIC = 25% v/v). These results are of particular relevance in tropical areas where pharmaceutical drugs are scarce but *Moringa* is widely available and often used as a nutritional supplement. Moreover, the rising threat of multi-drug resistant pathogens lends greater importance to the study of antibacterial plant products that ultimately may find application in the clinical setting.

Introduction

Recent explorations in herbal medicine among the scientific community have shown potential for the development of new antimicrobial products from various plant species for use in both developing regions having little access to pharmaceutical drugs and in developed areas that have experienced a rise in bacterial infections caused by antibiotic-resistant strains (2, 3, 4, 7, 17, 28, 30). One such medicinal plant that has experienced a degree of commercialization in recent years is *Moringa oleifera* (also called the "horseradish tree," "drumstick tree," and, more recently, the "miracle tree"), a drought-resistant and rapidly growing tree species native to India but which is now widespread in tropical and subtropical regions around the world. Growing to a maximum height of about 12 m but usually pruned yearly to ease harvesting, the use of *M. oleifera* leaves as a nutritional supplement and herbal medicine has been well documented (12, 15, 23, 24, 25, 27). *M. oleifera* leaf powder contains unusually high levels of protein, iron, calcium, magnesium, potassium, several vitamins (e.g., β-carotene and vitamins B_2, B_6, and C), and dietary fiber and other complex carbohydrates (15). Because of this, *M. oleifera* products have been incorporated into feeding programs where malnutrition is prevalent. *M. stenopetala* also has an unusually high nutrient content, but as this species occurs only in northeastern tropical Africa, the use of *M. stenopetala* as a nutritional supplement is limited mainly to regions in which the plant is indigenous (19).

In addition to their nutritional benefits, the potential of *Moringa spp.* as new sources of antimicrobial products is becoming more widely recognized (5, 8, 11, 20, 22, 27, 29). Extracts of seeds and leaves of *Moringa spp.* exhibit antibacterial properties through direct inhibition of growth in culture-based experiments. As has been shown using leaf extracts in experiments with *Xanthomonas campestris* (13) and *Erwinia amylovora* (14), this inhibition is primarily due to the production of compounds that compromise the structural integrity of the cytoplasmic membrane. Several decades ago, Eilert et al. (9) described both antibacterial and antifungal activity of *Moringa* extracts and identified 4-(a-L-rhamnosyloxy) benzyl isothiocyanate as an active compound in aqueous preparations. However, other compounds, including phenolic acids, flavonoids, and alkaloids, likely also contribute to the antibacterial activity of these extracts (13). Manilal et al. (20) recently showed antibacterial activity of *Moringa stenopetala* extracts on par with clindamycin and vancomycin controls against clinical isolates of methicillin-resistant *Staphylococcus aureus* (MRSA), and several other studies have shown inhibitory activity of *Moringa* extracts against a variety of human pathogens, including *Proteus mirabilis*, *Helicobacter pylori*, and *Bacillus cereus* (5, 11, 20, 27). Although documentation of the antibacterial activity of *Moringa* seed and leaf extracts is expanding, the clinical potential of these natural products is unknown, and further testing of these materials is both prudent and needed.

Based upon studies from other research groups and our own observations (21), we predicted that crude seed and leaf extracts from multiple species of *Moringa* would exhibit broad-spec-

trum activity against a variety of bacterial species. To test this prediction, we compared the growth-inhibitory activity of aqueous seed extracts and both aqueous and ethanolic leaf extracts from two *Moringa* species, *M. oleifera* and *M. stenopetala*, against selected species of Gram-positive and Gram-negative bacteria, some of which are known to cause opportunistic infections. In addition, the minimum inhibitory concentration (MIC) of aqueous *Moringa* leaf extracts was determined for several species of Gram-positive and Gram-negative bacteria. Finally, as *Moringa* leaves and seeds are commonly consumed as dietary supplements and could potentially have an inhibitory effect on susceptible members of the intestinal microbiota, we have simulated passage of these plant products through the stomach by testing the effect of a temporary shift to acid pH on the antibacterial activity of both aqueous and ethanolic *Moringa* extracts. Abolishment of the antibacterial efficacy of *Moringa* extracts following exposure to low pH would suggest that these plant products can be consumed for nutritional purposes without concern that the composition of the gut microbiota would be detrimentally or otherwise affected.

Materials and Methods

Bacterial Cultures

Species of bacteria used in this study consisted of strains commonly employed in general microbiology teaching laboratories. Gram-positive species included *Bacillus cereus* (ATCC 14579), *Staphylococcus aureus* (ATCC 29213), *Enterococcus durans* (ATCC 6056), *Corynebacterium xerosis* (ATCC 373), *Listeria monocytogenes* (ATCC 15313), *Streptococcus agalactiae* (ATCC 13813), and *Micrococcus luteus* (ATCC 4698). Gram-negative test bacteria included *Proteus vulgaris* (ATCC 6380), *Yersinia kristensenii* (ATCC 33639), *Serratia liquefaciens* (ATCC 27592), and *Escherichia coli* (ATCC 25922). Source cultures of all bacteria used to inoculate experimental media were routinely grown in BD Bacto™ tryptic soy broth (Becton, Dickinson and Company) at pH 7 and 37 °C.

Moringa Seed and Leaf Extract Preparation

Seeds of *Moringa oleifera* and *Moringa stenopetala* used in this study were obtained from Educational Concerns for Hunger Organization (ECHO; www.echonet.org, Fort Myers, Florida, USA). Leaves from each *Moringa* species were obtained from plants propagated from seeds in our laboratory. To obtain the seed extracts, the dried *Moringa* seed pods were husked by hand, revealing the small, white pit in each pod. The seeds were then ground into a fine powder using a mortar and pestle.

For preparation of *Moringa* seed extracts, 3 g of the powdered seed were combined with 15 ml of warm (60 °C) ddH2O and mixed by hand for 5 minutes using a glass rod. The slurry was then transferred to tubes and placed in a centrifuge at 3000 rpm for 10 minutes at room temperature. After centrifugation, the supernatant was extracted using a micropipette and vacuum filtered to remove any remaining suspended particles. The vacuum-filtered extract was then sterilized by pushing through a 0.45 μm cellulose acetate (CA) membrane filter into a sterile petri dish.

Moringa leaves used for extract preparation were washed and dried thoroughly prior to processing. Leaf extracts from *Moringa spp.* were obtained by macerating 12 g of leaf tissue in 20 ml ddH_2O. This slurry was then filtered through five layers of cheesecloth into two 15 ml conical tubes, which were placed in a centrifuge at 3000 rpm for 10 min. For each *Moringa* species, the leaf extract supernatant was collected, and 10 ml were filtered through a 0.45 μm CA membrane filter into a sterile 17 ml test tube. Preparation of the ethanolic leaf extracts was the same as water extraction except that the ddH_2O was replaced with 20 ml of 70% ethanol.

Disk Diffusion Assays

Using ethanol-flamed forceps, pre-sterilized blank disks (6 mm in diameter; Becton, Dickinson and Company) were aseptically placed in Petri dishes that contained a single, sterile plant extract (either *M. oleifera* or *M. stenopetala* seed or leaf extract) in order to test for antibacterial activity using a modification of the disk-diffusion method described by Bauer et al. (6). Other Petri dishes used for soaking blank disks contained either filter-sterilized ddH_2O or 70% ethanol to be used as negative controls. All disks were soaked for 15 min before experimental use.

To perform the disk diffusion plate assays, each species of bacteria was inoculated onto the entire surface of triplicate plates of Difco™ Mueller-Hinton agar. Plates were inoculated from fresh tryptic soy broth cultures (OD_{600} of 0.05) of each bacterial species using pre-sterilized cotton swabs that had been inserted into the cultures and spread in multiple directions on the agar surface to produce a "lawn" of bacterial growth after incubation. Disks containing either crude *Moringa* extract or sterile solvent (either ddH_2O or 70% ethanol, depending on the experiment) were placed on the inoculated plates in labeled quadrants using ethanol-flamed forceps. Four disks were placed on each agar plate: 1) a disk impregnated with *M. oleifera* seed or leaf extract; 2) a disk impregnated with *M. stenopetala* seed or leaf extract; 3) a disk infused with 30 μg of the broad-spectrum antibiotic tetracycline (Becton, Dickinson and Company) as a positive control; and 4) a disk containing only sterile solvent (i.e., no *Moringa* extract) as a negative control. Once in place, the disks were pressed gently into the agar surface with the forceps to ensure they would not move or become detached when inverted for incubation. All test plates were incubated at 37 °C for 24 h.

Following incubation, antibacterial activity was assayed by measuring the diameter (to the nearest mm) of zones of inhibition around the disks on each plate culture. Measurements of zones of inhibition shown in each graph are averages of triplicate cultures for each bacterial species tested and are expressed as the mean ± standard error. Statistical significance ($P \leq 0.05$) determinations of growth inhibition among tested groups and controls were performed using one-way analysis of variance (ANOVA) followed by Tukey's honest significant difference (HSD) test.

To simulate and test the effect of oral ingestion of *Moringa* leaf and seed products on antibacterial activity, we subjected both aqueous and ethanolic *Moringa* extracts to temporary acidification. For this procedure, the pH of

each extract was dropped to pH 2 using a sterile solution of 1 M HCl. After 1 h at room temperature (~23 °C), the pH of each extract was raised to neutral (pH 7) using sterile 1 M NaOH. Sterile blank disks were then soaked in the extracts, and disk diffusion experiments were conducted as described above.

Minimum Inhibitory Concentration (MIC) Assay

MIC assays were performed in triplicate using *Moringa oleifera* aqueous leaf extract. Ten test tubes were used for each MIC experiment, with tube 1 initially containing 10 ml of 100% crude *Moringa* leaf extract (obtained as described above) and tubes 2–10 containing 5 ml sterile tryptic soy broth (TSB). A serial dilution was then performed in which 5 ml of leaf extract from tube 1 was aseptically transferred to tube 2, producing a 1:2 dilution. After mixing well, 5 ml from tube 2 was transferred to tube 3 and mixed. Dilutions continued in this way through tube 9. After mixing, 5 ml was removed from tube 9 and discarded. This resulted in all 10 tubes having a final volume of 5 ml, with tube 1 containing 100% *Moringa* extract, tubes 2–9 containing two-fold decreasing concentrations of extract, and tube 10 serving as a control containing 100% TSB (i.e., no extract). All ten tubes were then inoculated with a test species of bacteria using a loop (a different 10-tube set was required for each species of bacteria tested for all three trials).

After a 24-h incubation (unshaken) at 37 °C, growth in each of the tubes was assessed by visual inspection for turbidity, and the MIC for each bacterial species was recorded as the tube containing the highest dilution of extract that showed no growth. The recorded MIC was confirmed by transferring a portion of the contents of each tube onto separate plates of tryptic soy agar (TSA) by streaking for isolation and checking for growth after incubation (37 °C for 24 h).

Results and Discussion

Antibacterial Activity of Aqueous *Moringa* Seed Extracts

In recent years, several studies have demonstrated the antibacterial activity of extracts from various species of *Moringa*, especially *Moringa oleifera* (5, 8, 11, 13, 14, 16, 18, 20, 21, 24, 26, 29). In agreement with these reports, most of which employed extracts from a single *Moringa* species against one or a few species of bacteria, we observed antibacterial activity of seed extracts made from two different *Moringa* species against a diversity of both Gram-positive and Gram-negative bacteria, some species of which, to our knowledge, have not been included in previous studies (e.g., *Enterococcus durans*, *Yersinia kristensenii*, *Serratia liquefaciens*, *Streptococcus agalactiae*, and *Corynebacterium xerosis*).

Disk diffusion assays showed that aqueous seed extracts of both *M. oleifera* and *M. stenopetala* inhibited the growth of a wide variety of bacteria, with Gram-positive bacteria being especially susceptible. Zones of inhibition from *Moringa* seed extracts against *Staphylococcus aureus* were equal in size (~22 mm) to zones of inhibition produced by a tetracycline control disk (a zone of inhibition of >22 mm for *Staphylococcus* spp. indicates susceptibility to tetracycline based on data from the European Committee on Antimicrobial Susceptibility Testing [10]).

Growth inhibition by *Moringa* extracts against other Gram-positive cocci, including *Streptococcus agalactiae* and *Micrococcus luteus*, produced zones of inhibition that were of similar size (20–25 mm) to those observed with *S. aureus* (Figure 1). For *Bacillus cereus*, an endospore-forming Gram-positive rod, the sizes of the observed zones of inhibition by *Moringa* seed extracts indicated significant growth inhibition ($P = 1.6 \times 10\text{-}6$) and actually exceeded that from tetracycline at about 20 mm versus 13 mm, respectively (Figure 1). Another opportunistic Gram-positive rod, *Listeria monocytogenes*, was also inhibited by seed extracts from both *Moringa* species. However, with zones of inhibition having an average diameter of 16 mm versus 30 mm, the antibacterial effect of the *Moringa* extracts was less than that observed with the tetracycline control (Figure 1).

Although an inhibitory effect was still evident against them, Gram-negative bacteria as a whole showed less sensitivity to aqueous *Moringa* seed extracts than Gram-positive bacteria. The four Gram-negative bacteria tested were all of the family *Enterobacteriaceae*. Of these species, *Proteus vulgaris*, an opportunistic pathogen often responsible for urinary tract infections, had the largest zones of inhibition (~15 mm) and was significantly affected ($P = 4.6 \times 10\text{-}6$) by the *Moringa* seed extracts (Figure 1). By contrast, *Escherichia coli*,

Figure 1

Antibacterial activity of aqueous seed extracts of Moringa oleifera *and* Moringa stenopetala *against selected mostly Gram-positive bacteria, as compared to tetracycline and sterile water controls.*

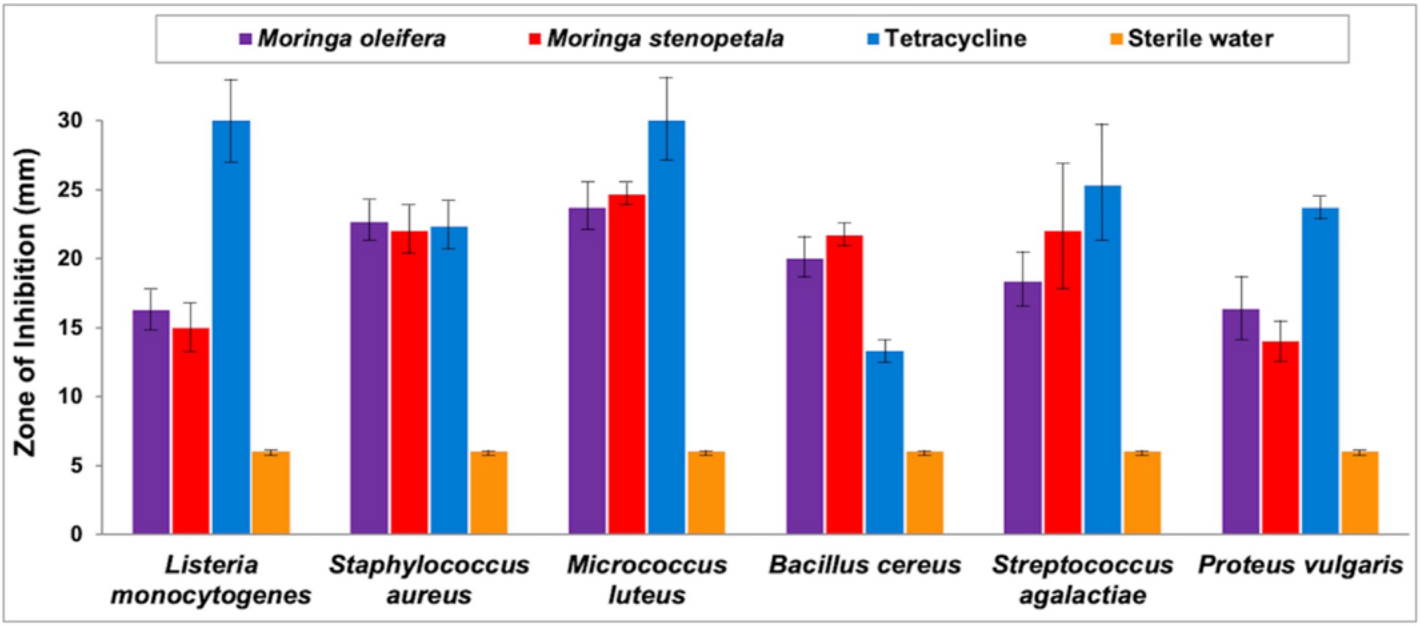

Note. The average sizes (from triplicate samples) of zones of inhibition on disk diffusion plate assays are shown. A measurement of 6 mm is a baseline representing the diameter of the disks themselves and equates to no visible zone of inhibition.

Serratia liquefaciens, and *Yersinia kristensenii* exhibited no significant susceptibility ($P > 0.05$) to the *Moringa* extracts over the sterile water control (data not shown). As was observed with the Gram-positive bacteria, there was no significant difference ($P > 0.05$) between the antibacterial activity of *Moringa oleifera* seed extract versus that of *Moringa stenopetala*.

Antibacterial Activity of *Moringa* Leaf Extracts

In addition to testing the antibacterial activity of *Moringa* seed extracts, we also collected and tested the potential for bacterial growth inhibition using both aqueous and ethanolic leaf extracts. Although a significant ($P \leq 0.05$) effect was observed over sterile water controls (Figure 2A), inhibition of bacterial growth by aqueous leaf extracts was less pronounced than that observed from aqueous seed extracts. This may be due to the antibacterial constituents being more concentrated in the seed extracts than in the leaf extracts, although other explanations, such as differences in the effectiveness of the extraction methods, are also possible.

For the Gram-positive bacteria tested, zones of inhibition around tetracycline control disks were approximately twice as large in diameter as zones of inhibition using *Moringa* leaf extracts, which ranged from 12–16 mm in diameter (mean = 13 mm) for both *Moringa* species (Figure 2A). As was the case using seed extracts, the inhibitory effect of the leaf extracts was generally less pronounced against the Gram-negative bacteria tested, which had zones of inhibition ranging from 7–11 mm in diameter (data not shown).

To potentially augment the antibacterial effect of the *Moringa* leaves, we repeated the test using ethanolic rather than water-based leaf extracts. Against the same bacteria, ethanolic *Moringa* leaf extracts produced larger zones of inhibition and, thus, a greater antibacterial effect than observed with water extraction. Other studies have shown a similar increase in antibacterial activity of ethanolic over aqueous *M. oleifera* extracts, and Hagos et al. observed greater antibacterial activity from methanol extraction over water extraction of *M. stenopetala* leaves (16, 26, 31). In the present study, sizes of the zones of inhibition using ethanolic leaf extracts from both *Moringa* species were similar and had average diameters ranging from 12–21 mm (mean = 17 mm) (Figure 2B), resulting in an approximately 30% increase in efficacy over aqueous leaf extracts.

Effect of Acidification on the Antibacterial Activity of *Moringa* Seed and Leaf Extracts

Moringa seed pods and leaves can be an important nutritional supplement for peoples living in tropical and subtropical regions around the world (15, 23). Although considerable work has been done to characterize the nutritive properties of *Moringa* products when prepared in various ways for human consumption (15), to our knowledge, the potential effect of ingestion—and in particular the temporary acidification that occurs during passage through the stomach—on the antibacterial properties of *Moringa* has not been investigated.

In testing the effect of low pH on the antibacterial properties of *Moringa* extracts, a significant decrease ($P \leq 0.05$) in antibacterial activity occurred against most species and under most conditions as a result of temporary acidification.

Figure 2

Antibacterial activity of A) aqueous Moringa *leaf extracts, and B) ethanolic* Moringa *leaf extracts against selected Gram-positive bacteria, as compared to tetracycline and sterile solvent (ddH_2O for part A; 70% ethanol for part B) controls.*

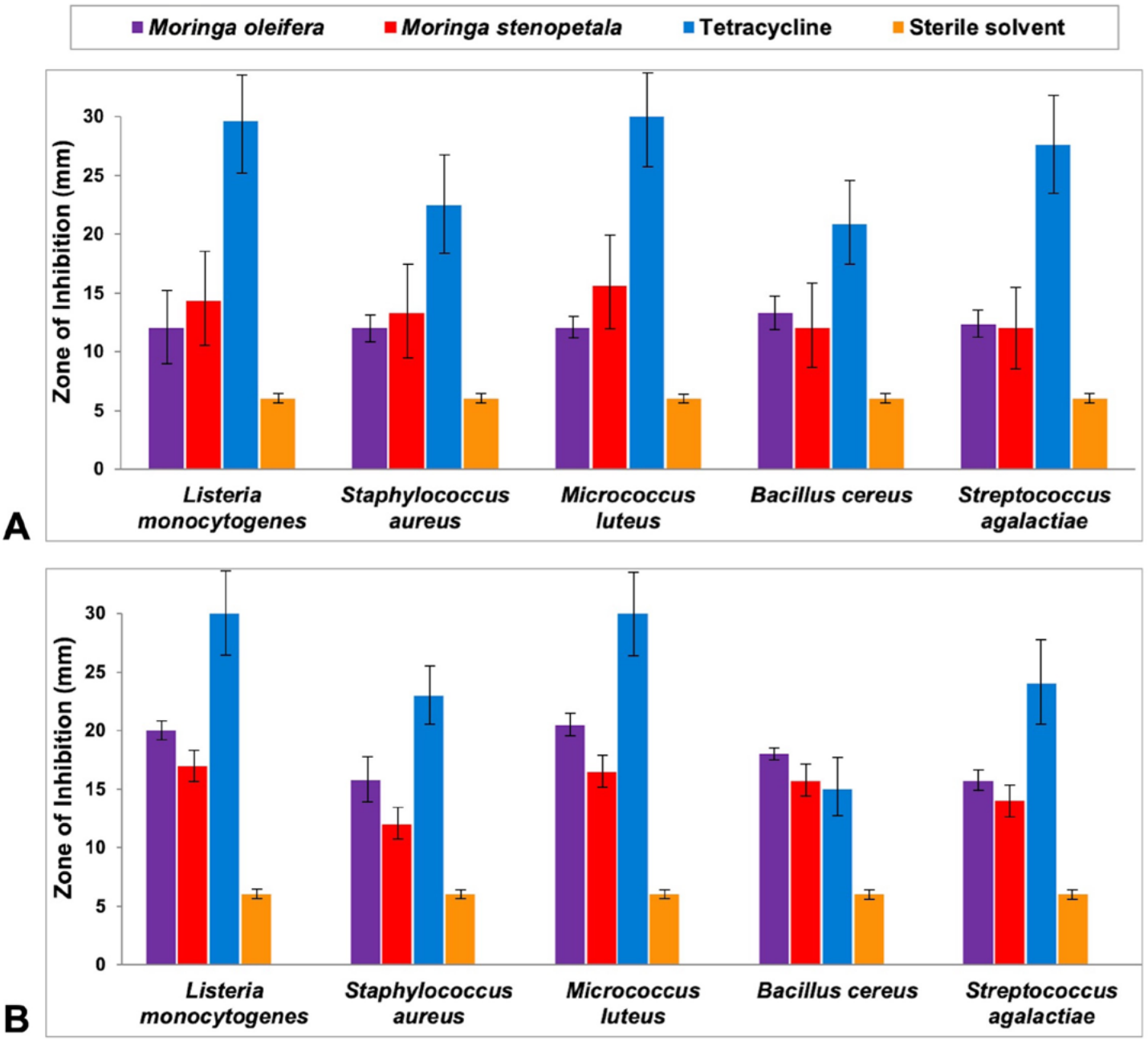

Note. The average sizes (from triplicate samples) of zones of inhibition on disk diffusion plate assays are shown. A measurement of 6 mm is a baseline representing the diameter of the disks themselves and equates to no visible zone of inhibition.

As aqueous seed extracts and ethanolic leaf extracts both showed strong antibacterial activity in previous experiments, we limited testing to these preparations from both *M. oleifera* and *M. stenopetala* against a selection of Gram-positive and Gram-negative bacteria.

After 1 hour at pH 2 (23 °C), activity against the tested Gram-positive bacteria was significantly ($P \leq 0.05$) diminished, and in several cases entirely abolished, for aqueous seed extracts of both *M. oleifera* and *M. stenopetala* versus the untreated (nonacidified) control extract (Figure 3A, B). The same trend was observed for the seed extracts against the tested Gram-negative bacteria; in every case, antibacterial activity was severely diminished or entirely absent after the acidification treatment (Figure 3C, D). Similarly, with the exception of *Staphylococcus aureus* among the Gram-positive bacteria (Figure 3E) and *Escherichia coli* among the Gram-negative bacteria (Figure 3G), acidification of *Moringa* ethanolic leaf extracts consistently produced smaller zones of inhibition around the test disks compared to the untreated controls (Figure 3E–H). Against the Gram-negative bacteria in particular, zones of inhibition were entirely absent around most of the disks containing acid-treated extracts (Figure 3G, H).

These results suggest that antibacterial constituents occurring in seeds and leaves of *Moringa spp.* are acid-labile and are likely broken down by digestive chemicals of the stomach when ingested (1, 9, 12). This brings into question the curative potential of ingested natural *Moringa* seed and leaf products for the treatment of gastrointestinal bacterial infections, such as gastric ulcers caused by *Helicobacter pylori* [even if antibacterial activity has been demonstrated in vitro (11)], and is a topic warranting further study.

MIC Assays Using *Moringa* Leaf Extracts

The results of minimum inhibitory concentration (MIC) assays confirmed the antibacterial effect of *Moringa* leaf extracts. Crude aqueous leaf extracts from *M. oleifera* inhibited the growth of all bacteria tested to varying degrees. As with the disk diffusion test, the MIC assays showed that Gram-positive bacteria were generally more susceptible to the inhibitory effect of *M. oleifera* leaf extracts, with most species showing susceptibility at >50% dilution of crude extract (Table 1). A representative MIC preparation is shown in Figure 4. Only two of the four Gram-negative bacteria tested (*P. vulgaris* and *Y. kristensenii*) were inhibited beyond a 50% dilution of crude leaf extract, and no Gram-negative species were inhibited beyond a 25% dilution (Table 1).

Conclusions

The results of this study and others cited in this report show that seed and leaf extracts of multiple species of the fast-growing, tropical to subtropical tree *Moringa* exhibit clear antibacterial properties. Both disk diffusion and MIC assays indicated that among the species tested, Gram-positive bacteria were more susceptible to *Moringa*-derived antibacterial compounds than were Gram-negative bacteria, possibly due to the presence of an outer membrane in the cell wall of the latter. Moreover, this work presents evidence that the antibacterial components of crude *Moringa* extracts are acid-labile and

Figure 3

Effect of acidification on the antibacterial activity of Moringa *seed and leaf extracts.*

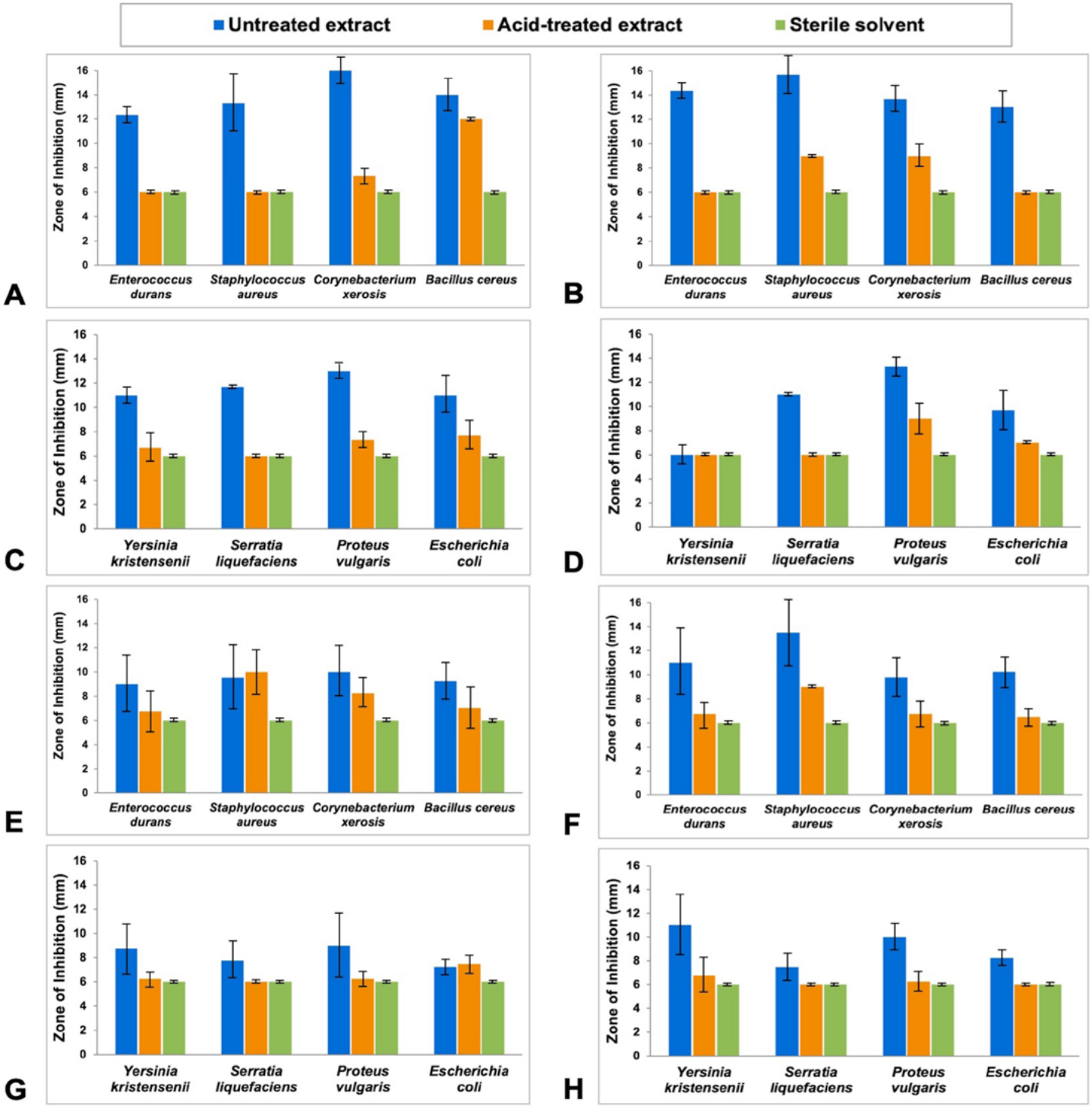

Note. The average sizes (from triplicate samples) of zones of inhibition on disk diffusion plate assays are shown. A measurement of 6 mm is a baseline representing the diameter of the disks themselves and equates to no visible zone of inhibition. A) *Moringa oleifera* aqueous seed extract against selected

Continued on page 69

Continued from page 68

Gram-positive bacteria; B) *Moringa stenopetala* aqueous seed extract against Gram-positive bacteria; C) *M. oleifera* aqueous seed extract against selected Gram-negative bacteria; D) *M. stenopetala* aqueous seed extract against Gram-negative bacteria; E) *M. oleifera* ethanolic leaf extract against Gram-positive bacteria; F) *M. stenopetala* ethanolic leaf extract against Gram-positive bacteria; G) *M. oleifera* ethanolic leaf extract against Gram-negative bacteria; H) *M. stenopetala* ethanolic leaf extract against Gram-negative bacteria. Controls are sterile ddH_2O (A–D) or sterile 70% ethanol (E–H).

Table 1

Antibacterial minimum inhibitory concentration (MIC) assay results for Moringa oleifera *aqueous crude leaf extract.*

Bacterial Species	Gram Reaction	Two-Fold Tube Dilution Series*				
		1	2	3	4	5
Bacillus cereus	Positive	-	-	-	-	+
Corynebacterium xerosis	Positive	-	-	-	+	+
Enterococcus durans	Positive	-	-	+	+	+
Listeria monocytogenes	Positive	-	-	-	+	+
Micrococcus luteus	Positive	-	-	+	+	+
Staphylococcus aureus	Positive	-	-	-	+	+
Streptococcus agalactiae	Positive	-	-	+	+	+
Escherichia coli	Negative	-	-	+	+	+
Proteus vulgaris	Negative	-	-	-	+	+
Serratia liquefaciens	Negative	-	-	+	+	+
Yersinia kristensenii	Negative	-	-	-	+	+

Note. *Although the dilution series for all species tested contained 9 tubes, the results for only five tubes are shown because growth occurred for all species in tubes 6–9; growth also occurred in every case in tube 10, a positive control containing no *Moringa* extract. The concentration (v/v) of total extract in each tube was as follows: tube 1, 100%; tube 2, 50%; tube 3, 25%; tube 4, 12.5%; tube 5, 6.25%. (+) growth present; (–) growth absent.

Figure 4

Representative minimum inhibitory concentration (MIC) assay using crude aqueous leaf extract from M. oleifera.

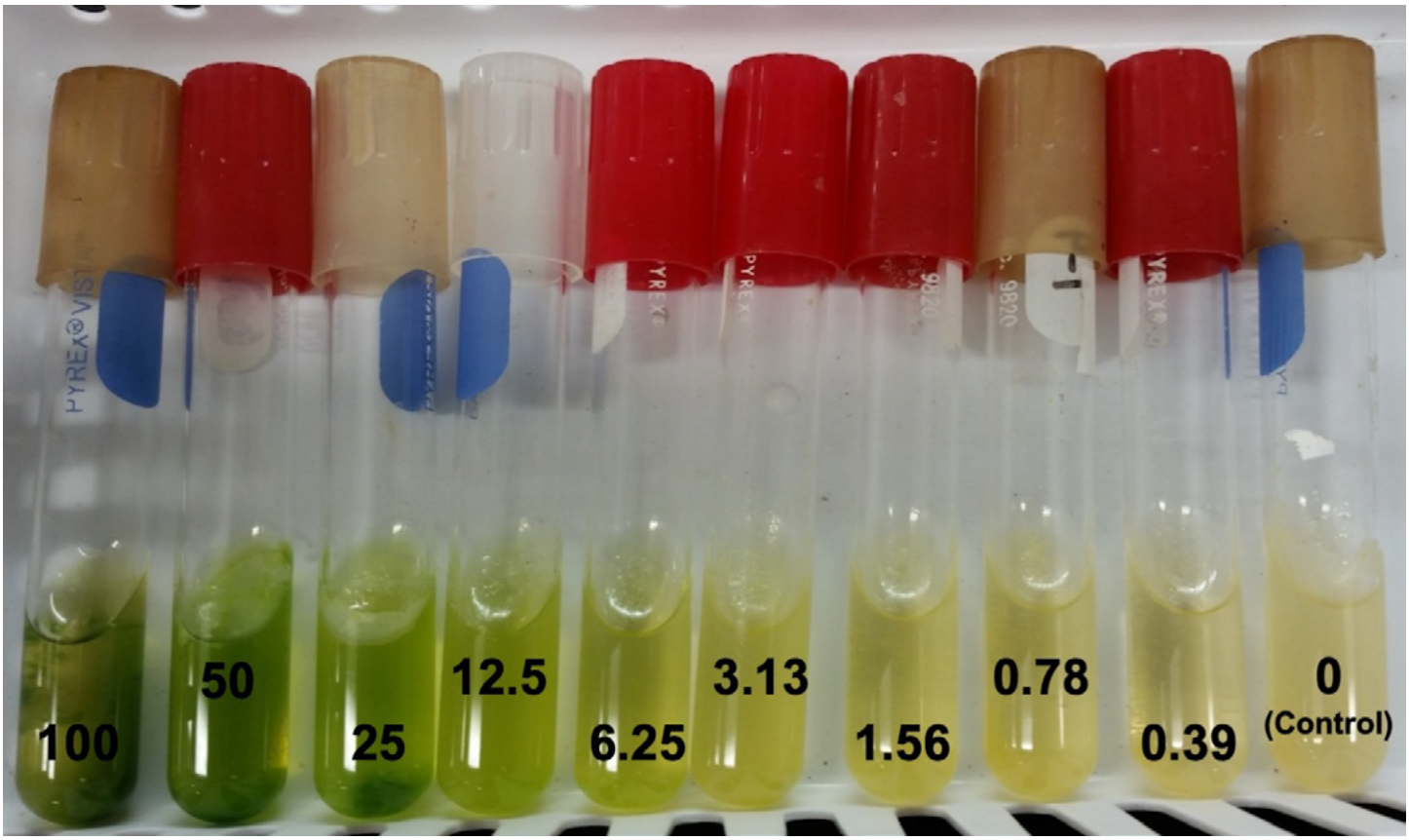

Note. A two-fold MIC serial dilution protocol was employed using 9 tubes, as well as a positive control containing no *Moringa* extract; the numbers indicate the % dilution of the extract.

subject to inactivation by conditions of low pH. Thus, although still highly nutritive, it is likely that the antibacterial properties of *Moringa* plant products are diminished upon ingestion.

Antibacterial compounds isolated from *Moringa* seeds and/or leaves may prove beneficial and find application in the clinical setting, either in native form or by contributing to the development of highly effective semi-synthetic pharmaceuticals. The many nutritional benefits of *Moringa* products have been well documented for some time and have gained considerable commercial promotion in recent years. With the rise in antibiotic resistance reaching alarming levels in the contemporary healthcare sector, the search for new antimicrobial drug options is of utmost importance. There could hardly be a more pertinent time than now to invest in the study of promising alternatives to traditional antibiotics, including those offered by species of *Moringa* and other medicinal plants.

Acknowledgments

The authors thank the IWU Division of Natural Sciences and the IWU Hodson Research Insti-

tute for financial support of this work. We thank ECHO (Fort Myers, Florida, USA) for providing seeds of *Moringa oleifera* and *Moringa stenopetala* in support of this work. We also thank Garth Miller for assistance with our statistical analyses and Angela Davidson for technical assistance in the laboratory.

Author Correspondence

Correspondence concerning this article should be addressed to: Grace J. Miller, gmiller@echonet.org; or
W. Matthew Sattley,
matthew.sattley@indwes.edu.

References

1. Adane, L., Teshome, M., & Tariku, Y. (2019) Isolation of compounds from root bark extracts of *Moringa stenopetala* and evaluation of their antibacterial activities. *Journal of Pharmacognosy and Phytochemistry, 8*, 4228–4244.

2. Aissani, N., Coroneo, V., Fattouch, S., & Caboni, P. (2012) Inhibitory effect of carob (*Ceratonia siliqua*) leaves methanolic extract on *Listeria monocytogenes*. *Journal of Agricultural and Food Chemistry*, 60, 9954–9958. https://pubs.acs.org/doi/pdf/10.1021/jf3029623

3. Alviano, D. S., Barreto, A. L. S., Dias, F. d. A., Rodrigues, I. d. A., dos Santos Rosa, M. d. S, Alviano, C. S., & de Araújo Soares, R. M. (2012) Conventional therapy and promising plant-derived compounds against trypanosomatid parasites. *Frontiers in Microbiology, 3*, 283. https://doi.org/10.3389/fmicb.2012.00283

4. Ambrose, O. M., Nguyen, T. T. M., & Nowicki, E. M. (2022) Antibacterial effects of bitter melon extract in combination with commonly prescribed antibiotics. *Fine Focus, 8*, 74–85

5. Arun, T., & Rao, P. (2011) Phytochemical screening and antibacterial activity of *Moringa oleifera* Lam. against *Proteus mirabilis* from urinary tract infected patients. *International Journal of PharmTech Research, 3*, 2118–2123.

6. Bauer, A. W., Kirby, W. M. M., Sherris, J. C., & Turck, M. (1966) Antibiotic susceptibility testing by a standardized single disc method. *American Journal of Clinical Pathology, 45*, 493–496.

7. Biswas, B., Rogers, K., McLaughlin, F., Daniels, D., & Yadav, A. (2013) Antimicrobial activities of leaf extracts of guava (*Psidium guajava* L.) on two gram-negative and gram-positive bacteria. *International Journal of Microbiology*, 746165. https://doi.org/10.1155/2013/746165

8. Chekesa, B., & Mekonnen, Y. (2015) Antibacterial activity of *Moringa stenopetala* against some human pathogenic bacterial strains. *Science, Technology and Arts Research Journal, 4*, 190–198. https://doi.org/10.4314/star.v4i2.23

9. Eilert, U., Wolters, B., & Nahrstedt, A. (1981) The antibiotic principle of seeds of *Moringa oleifera* and *Moringa stenopetala*. *Planta Medica Journal of Medicinal Plant Research, 42*, 55–61.

10. European Committee on Antimicrobial Susceptibility Testing. (2023) Breakpoint Tables for Interpretation of MICs and Zone Diameters. Version 13.0. http://www.eucast.org

11. Ezugwu, R. I., & Chukwubike, C. (2014) Evaluation of the antimicrobial activity of *Moringa oleifera* leaves extract on *Helicobacter pylori*. *IOSR Journal of Pharmacy and Biological Sciences, 9*, 57–60.

12. Fahey, J. W. (2005) *Moringa oleifera*: A review of the medical evidence for its nutritional, therapeutic, and prophylactic properties. Part 1. *Trees for Life Journal, 1*, 5.

13. Fontana, R., Caproni, A., Buzzi, R., Sicurella, M., Buratto, M., Salvatori, F., Pappadà, M., Manfredini, S., Baldisserotto, A., & Marconi, P. (2021) Effects of *Moringa oleifera* leaf extracts on *Xanthomonas campestris* pv. *campestris*. *Microorganisms, 9*, 2244. https://doi.org/10.3390/microorganisms9112244

14. Fontana R, Machi G, Caproni A, Sicurella, M., Buratto, M., Salvatori, F., Pappadà, M., Manfredini, S., Baldisserotto, A., & Marconi, P. (2022) Control of *Erwinia amylovora* growth by *Moringa oleifera* leaf extracts: In vitro and in planta effects. *Plants, 11*, 957. https://doi.org/10.3390/plants11070957

15. Gopalakrishnan, L., Doriya, K., & Kumar, D. S. (2016) *Moringa oleifera*: A review on nutritive importance and its medicinal application. *Food Science and Human Wellness, 5*, 49–56. https://doi.org/10.1016/j.fshw.2016.04.001

16. Hagos, Z., Teka, M. Z., Brhane, M. Y., Chaithanya, K. K., Gopalakrishnan, V. K., & Weletnsae, T. (2018) *In vitro* antibacterial activities of the methanolic and aqueous extracts of *Moringa stenopetala* leaves. *Journal of Pharmacy Research, 12*, 788–793.

17. Hayek, S. A., & Ibrahim, S. A. (2012) Antimicrobial activity of xoconostle pears (*Opuntia matudae*) against *Escherichi coli* O157:H7 in laboratory medium. *International Journal of Microbiology*, 368472. https://doi.org/10.1155/2012/368472

18. Jerri, H. A., Adolfsen, K. J., McCullough, L. R., Velegol, D., & Velegol, S. B. (2012) Antimicrobial sand via adsorption of cationic *Moringa oleifera* protein. *Langmuir, 28*, 2262–2268. https://doi.org/10.1021/la2038262

19. Kim, Y-J., & Kim, H. S. (2019) Screening Moringa species focused on development of locally available sustainable nutritional supplements. *Nutrition Research and Practice, 13*, 529–534. https://doi.org/10.4162/nrp.2019.13.6.529

20. Manilal, A., Sabu, K. R., & Shewangizaw, M. (2020) *In vitro* antibacterial activity of medicinal plants against biofilm-forming methicillin-resistant *Staphylococcus aureus*: efficacy of *Moringa stenopetala* and *Rosmarinus officinalis* extracts. *Heliyon, 6*, e03303. https://doi.org/10.1016/j.heliyon.2020.e03303

21. Miller, G. J., Cunningham, A. M. G., Iwase, Y., Lautensack, N. L., & Sattley, W. M. (2017) A laboratory activity demonstrating the antibacterial effects of extracts from two plant species, *Moringa oleifera* and *Allium sativum* (garlic). *Journal of Microbiology and Biology Education, 18*, 3. https://doi.org/10.1128/jmbe.v18i3.1306

22. Mubarek, A. K., Arbab, M. H., Mohammed, S. E., Kabbashi, A. S., Baraka, A. A., & Ahmed, N. M. (2022) Antimicrobial activity of *Lepidium sativum* against multi-drug resistant and sensitive *Pseudomonas aeruginosa*: A microbiological study from Khartoum State, Sudan. *Al-Kindy College Medical Journal, 18*, 96–100. https://doi.org/10.47723/kcmj.v18i2.807

23. Parrotta, J. A. (1993) *Moringa oleifera* Lam. Resedá, horseradish tree, Moringaceae, horseradish-tree family. SO-ITF-SM, United States Department of Agriculture, pp. 1–6.

24. Peixoto, J. R. O., Silva, G. C., Costa, R. A., de Sousa Fontenelle, J. L., Vieira, G. H. F., Filho, A. A. F., & Vieira, R. H. S. F. (2011) *In vitro* antibacterial effect of aqueous and ethanolic *Moringa* leaf extracts. *Asian Pacific Journal of Tropical Medicine, 4*, 201–204. https://doi.org/10.1016/S1995-7645(11)60069-2

25. Posmontier, B. (2011) The medicinal qualities of *Moringa oleifera*. *Holistic Nursing Practice, 25*, 80–87. https://doi.org/10.1097/HNP.0b013e31820dbb27

26. Rahman, M. M., Sheikh, M. I., Sharmin, S. A., Islam, M. S., Rahman, M. A., Rahman, M. M., & Alam, M.F. (2009) Antibacterial activity of leaf juice and extracts of *Moringa oleifera* Lam. against some human pathogenic bacteria. *CMU Journal of Natural Science, 8*, 219–227. https://www.thaiscience.info/journals/Article/CMUJ/10557966.pdf

27. Razis, A. F. A., Ibrahim, M. D., & Kntayya, S. B. (2014) Health benefits of *Moringa oleifera*. *Asian Pacific Journal of Cancer Prevention, 15*, 8571–8576. https://doi.org/10.7314/APJCP.2014.15.20.8571

28. Reygaert, W., & Jusufi, I. (2013) Green tea as an effective antimicrobial for urinary tract infections caused by *Escherichia coli*. *Frontiers in Microbiology, 4*, 162. https://doi.org/10.3389/fmicb.2013.00162

29. Seleshe, S., & Kang, S. N. (2019) *In vitro* antimicrobial activity of different solvent extracts from *Moringa stenopetala* leaves. *Preventive Nutrition and Food Science, 24*, 70–74. https://doi.org/10.3746/pnf.2019.24.1.70

30. Shalayel, M. H. F., Asaad, A. M., Qureshi, M. A., & Elhussein, A. B. (2017) Anti-bacterial activity of peppermint (*Mentha piperita*) extracts against some emerging multi-drug resistant human bacterial pathogens. *Journal of Herbal Medicine, 7*, 27–30. https://doi.org/10.1016/j.hermed.2016.08.003

31. Vieira, G. H. F., Mourão, J. A., Ângelo, Â. M., Costa, R. A., & Vieira, R. H. S. F. (2010) Antibacterial effect (*in vitro*) of *Moringa oleifera* and *Annona muricata* against gram-positive and gram-negative bacteria. *Revista do Instituto de Medicina Tropical de São Paulo, 52*, 129–132. https://doi.org/10.1590/S0036-46652010000300003

Polymicrobial Conditions Affect Antibiotic Susceptibility in Clinically Relevant Bacterial Species

William Little[1]

Andrea J. Lopez[1]

Eleanna Carris[1]

Allie Clinton Smith[1]

[1] **Honors College, Texas Tech University, Lubbock TX**

Abstract

Chronic wounds, defined as those which remain open and inflamed for greater than six weeks, are a major area of clinical concern. Resulting in thousands of amputations per year and billions of dollars spent globally in treatment, chronic wounds are notoriously difficult to successfully treat. Two hallmarks of chronic wounds are that they are thought to harbor biofilm-associated bacteria and tend to be polymicrobial. While the research literature has repeatedly demonstrated the effects of biofilms on wound persistence and the changes to the efficacy of antibiotics, few studies have demonstrated what effect the polymicrobial condition has on the antibiotic tolerance of bacteria. To further explore this, four species of clinically relevant wound pathogens (*Pseudomonas aeruginosa, Acinetobacter baumanii, Staphylococcus aureus, and Enterococcus faecalis*) were tested in mono- and polymicrobial conditions using the current gold-standard methods for determining antibiotic susceptibility. Noticeable differences in antibiotic tolerance were observed in the polymicrobial condition, including both increased and decreased susceptibility, depending on the antibiotic used. Our data demonstrate that the current clinical methods used for testing antibiotic susceptibility can generate results that are not representative of the infection environment, which may contribute to treatment failure and persistence of polymicrobial infections.

Keywords: Minimum inhibotry concentration (MIC), antimicrobial susceptibility testing (AST), wound, diagnostics, synergism

Manuscript received 22 April 2023; accepted 26 September 2023

Fine Focus, 10(1), 74-89. doi: 10.33043/FF.10.1.74-89.

Introduction

While a variety of chronic conditions affect Americans each year, less prominent, yet still clinically-impactful conditions manage to slip under the radar of the popular consciousness; one of these is chronic wounds. Often occurring in diabetic patients, the bed-ridden, and those with vascular diseases, chronic wounds are currently an area of major clinical concern- costing billions of dollars every year to treat and resulting in thousands of amputations in the United States alone.[1, 2] The most common definition of these wounds is those which remain open and in a prolonged state of inflammation for greater than six weeks.[3] Standard treatment protocols do exist for the management of chronic wounds, including the use of oral antibiotics, cleaning of the wound via physical means (commonly called debridement), and even the use of strong, topical antibiotics, yet as seen in the treatment costs listed above, those protocols remain of mixed efficacy.[4] To illustrate how these wounds occur, the case of a proto-typical diabetic patient will be used. For patients with diabetes, a gradual loss of sensation in the limbs, termed diabetic peripheral neuropathy, can often occur.[5] When combined with decreased circulation to the extremities, such a patient may receive a wound on their foot, and due to the lack of sensation, the patient will remain largely unaware of the existence of the damage, continuing with their normal activities of daily life. [5,6] As the wound progresses in its infection and tissue necrosis, it may become apparent to the patient or to caregivers who are assisting them, and the patient will be brought in for treatment. The open wound will be treated with antibiotics, but the wound will often persist, and refuse to heal or reduce its inflammatory condition.[5] At that point, debridement, specialized wound dressings, and further antibiotic treatment will be attempted, but the wound will often continue to remain infected, and amputation of the affected digit, appendage, or limb may be necessary to ensure the patient's survival.[5] As mentioned above, many thousands of patients receive amputations on the basis of chronic wound treatment failure every year, and so this area of study is a critical one to improving health outcomes in the United States.[1, 2] A question remains, though. Why do the current clinical best-practices in the treatment of these wounds fail so often? While it may be obvious that there exists some gap in the understanding of these wounds, it is by no means clear *where* that gap exists. In order to elucidate these gaps, it is imperative to first understand what is currently known by both the scientific and clinical communities around the structure and composition of these wounds.

It is widely understood that two major features characterize chronic wounds.[4] The first is that the bacteria within the wounds form biofilms. Biofilms are defined by the secreted extracellular polysaccharide (EPS) matrices that bacteria form to protect against dislodgement, to better control their microenvironment, and to serve as a mechanical barrier to external conditions.[7] More simply put, biofilms are a structure by which bacteria protect themselves and adhere to their infection site.[7, 8] For example, the necessity of brushing one's teeth with an abrasive compound such as a toothbrush arises from the biofilms that oral bacteria form as they grow; this can be observed from the off-white

plaque that is physically removed from teeth during this cleaning. Without the abrasive removal of biofilm, the bacteria would continue to adhere to the surface of the teeth, with poor outcomes for one's oral health.[9] The second well known characteristic of chronic wounds is that they tend to be polymicrobial- meaning that an infected wound is colonized by multiple species of bacteria, and almost without exception contain multiple species of pathogenic bacteria.[10, 11] It is more commonly thought that infections consist of a single species of bacteria or infectious agent (fulfilling Koch's postulates), but the research literature has shown extensively that, once within a biofilm, numerous species of bacteria can happily coexist. Next-generation sequencing (an advanced method of genetic analysis) of wound samples has revealed that up to several hundred different species of bacteria may infect chronic wounds, though not necessarily all simultaneously (demonstrating a dynamic and ever-changing nature of a chronic wound).[12] This polymicrobial environment can also promote synergistic interactions among bacteria within the wound. Synergistic interactions in bacteria are those in which multiple bacterial species inhabiting the same environment creates differences in behavior from a single species condition.[13, 14] This often occurs by the upregulation of virulence factors among bacteria in those communities, and is associated with poorer patient outcomes.[15] The synergistic interactions within the polymicrobial biofilm environment are also known to increase both the antimicrobial tolerance and resistance in constituent microbes through increased rates of horizontal gene transfer and differential gene expression.[8, 16-19] Tolerance to antibiotics is characterized by transient changes in a bacterial population in response to their environment, usually via differential gene expression (DGE), which allows them to survive when exposed to antibiotics (Fig. 1).[20] This change in metabolism as a result of the synergistic interaction-caused DGE often decreases the efficacy of antibiotics by changing the availability of target sites or processes, which leads to bacteria surviving a normally lethal treatment.[20] Resistance, on the other hand, involves the acquisition of specific genes that allow the bacteria to counter the effect of the antibiotic (Fig. 1), and is a 'permanent' change in their genetic makeup, often associated with horizontal gene transfer (HGT).[21] HGT is the method by which antimicrobial resistance genes are shared within a mature bacterial population, and the polymicrobial environment favors these interactions.[12] Using *in vitro* research models, biofilms have also been shown to play a major role in the antibiotic tolerance of pathogens via the mechanical barrier that the biofilm forms, as well as the increased DGE that affects the efficacy of therapeutic compounds of the bacteria within the biofilm. The effect of biofilm formation alone can result in a one thousand fold decrease in antibiotic susceptibility due to the conditions within that microenvironment.[20, 22, 23] While this has been extensively demonstrated in the literature, most studies investigating the contribution of a biofilm to changes in susceptibility have focused on monomicrobial, or single-species, bacterial suspensions.[24-32] Because of this, our aim was to determine what effects a polymicrobial condition has on the antimicrobial susceptibility of a group of bacteria- an effect independent of biofilm formation- and one that is currently a gap in the research knowledge, especially

when compared to the large body of research on the effects of biofilm formation on antibiotic susceptibility.

Methods and Materials

Species and Strains

Four species were chosen for use in the polymicrobial culture: *Acinetobacter baumanii* (AB), *Pseudomonas aeruginosa* (PA), *Staphylococcus aureus* (SA), and *Enterococcus faecalis* (EF). Each of these species is both a common infector of chronic wounds and a member of the ESKAPE pathogen family, which are a leading cause of nosocomial infections.[17,37] Clinical and Laboratory Standards Institute (CLSI) -recommended quality control strains of *A. baumanii* (ATCC® 19606), *P. aeruginosa* (ATCC® 27853), *E. faecalis* (ATCC® 29212), and *S. aureus* (ATCC® 29213) were used.[38] These strains are pan-susceptible and were used to ensure the reliability of the established MIC breakpoints provided by CLSI while eliminating any possibility of antibiotic resistance genes affecting the results of the experiments.

Figure 1

Antibiotic Resistance Versus Tolerance. (Taken from [21])

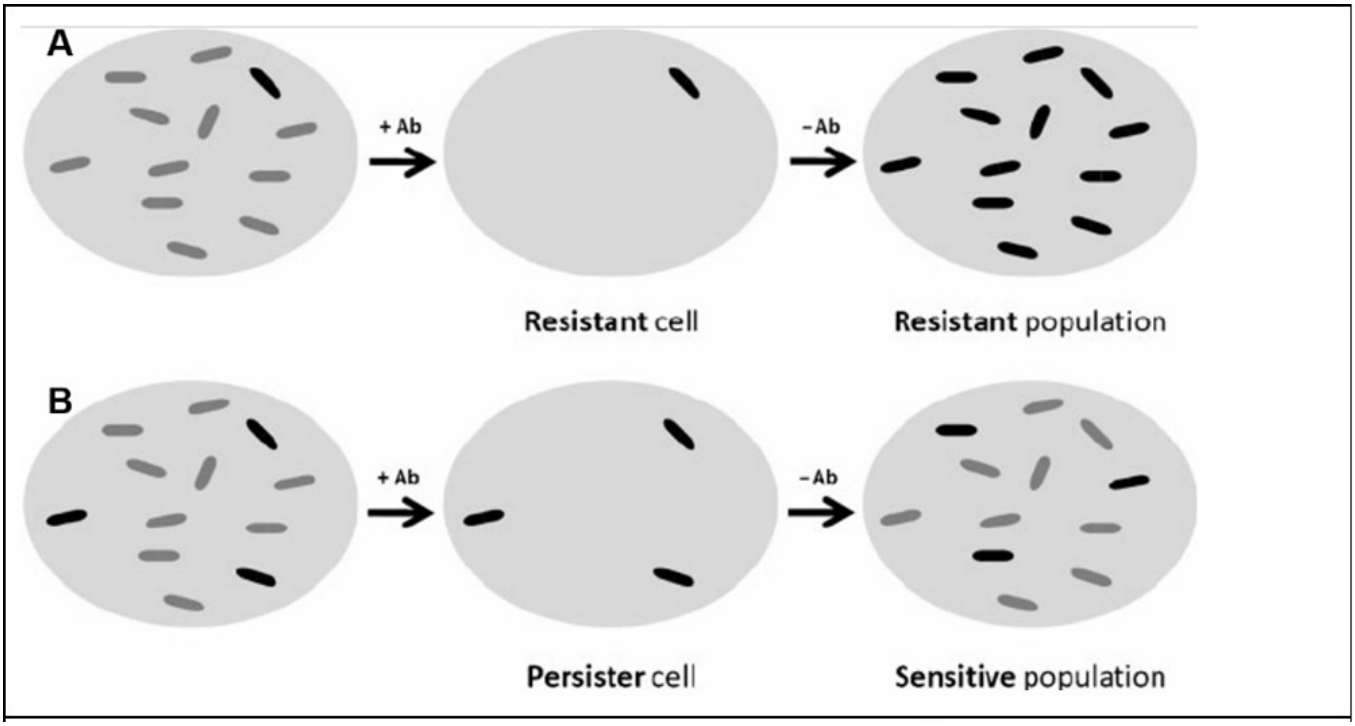

Note. A microbial population (confined by a light-grey ellipse) initially consists of mainly antibiotic-sensitive cells (dark-grey). (A) In addition, the population may also contain resistant cells (black), resulting from a permanent change at the genetic level. After antibiotic treatment (+Ab), only resistant cells remain. Upon regrowth (-Ab), the entire population is composed of resistant individuals. (B) Alternatively, the population may contain persister cells (black), resulting from a reversible phenotypic switch to a tolerant state. After antibiotic treatment, only persister cells remain. Upon regrowth, the population will exhibit the same sensitivity as the original population.

Minimum Inhibitory Concentration (MIC)

Our experiments were conducted in accordance with the CLSI M100 and M7 guidelines for determining antibiotic susceptibility.[38, 39] MICs were determined by first conducting mono-species MICs in 96-well plates and the results were cross-checked with the CLSI's established MIC breakpoints for each species used stratified by drug. Bacterial cryo-stocks were grown overnight in lysogeny (LB) broth (Thermo Fisher Scientific, Hampton, NH) , then the above CLSI protocol was followed. Mono-species MICs were conducted first to ensure that the results were in accordance with published guidelines as an internal control. Then, each of the four species was grown in lysogeny (LB) broth (Thermo Fisher Scientific, Hampton, NH) overnight separately, then combined in a 1:1:1:1 ratio inoculating dose, which ensured that total colony forming units (CFUs) of bacteria and volume added was equivalent between the mono and poly-microbial conditions. Antibiotic concentration was diluted across the 96-well

Figure 2

An Example of Broth Microdilution Technique as Directed by CLSI.

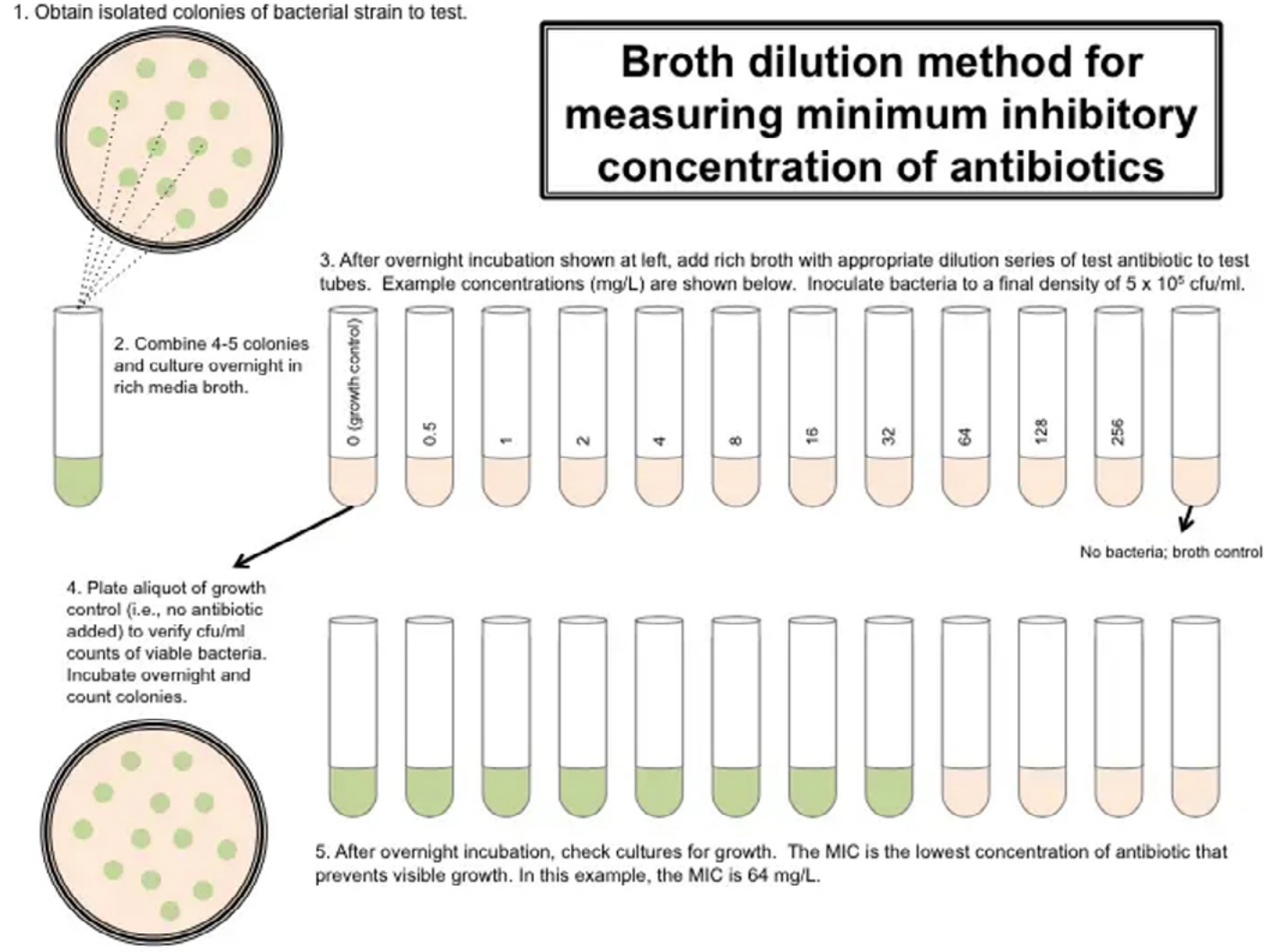

Note. A brief visual outline of the current diagnostic MIC protocol, as used via CLSI guidelines. Taken from [42]

plate in accordance with CLSI M7 and M100 guidelines, with the highest concentration at 128ug/ml; concentrations were serially halved across the 12 wells in a row down to 0.06ug/mL. Cation-Adjusted Mueller Hinton Broth (CAMHB) (Thermo Fisher Scientific, Hampton, NH) was used as the media, and after inoculation with the bacterial dose, the plate was sealed and incubated at 37^0C. After 18-24 hours of incubation, the plates were removed and MICs were determined visually via turbidity, as described as best-practice by the CLSI (Fig. 2).[39] All experiments were conducted in triplicate with biological replicates. The results were recorded and compared with the mono-species results for that antibiotic to determine if any notable differences were observed.

It has previously been observed that polymicrobial cultures gave results not in accordance with CLSI breakpoint guidelines, but since those assays were conducted with the disk diffusion method, their results cannot directly compared to the broth microdilution methods commonly used in US clinical laboratories.[40, 41] Given the lack of consistency in experimental conditions from previous in vitro research, we aimed to use the current clinical method of broth microdilution to determine what effect a polymicrobial community had on individual MICs among the species in a polymicrobial suspension. Using the current clinical model allowed for effective comparison both across antibiotics and species in the polymicrobial environment and ensured the validity of results in the current clinical standards. Limitations to this method do exist, however. Given that the bacteria in a polymicrobial condition cannot be differentiated visually, it is not possible to establish changes for individual species' MIC in this condition on the basis of turbidity alone. Because of this, an additional viability method was used to assess changes in antibiotic tolerance for each individual species (described below).

Viability

Two antibiotics - penicillin and ceftazidime - were tested with a modification of the MIC protocol. After following the previously described MIC protocol, the bacterial suspensions were extracted from the wells, diluted to the first order in phosphate buffered saline (1XPBS), then 10µl volume was spot-plated on selective and differential media for each bacteria (*Pseudomonas* Isolation Agar for the recovery of PA (Thermo Fisher Scientific, Hampton, NH), Mannitol Salt Agar (Thermo Fisher Scientific, Hampton, NH) for the recovery of SA, Bile Esculin Agar for the recovery of EF, and Leeds Agar (Thermo Fisher Scientific, Hampton, NH) for the recovery of AB, to observe any possible differences in viability of those cells in mono- and polymicrobial conditions. Selective and differential agars were used to allow for the differentiation of individual species within the polymicrobial condition, though the results of these assays are not directly comparable to the MICs for either of those antibiotics as they do not rely on the turbidity assessment used by the CLSI. In addition, the scientific literature has demonstrated that the visual assessment of turbidity corresponds only to an approximately 50 percent decrease in OD reading, so viable bacteria will still be present in wells above the visually assessed MIC.[43]

Results

Our results are demonstrated in the following figures, which are divided into two parts. The first covers our MIC data, and the second shows our viability data. For the MIC charts, the values listed show the individual MICs for each bacterium per antibiotic treatment, then the MIC polymicrobial value from our data, when read in accordance with CLSI guidelines. The viability data shows the comparison of spot plated viability values between the individual and polymicrobial conditions for a particular antibiotic treatment.

MIC Values

These data reflect comparisons of results obtained following the CLSI gold standard broth microdilution method for individual suspensions versus a polymicrobial planktonic suspension. MIC results were obtained for gentamicin, tobramycin, penicillin, tetracycline, doxycycline, and ceftazidime (Fig. 3). For gentamicin (Fig. 3A) and penicillin (Fig. 3C) the polymicrobial MIC was the same as the highest individual MIC result. This demonstrates that there was no observable change in the polymicrobial community MIC determinable by turbidity alone. For tetracycline (Fig. 3B), the highest observable individual MIC was *E. faecalis* at 32 μg/mL; however, the polymicrobial MIC result was 128 μg/mL. This demonstrates that mixing the four species together changes antimicrobial susceptibility of the population by 4-fold for at least one species in the suspension. For ceftazidime (Fig. 3D), the highest individual MIC value was *E. faecalis* at >128 μg/mL; however, the polymicrobial MIC result was 16 μg/mL. This demonstrates that the polymicrobial condition increases the susceptibility of *E. faecalis* by 4-fold. It is worth noting that any changes to individual MICs within the predetermined minimum and maximum ranges cannot be evaluated via turbidity and MIC alone in a polymicrobial condition.

Viability Values

The viability assays were run in order to determine changes in viability of the individual and polymicrobial conditions following antimicrobial challenge. All viability assays were conducted in triplicate with biological replicates. These results are not comparable to conventional MICs because the turbidity reduction observed in MICs correlates to an estimated 50% reduction in viable cells, whereas these data relate to the total elimination of viable bacteria.[43] For penicillin (Fig. 4A), both SA and AB observed decreases to antimicrobial susceptibility, at 64 and 8-fold respectively, in the polymicrobial versus individual conditions. For ceftazidime (Fig. 4B), AB observed a reduction in susceptibility by 2.86-fold, while SA observed an increase in susceptibility by 3-fold in the polymicrobial versus individual conditions. PA and EF do not exhibit any observable changes in susceptibility.

Discussion

Our data across the two methods - MIC and viability - demonstrate several notable results. In the first case, gentamicin, tobramycin, penicillin, and doxycycline did not show a difference in the observable MIC in the polymicrobial condition over the given values for the individual. In other words, the range of possible MIC values of the individual condition overlapped with that of the polymicrobial.

Because of this, and because the samples were assessed visually, it is not possible to determine the contribution of each individual species to the turbidity observed in the polymicrobial condition. For instance, in the case of gentamicin, the polymicrobial MIC is 8μg/ml. Given that the MIC value in the individual condition for *A. baumannii* is 4μg/mL, it is not possible for us to determine if any changes in MIC for that species occurred, because the individual MIC result for *E. faecalis* at 8μg/mL is the same as the polymicrobial result. Put another way, in the case of gentamicin, the polymicrobial condition having the same MIC as one of the individual MICs (in this case *E. faecalis*) might represent that the individual species had no

Figure 3

Comparison of Minimum Inhibitory Concentrations (MIC) in Mono- and Polymicrobial Conditions.

(A) Gentamicin

Species	MIC Value (μg/mL)
P. aeruginosa	0.5±0†
S. aureus	0.5±0†
A. baumannii	4±0†
E. faecalis	8±0†
Polymicrobial	8±0

(B) Tetracycline

Species	MIC Value (μg/mL)
P. aeruginosa	32±0†
S. aureus	0.5±0†
A. baumannii	4±0†
E. faecalis	32±0†
Polymicrobial	128±0

(C) Penicillin

Species	MIC Value (μg/mL)
P. aeruginosa	>128±0
S. aureus	2±0†
A. baumannii	16±0
E. faecalis	4±0†
Polymicrobial	>128

(D) Ceftazidime

Species	MIC Value (μg/mL)
P. aeruginosa	2±0†
S. aureus	16±0†
A. baumannii	1±0†
E. faecalis	>128±0
Polymicrobial	16±0

Note. Monomicrobial versus Polymicrobial MIC results for gentamicin (A), tetracycline (B), penicillin (C), and ceftazidime (D). † denotes that the value is within the published guidelines from the Clinical Laboratory Science Institute's M7 and M100 manuals for MIC breakpoints (CLSI, 2018a, 2018b). MIC values greater than 128 μL have been calculated as that number. CLSI does not publish established breakpoint values for *P. aeruginosa* and *A. baumanii* when treated with penicillin and for *E. faecalis* when treated with ceftazidime. n=3.

change in MIC, or it could represent that one or more of the species increased in MIC up to the polymicrobial MIC, but that change cannot be determined because the contribution of each individual species in the polymicrobial condition is not observable via an assessment of turbidity.

Two notable differences in MIC were observed in the polymicrobial condition. With tetracycline, a decrease in susceptibility was observed in the polymicrobial condition, which correlates to a decreased antibiotic efficacy, presumably via tolerance as all strains of bacteria used are pan-susceptible. As the polymicrobial MIC is substantially greater than any of the component individual MICs, it is not possible to determine which bacterial species' tolerance was increased, or which combination of those species was affected. With ceftazidime, however, an opposite effect was observed, where a sensitization interaction occurred. In this case, *E. faecalis* can be identified as the bacteria whose tolerance decreased, as its individual MIC is substantially higher than the polymicrobial value, whereas *P. aeruginosa*, *S. aureus*, and *A. baumanii*'s individual MIC values are equal to or lower than the polymicrobial MIC. As tetracycline and ceftazidime are both clinically important antibiotics, these results demonstrate a notable and potentially clinically significant change.[44, 45]

For the viability experiments, bacteria treated with penicillin and ceftazidime both showed notable differences in antibiotic susceptibility in the polymicrobial condition. When treated with penicillin in the polymicrobial environment, both *S. aureus* and *A. baumanii* showed notable increases in tolerance to the antibi-

Figure 4

Comparison of Viability in Mono- and Polymicrobial Conditions.

(A) Penicillin

Species	Individual Viability Value (µg/mL)	Polymicrobial Viability Value (µg/mL)
P. aeruginosa	>128±0	>128±0
S. aureus	2±0†	128±0
A. baumannii	16±0	>128±0
E. faecalis	4±0†	4±0

(B) Ceftazidime

Species	Individual Viability Value (µg/mL)	Polymicrobial Viability Value (µg/mL)
P. aeruginosa	>128±0†	>128±0
S. aureus	96±55.43†	32±27.71
A. baumannii	37.33±24.44†	106.67±37.0
E. faecalis	>128±0	>128±0

Note. Monomicrobial versus Polymicrobial Viability results for penicillin (A) and ceftazidime (B). † denotes that the value is within the published guidelines from the Clinical Laboratory Science Institute's M7 and M100 manuals for MIC breakpoints (CLSI, 2018a, 2018b). Viability values greater than 128 µL have been calculated as that number. CLSI does not publish established breakpoint values for *P. aeruginosa* and *A. baumanii* when treated with penicillin and for *E. faecalis* when treated with ceftazidime. n=3.

otic challenge. For *S. aureus,* this difference amounts to a 64-fold increase in concentration necessary to successfully kill the bacteria, and for *A. baumanii*, an 8-fold increase. However, when treated with ceftazidime, *S. aureus* demonstrated a decreased tolerance of 3-fold, but *A. baumanii* showed an almost three-fold increase in tolerance to the compound. As penicillin and ceftazidime are both clinically important, oft-prescribed antibiotics, this shift in tolerances is highly relevant for care practitioners in the wound and lab environments.

Given that our results are consistent with both the existing literature around the polymicrobial effect on antibiotic susceptibility and uses the current clinical model, these data demonstrate that there exists a gap in the current clinical diagnostic schema for determining the antimicrobial susceptibility of polymicrobial infections. As it has also been repeatedly demonstrated in the literature that synergistic interactions among bacteria within a wound produce more negative outcomes clinically, and that chronic wounds harbor polymicrobial infections, our data is consistent both internally and externally with the observations found in clinical practice.[10, 11, 15] Since both tolerance and resistance can play important roles in the success of infection treatment, and as our data demonstrates, tolerance alone can notably change the susceptibility of bacteria to antibiotic treatments, it is critical that the clinical models be adapted to allow for the presence of polymicrobial cultures during the assessment process. This change could potentially result in more accurate assessments of antibiotic susceptibility across the clinical spectrum, and may be of particular benefit to the treatment of the notoriously intractable chronic wounds. Though the rise of sequencing technologies in the clinical laboratory is no doubt of great value for clinical microbiologists and provides valuable data in the diagnostic process (particularly for microbial identification), it is important to note that because the above data assesses transient changes to antibiotic tolerance rather than antibiotic resistance, the former of which is the result of phenotypic rather than genotypic differences, methods such as 16S next-generation sequencing (NGS) or rapid qPCR will not be able to determine these changes in tolerance, since those technologies rely on and assess for the presence of antibiotic resistance genes.[46]

It is noteworthy that the differing combinations of bacterial species and antimicrobial drug yield different results. In some instances, the susceptibility is decreased, and in other instances the susceptibility of one or more species is increased. This implies that there is no 'one size fits all' approach to changes in susceptibility due to the polymicrobial condition, and that more research is necessary to understand why different bacterial consortia respond differently to antimicrobial challenges in clinical settings. It is also noteworthy that most of the existing literature, including this study, focus on either the contribution of either the polymicrobial or biofilm condition to changes in susceptibility, when in the clinical setting both of these conditions commonly exist simultaneously. This implies that the effects seen in these studies might be compounded when combined in the clinical setting, and more research needs to be done to understand both the cumulative effect of those conditions in the clinical wound setting and how the entirety of the microbial

environment can be taken into account when considering antimicrobial susceptibility in clinical diagnostic procedures.

In conclusion, antibiotic susceptibility testing is a crucial part of the chronic wound treatment process. Healthcare practitioners rely on the information that clinical microbiologists provide to determine the most appropriate antibiotic treatment, and it is critical that the information the clinical laboratory generates is representative of the infection, accurate, and applicable to the patient. Using clinically-relevant models based upon the current gold-standard guidelines, our results show that the polymicrobial condition of wounds may be modifying their response to antimicrobial chemotherapy, and therefore the results from the current method may not be an accurate reflection of susceptibility in the chronic wound infection environment. In adapting the method of assessment to better reflect the wound environment by including polymicrobial cultures, it is entirely possible that the costs, both physical and economic, of chronic wound care might be minimized, leading to improved patient care and outcomes.

References

1. Järbrink, K., Ni, G., Sönnergren, H., Schmidtchen, A., Pang, C., Bajpai, R., & Car, J. (2017). The humanistic and economic burden of chronic wounds: A Protocol for a systematic review. *Systematic Reviews*, *6*(1). https://doi.org/10.1186/s13643-016-0400-8

2. Nussbaum, S. R., Carter, M. J., Fife, C. E., DaVanzo, J., Haught, R., Nusgart, M., & Cartwright, D. (2018). An economic evaluation of the impact, cost, and Medicare policy implications of chronic nonhealing wounds. *Value in Health*, *21*(1), 27–32. https://doi.org/10.1016/j.jval.2017.07.007

3. Iheozor-Ejiofor, Z., Newton, K., Dumville, J. C., Costa, M. L., Norman, G., & Bruce, J. (2018). Negative pressure wound therapy for open traumatic wounds. *Cochrane Database of Systematic Reviews*, *2018*(7). https://doi.org/10.1002/14651858.cd012522.pub2

4. Snyder RJ, Bohn G. Hanft J. et al. (2017). Wound Biofilm: Current Perspectives and Strategies on Biofilm Disruption and Treatments. *Wounds,*29(6):S1-S17.

5. Torkington-Stokes, R., Metcalf, D., & Bowler, P. (2016). Management of diabetic foot ulcers: Evaluation of case studies. *British Journal of Nursing*, *25*(15). https://doi.org/10.12968/bjon.2016.25.15.s27

6. Barrell, K., & Smith, A. G. (2019). Peripheral neuropathy. *Medical Clinics of North America*, *103*(2), 383–397. https://doi.org/10.1016/j.mcna.2018.10.006

7. Myckatyn, T. M., Cohen, J., & Chole, R. A. (2016). Clarification of the definition of a "biofilm." *Plastic and Reconstructive Surgery*, *137*(1), 237–238. https://doi.org/10.1097/prs.0000000000001911

8. Tolker-Nielsen, T. (2015). Biofilm development. *Microbiology Spectrum*, *3*(2). https://doi.org/10.1128/microbiolspec.mb-0001-2014

9. Arweiler, N. B., & Netuschil, L. (2016). The oral microbiota. *Microbiota of the Human Body*, 45–60. https://doi.org/10.1007/978-3-319-31248-4_4

10. Körber, A., Schmid, E. N., Buer, J., Klode, J., Schadendorf, D., & Dissemond, J. (2010). Bacterial colonization of chronic leg ulcers: Current results compared with data 5 years ago in a specialized dermatology department. *Journal of the European Academy of Dermatology and Venereology*, 1017–1025. https://doi.org/10.1111/j.1468-3083.2010.03570.x

11. Beaudoin, T., Yau, Y. C., Stapleton, P. J., Gong, Y., Wang, P. W., Guttman, D. S., & Waters, V. (2017). Staphylococcus aureus interaction with pseudomonas aeruginosa biofilm enhances tobramycin resistance. *Npj Biofilms and Microbiomes*, *3*(1). https://doi.org/10.1038/s41522-017-0035-0

12. Dowd, S. E., Sun, Y., Secor, P. R., Rhoads, D. D., Wolcott, B. M., James, G. A., & Wolcott, R. D. (2008). Survey of bacterial diversity in chronic wounds using pyrosequencing, DGGE, and full ribosome shotgun sequencing. *BMC Microbiology*, *8*(1), 43. https://doi.org/10.1186/1471-2180-8-43

13. DeLeon, S., Clinton, A., Fowler, H., Everett, J., Horswill, A. R., & Rumbaugh, K. P. (2014). Synergistic interactions of pseudomonas aeruginosa and Staphylococcus aureus in an *in vitro* wound model. *Infection and Immunity*, *82*(11), 4718–4728. https://doi.org/10.1128/iai.02198-14

14. Deng, Y.-J., & Wang, S. Y. (2016). Synergistic growth in bacteria depends on substrate complexity. *Journal of Microbiology*, *54*(1), 23–30. https://doi.org/10.1007/s12275-016-5461-9

15. Korgaonkar, A., Trivedi, U., Rumbaugh, K. P., & Whiteley, M. (2012). Community surveillance enhances *pseudomonas aeruginosa* virulence during polymicrobial infection. *Proceedings of the National Academy of Sciences*, *110*(3), 1059–1064. https://doi.org/10.1073/pnas.1214550110

16. Bahamondez-Canas, T. F., Heersema, L. A., & Smyth, H. D. (2019). Current status of in vitro models and assays for susceptibility testing for wound biofilm infections. *Biomedicines*, *7*(2), 34. https://doi.org/10.3390/biomedicines7020034

17. Citron, D. M., Goldstein, E. J., Merriam, C. V., Lipsky, B. A., & Abramson, M. A. (2007). Bacteriology of moderate-to-severe diabetic foot infections and in vitro activity of antimicrobial agents. *Journal of Clinical Microbiology*, *45*(9), 2819–2828. https://doi.org/10.1128/jcm.00551-07

18. Estrela, S., & Brown, S. P. (2018). Community interactions and spatial structure shape selection on antibiotic resistant lineages. *PLOS Computational Biology*, *14*(6). https://doi.org/10.1371/journal.pcbi.1006179

19. Madsen, J. S., Burmølle, M., Hansen, L. H., & Sørensen, S. J. (2012). The interconnection between biofilm formation and horizontal gene transfer. *FEMS Immunology & Medical Microbiology*, *65*(2), 183–195. https://doi.org/10.1111/j.1574-695x.2012.00960.x

20. Orazi, G., & O'Toole, G. A. (2019). "it takes a village": Mechanisms underlying antimicrobial recalcitrance of polymicrobial biofilms. *Journal of Bacteriology*, *202*(1). https://doi.org/10.1128/jb.00530-19

21. Fauvart, M., De Groote, V. N., & Michiels, J. (2011). Role of persister cells in chronic infections: Clinical relevance and perspectives on anti-persister therapies. *Journal of Medical Microbiology*, *60*(6), 699–709. https://doi.org/10.1099/jmm.0.030932-0

22. Hall, C. W., & Mah, T.-F. (2017). Molecular mechanisms of biofilm-based antibiotic resistance and tolerance in pathogenic bacteria. *FEMS Microbiology Reviews*, *41*(3), 276–301. https://doi.org/10.1093/femsre/fux010

23. Mah, T.-F. C., & O'Toole, G. A. (2001). Mechanisms of biofilm resistance to antimicrobial agents. *Trends in Microbiology*, *9*(1), 34–39. https://doi.org/10.1016/s0966-842x(00)01913-2

24. Mottola, C., Matias, C. S., Mendes, J. J., Melo-Cristino, J., Tavares, L., Cavaco-Silva, P., & Oliveira, M. (2016). Susceptibility patterns of Staphylococcus aureus biofilms in diabetic foot infections. *BMC Microbiology*, *16*(1). https://doi.org/10.1186/s12866-016-0737-0

25. Kosikowska, U., Andrzejczuk, S., Plech, T., & Malm, A. (2016). Inhibitory effect of 1,2,4-triazole-ciprofloxacin hybrids on haemophilus parainfluenzae and haemophilus influenzae biofilm formation in vitro under stationary conditions. *Research in Microbiology*, *167*(8), 647–654. https://doi.org/10.1016/j.resmic.2016.05.009

26. Velez Perez, A. L., Schmidt-Malan, S. M., Kohner, P. C., Karau, M. J., Greenwood-Quaintance, K. E., & Patel, R. (2016). In vitro activity of ceftolozane/tazobactam against clinical isolates of pseudomonas aeruginosa in the planktonic and biofilm states. *Diagnostic Microbiology and Infectious Disease*, *85*(3), 356–359. https://doi.org/10.1016/j.diagmicrobio.2016.02.014

27. Er, B., Demirhan, B., Onurdağ, F. K., Özgacar, S. Ö., & Öktem, A. B. (2014). Antimicrobial and antibiofilm effects of selected food preservatives against salmonella spp. isolated from chicken samples. *Poultry Science*, *93*(3), 695–701. https://doi.org/10.3382/ps.2013-03404

28. Luque-Sastre, L., Fox, E. M., Jordan, K., & Fanning, S. (2018). A comparative study of the susceptibility of listeria species to sanitizer treatments when grown under planktonic and biofilm conditions. *Journal of Food Protection*, *81*(9), 1481–1490. https://doi.org/10.4315/0362-028x.jfp-17-466

29. Desai, M. (1998). Increasing resistance of planktonic and biofilm cultures of burkholderia cepacia to ciprofloxacin and ceftazidime during exponential growth. *Journal of Antimicrobial Chemotherapy*, *42*(2), 153–160. https://doi.org/10.1093/jac/42.2.153

30. Pascual, A., de Arellano, E. R., Martínez, L. M., & Perea, E. J. (1993). Effect of polyurethane catheters and bacterial biofilms on the in-vitro activity of antimicrobials against Staphylococcus epidermidis. *Journal of Hospital Infection*, *24*(3), 211–218. https://doi.org/10.1016/0195-6701(93)90050-a

31. Théraud, M., Bédouin, Y., Guiguen, C., & Gangneux, J.-P. (2004). Efficacy of antiseptics and disinfectants on clinical and environmental yeast isolates in planktonic and biofilm conditions. *Journal of Medical Microbiology*, *53*(10), 1013–1018. https://doi.org/10.1099/jmm.0.05474-0

32. Martins, K. B., Ferreira, A. M., Pereira, V. C., Pinheiro, L., Oliveira, A. de, & Cunha, M. de. (2019). In vitro effects of antimicrobial agents on planktonic and biofilm forms of Staphylococcus saprophyticus isolated from patients with urinary tract infections. *Frontiers in Microbiology*, *10*. https://doi.org/10.3389/fmicb.2019.00040

33. Humphries, R. M., Ambler, J., Mitchell, S. L., Castanheira, M., Dingle, T., Hindler, J. A., Koeth, L., Sei, K., Hardy, D., Zimmer, B., Butler-Wu, S., Dien Bard, J., Brasso, B., Shawar, R., Dingle, T., Humphries, R., Sei, K., & Koeth, L. (2018). CLSI methods development and standardization working group Best Practices for evaluation of antimicrobial susceptibility tests. *Journal of Clinical Microbiology*, *56*(4). https://doi.org/10.1128/jcm.01934-17

34. Syal, K., Mo, M., Yu, H., Iriya, R., Jing, W., Guodong, S., Wang, S., Grys, T. E., Haydel, S. E., & Tao, N. (2017). Current and emerging techniques for antibiotic susceptibility tests. *Theranostics*, *7*(7), 1795–1805. https://doi.org/10.7150/thno.19217

35. Orazi, G., & O'Toole, G. A. (2017). *pseudomonas aeruginosa* alters *staphylococcus aureus* sensitivity to vancomycin in a biofilm model of cystic fibrosis infection. *MBio*, *8*(4). https://doi.org/10.1128/mbio.00873-17

36. Orazi, G., Ruoff, K. L., & O'Toole, G. A. (2019). Pseudomonas aeruginosa increases the sensitivity of biofilm-grown staphylococcus aureus to membrane-targeting antiseptics and antibiotics. *MBio*, *10*(4). https://doi.org/10.1128/mbio.01501-19

37. Pendleton, J. N., Gorman, S. P., & Gilmore, B. F. (2013). Clinical relevance of the ESKAPE pathogens. *Expert Review of Anti-Infective Therapy*, *11*(3), 297–308. https://doi.org/10.1586/eri.13.12

38. CLSI (2018). Performance Standards for Antimicrobial Susceptibility Testing. 28th ed. Wayne, PA:Clinical Laboratory Standards Institute

39. CLSI (2018). Methods for Dilution Antimicrobial Susceptibility Tests for Bacteria That Grow Aerobically. 11th ed. Wayne, PA: CLSI

40. Shahidi, A., & Ellner, P. D. (1969). Effect of mixed cultures on antibiotic susceptibility testing. *Applied Microbiology*, *18*(5), 766–770. https://doi.org/10.1128/am.18.5.766-770.1969

41. Linn BS, Szabo S. (1975). The Varying Sensitivity to Antibacterial Agents of Micro-organisms in Pure vs. Mixed Cultures. *Surgery*. 77(6): 780-785

42. Maughan, H. (2012). Laboratory tests for venereal diseases. *Materials and Methods*, *2*. https://doi.org/10.13070/mm.en.2.127

43. Arthington-Skaggs, B. A., Lee-Yang, W., Ciblak, M. A., Frade, J. P., Brandt, M. E., Hajjeh, R. A., Harrison, L. H., Sofair, A. N., & Warnock, and D. (2002). Comparison of visual and spectrophotometric methods of broth microdilution mic end point determination and evaluation of a sterol quantitation method for in vitro susceptibility testing of fluconazole and itraconazole against trailing and nontrailing *candida* isolates. *Antimicrobial Agents and Chemotherapy*, *46*(8), 2477–2481. https://doi.org/10.1128/aac.46.8.2477-2481.2002

44. Chopra, I., & Roberts, M. (2001). Tetracycline antibiotics: Mode of action, applications, molecular biology, and epidemiology of bacterial resistance. *Microbiology and Molecular Biology Reviews*, *65*(2), 232–260. https://doi.org/10.1128/mmbr.65.2.232-260.2001

45. Richards, D. M., & Brogden, R. N. (1985). Ceftazidime. *Drugs*, *29*(2), 105–161. https://doi.org/10.2165/00003495-198529020-00002

46. Motro, Y., & Moran-Gilad, J. (2017). Next-generation sequencing applications in clinical bacteriology. *Biomolecular Detection and Quantification*, *14*, 1–6. https://doi.org/10.1016/j.bdq.2017.10.002

Investigation of the Effects of Mutating Iron-Coordinating Residues in Rieske Dioxygenases

Phillip C. Betts

Jordan T. Froese*

Department of Chemistry, Ball State University, Muncie, IN 47306

Abstract

Rieske dioxygenases are multi-component enzyme systems, naturally found in many soil bacteria, that have been widely applied in the production of fine chemicals, owing to the unique and valuable oxidative dearomatization reactions they catalyze. The range of practical applications for these enzymes in this context has historically been limited, however, due to their limited substrate scope and strict selectivity. To overcome these limitations, our research group has employed the tools of enzyme engineering to expand the substrate scope or improve the reactivity of these enzyme systems in specific contexts. Traditionally, enzyme engineering campaigns targeting metalloenzymes have avoided mutations to metal-coordinating residues, based on the assumption that these residues are essential for enzyme activity. Inspired by the success of other recent enzyme engineering reports, our research group investigated the potential to alter or improve the reactivity of Rieske dioxygenases by altering or eliminating iron coordination in the active site of these enzymes. Herein, we report the modification of all three iron-coordinating residues in the active site of toluene dioxygenase both to alternate residues capable of coordinating iron, and to a residue that would eliminate iron coordination. The enzyme variants produced in this way were tested for their activity in the *cis*-dihydroxylation of a small library of potential aromatic substrates. The results of these studies demonstrated that all three iron-coordinating residues, in their natural state, are essential for enzyme activity in toluene dioxygenase, as the introduction of any mutations at these sites resulted in a complete loss of *cis*-dihydroxylation activity for all substrates tested.

Keywords: Rieske dioxygenase, toluene dioxygenase, oxidative dearomatization, green chemistry, enzyme engineering, bioremediation

Manuscript received 8 April 2023; accepted 19 May 2023

Fine Focus, 10(1), 90-108. doi: 10.33043/FF.10.1.90-108.

Introduction

In recent years, the environmentally deleterious effects of the chemical industry have increasingly been recognized, leading to a concerted effort to employ more sustainable methods for the production of fine chemicals (19, 36). These environmentally sustainable chemical methods have collectively been referred to as "green chemistry", which has been defined by a series of principles that serve to guide the application of sustainable chemistry (15, 34). Owing to this increased focus on green chemistry, the application of enzymes as catalysts in the chemical industry has grown in popularity (7). Enzymatic catalysts are entirely biodegradable, they operate in aqueous media as opposed to petroleum-derived solvents, they do not require high-temperature applications, and they are produced from renewable resources, complying with many of the principles of green chemistry (15, 34).

One class of enzymes that have been widely applied as catalysts in the production of fine chemicals are the Rieske dioxygenases (16, 23). Rieske dioxygenases are non-heme iron dioxygenases that are commonly found in soil bacteria (39). These enzymes have frequently evolved as a means for soil bacteria to metabolize aromatic pollutants in their environment and to use these pollutants as carbon and energy sources (**Figure 1**) (12, 42). The ability of these enzymes to catalyze the *cis*-dihydroxylation of aromatics to produce chemically versatile *cis*-diene-diol metabolites with high selectivity has made them very useful catalysts in the production of valuable compounds (16, 23).

Rieske dioxygenases are produced by a wide range of soil bacteria strains, including *Pseudomonas* (42), *Burkholderia* (6), *Nocardioides* (32), and *Comamonas* (22). In fact, metagenomic sequencing studies have revealed that aromatic dioxygenases are ubiquitous, particularly in contaminated environments (17). Owing to their natural role in the remediation of aromatics in the soil and therefore the detoxification of these environments (12,42), these enzymes play crucial roles in soil ecology. Because of this role for Rieske dioxygenases, these enzymes also have tremendous potential for utility in the field of bioremediation, the use of microorganisms to degrade anthropogenic pollutants in an environment. Aromatic pollutants such as benzene and toluene are ubiquitous in the environment and pose significant threats to human health, as these compounds are often

Figure 1

Metabolic pathway by which soil organisms break down aromatic pollutants in their environment (12, 42).

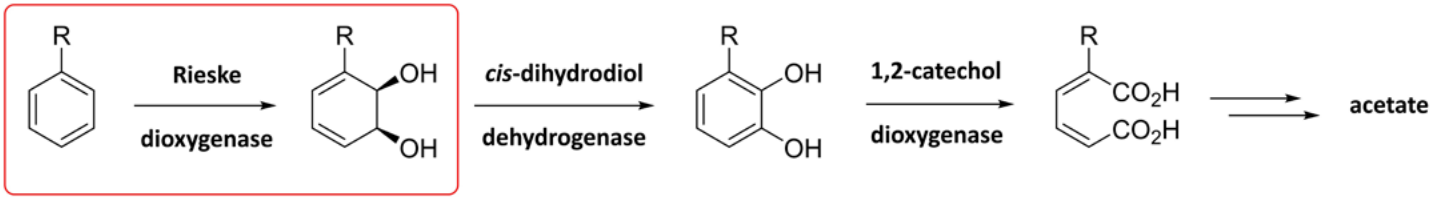

Note. The role of Rieske dioxygenases in this metabolic pathway is highlighted (red).

carcinogenic and endocrine disruptors (4). These aromatic pollutants are frequently introduced into the environment through fossil fuel combustion, oil spills, and the misuse of petroleum products and solvents, creating a need for a means to remove these toxic compounds from the environment (4). To this end, Rieske dioxygenases have been employed as bioremediation catalysts, including applications in the degradation of polychlorinated biphenyls (PCBs), which remain a hazardous presence in many environments (14, 21).

Despite their applications in chemical synthesis and in bioremediation, the utility of Rieske dioxygenases in these contexts has remained limited by their strict selectivity and by their finite substrate scopes. As many Rieske dioxygenases have evolved to metabolize non-polar aromatics, their active sites are organized to effectively bind non-polar substrates and orient them for 2,3-dihydroxylation (9, 18, 28). This results in the substrate scopes and the activities of these enzymes being restricted by the size and by the electronics of any potential substrates (10, 35). To alleviate these restrictions on the utility of Rieske dioxygenases, multiple research groups have applied the tools of enzyme engineering to improve their reactivity or to expand their substrate scopes (5, 3, 11, 20, 26, 33, 37, 38). This has included studies that have engineered Rieske dioxygenases specifically to improve their utility in the bioremediation of aromatic pollutants in the soil (1, 21). Our lab has recently reported the development of improved Rieske dioxygenase variants through the application of rational enzyme engineering (27). These studies have led to the development of Rieske dioxygenases with improved reactivity or expanded substrate scopes, increasing the practical utility of these green chemical tools (1, 3, 5, 11, 20, 21, 26, 27, 33, 37, 38).

When engineering metalloenzymes, studies have traditionally avoided mutations to the residues responsible for coordinating metal ions, based upon the assumption that these residues are essential for enzyme activity. Recently, however, studies have shown this assumption to be incorrect (29, 40). These studies have shown that mutations altering, or even eliminating, iron coordination in heme proteins can alter or improve the reactivity of these proteins in specific contexts (29, 40). Our laboratory was inspired by these studies to investigate whether a similar strategy could result in the development of improved Rieske dioxygenase variants. To our knowledge, no such study has been reported for Rieske dioxygenases, thus this investigation would serve to inform future engineering studies performed with this enzyme class. Based upon reported results with other metalloenzymes (29, 40), it is predicted that mutating the iron-coordinating residues of a Rieske dioxygenase enzyme will result in altered enzyme activity and/or substrate scope. This strategy has the potential to improve the activity of Rieske dioxygenases for specific substrates or expand their substrate scopes.

Materials and Methods

General Experimental

E. coli BL21 (DE3) competent cells were obtained from ThermoFisher. Plasmid isolation/purification was performed using New

Table 1

Sequences of mutagenic primers used.

Primer Name	Primer Sequence
TDO H222A fwd	CGACATGTAC**GCG**GCCGGGACGACCTCGCATCTGTCTGGCATCCTG
TDO H222A rev	GTCGTCCCGGC**CGC**GTACATGTCGCTGCAAAACTGCTCTGCGGCG
TDO H222C fwd	CGACATGTAC**TGC**GCCGGGACGACCTCGCATCTGTCTGGCATCCTG
TDO H222C rev	GTCGTCCCGGC**GCA**GTACATGTCGCTGCAAAACTGCTCTGCGGCG
TDO H222D fwd	CGACATGTAC**GAT**GCCGGGACGACCTCGCATCTGTCTGGCATCCTG
TDO H222D rev	GTCGTCCCGGC**ATC**GTACATGTCGCTGCAAAACTGCTCTGCGGCG
TDO H222E fwd	CGACATGTAC**GAA**GCCGGGACGACCTCGCATCTGTCTGGCATCCTG
TDO H222E rev	GTCGTCCCGGC**TTC**GTACATGTCGCTGCAAAACTGCTCTGCGGCG
TDO H228A fwd	GACGACCTCG**GCG**CTGTCTGGCATCCTGGCAGGCCTGCCAGAAGAC
TDO H228A rev	GATGCCAGACAG**CGC**CGAGGTCGTCCCGGCATGGTACATGTCGCTGC
TDO H228C fwd	GACGACCTCG**TGC**CTGTCTGGCATCCTGGCAGGCCTGCCAGAAGAC
TDO H228C rev	GATGCCAGACAG**GCA**CGAGGTCGTCCCGGCATGGTACATGTCGCTGC
TDO H228D fwd	GACGACCTCG**GAT**CTGTCTGGCATCCTGGCAGGCCTGCCAGAAGAC
TDO H228D rev	GATGCCAGACAG**ATC**CGAGGTCGTCCCGGCATGGTACATGTCGCTGC
TDO H228E fwd	GACGACCTCG**GAA**CTGTCTGGCATCCTGGCAGGCCTGCCAGAAGAC
TDO H228E rev	GATGCCAGACAG**TTC**CGAGGTCGTCCCGGCATGGTACATGTCGCTGC
TDO D376A fwd	CGAGCAGGAC**GCG**GGGGAGAACTGGGTCGAGATCCAGCACATCCTG
TDO D376A rev	CAGTTCTCCCC**CGC**GTCCTGCTCGAACACGCCACCGGCAGAGAAGG
TDO D376C fwd	CGAGCAGGAC**TGC**GGGGAGAACTGGGTCGAGATCCAGCACATCCTG
TDO D376C rev	CAGTTCTCCCC**GCA**GTCCTGCTCGAACACGCCACCGGCAGAGAAGG
TDO D376E fwd	CGAGCAGGAC**GAA**GGGGAGAACTGGGTCGAGATCCAGCACATCCTG
TDO D376E rev	CAGTTCTCCCC**TTC**GTCCTGCTCGAACACGCCACCGGCAGAGAAGG
TDO D376H fwd	CGAGCAGGAC**CAT**GGGGAGAACTGGGTCGAGATCCAGCACATCCTG
TDO D376H rev	CAGTTCTCCCC**ATG**GTCCTGCTCGAACACGCCACCGGCAGAGAAGG

England Biolabs Monarch® miniprep kit. Transformations of electrocompetent cells were performed on an Eppendorf Eporator®. Whole-cell assay cultures were grown in Greiner Bio-One polystyrene clear, round-bottom 96-well plates. All cultures were incubated in a Barnstead MaxQ 4000 Digital Orbital Incubator Shaker equipped with an Enzyscreen universal clamp system unless otherwise stated. Fluorescence analyses were performed using a Biotek® Synergy™ H1 monochromator-based multi-mode plate reader, using Corning® polystyrene black, opaque, flat-bottom 96-well plates. All reagents were obtained from MilliporeSigma unless otherwise stated. Media were made at pH 7.2 and streptomycin was added at 50 μg mL^{-1}. All *E. coli* cultures were maintained at 37 °C unless otherwise stated.

Targeted Mutagenesis Protocol

The pCP-02 expression system was used as the template for toluene dioxygenase mutant generation (30). Saturation mutagenesis was performed following the polymerase chain reaction (PCR)-based procedure of Liu and Naismith (24, 41). Amplification was performed using an ABI GeneAmp® 9700 Thermal Cycler and Q5® DNA polymerase (New England Biolabs). Mutagenic primers were designed according to the procedure of Liu and Naismith (24, 41). Primer sequences are shown below (**Table 1**). Parameters for the relevant PCR reactions are shown below (**Table 2**). Sequencing analyses were performed by Eurofins Genomics© (Louisville, KY).

Whole-cell fermentation 96 well-plate assay protocol

E. coli (BL21 (DE3)) electrocompetent cells were transformed with isolated pCP-02 plasmids expressing toluene dioxygenase (parent and/or mutant libraries), and with isolated pCP-01 plasmids as negative controls (30). The transformation cultures were selected on LB + streptomycin plates overnight. Single colonies were inoculated into 160 μL LB + streptomycin media with 0.3% glucose in a 96-well round bottom seed plate and incubated

Table 2

PCR reaction components and thermocycling protocol utilized for the generation of toluene dioxygenase mutants.

PCR reaction components	Thermocycling protocol
Sterile H2O – 22.5 μL	98 °C – 30 s
Q5® reaction buffer – 10 μL	98 °C – 10 s
Q5® high GC enhancer – 10 μL	72 °C – 4 min } x20
dNTPs (10 mM) – 1 μL	72 °C – 2 min
Forward primer (10 μM)- 2.5 μL	
Reverse primer (10 μM)- 2.5 μL	
Template DNA (pCP-02) – 1 μL	
Q5® DNA polymerase – 0.5 μL	
Total – 50 μL	

with shaking overnight. All plates included 3 or more wells containing *E. coli* (BL21 (DE3)) pCP-02 cells expressing the parent toluene dioxygenase enzyme, and 3 or more wells containing *E. coli* (BL21 (DE3)) pCP-01 (negative control) (30). Seed plates were used to inoculate 5 μL into 155 μL LB media containing streptomycin in a fresh 96-well round bottom assay plate, and the cultures were incubated with shaking for 2.75 h. The assay plates were then pelleted, and the supernatant discarded. Cultures were resuspended in 150 μL minimal media (KH_2PO_4 – 7.5 g L^{-1}; citric acid – 2 g L^{-1}; $MgSO_4 \cdot 7H_2O$ – 5 g L^{-1}; trace metal solution – 2 mL L^{-1} [Na_2SO_4 – 1 g L^{-1}; $MnSO_4$ – 2 g L^{-1}; $ZnCl_2$ – 2 g L^{-1}; $CoCl_2 \cdot 6H_2O$ – 2 g L^{-1}; $CuSO_4 \cdot 5H_2O$ – 0.3 g L^{-1}; $FeSO_4 \cdot 7H_2O$ – 10 g L^{-1}; pH 1.0]; conc. H_2SO_4 – 1.2 mL L^{-1}; ferric ammonium citrate – 0.3 g L^{-1}; glucose – 4 g L^{-1}; thiamine – 0.034 g L^{-1}; pH 7.2) (8) containing streptomycin and incubated for a 1 h recovery period. Following this, the cultures were induced to a final concentration of 0.5 mM IPTG and the incubation temperature was reduced to 30 °C. After a 2 h induction period, aromatic substrates were added as 68 mM stock solutions in DMSO to a final concentration of 2 mM. Cultures were incubated with aromatic substrates for 1.5 h at 30 °C, after which the cultures were pelleted. A 100 μL portion of supernatant from each well was transferred to 96-well black opaque assay plates. The reaction was initiated by adding a 50 μL of $NaIO_4$ stock solution to each well to a final concentration of 10 mM, and the assay plates were incubated with shaking at room temperature for 30 min. Cleaved diols were detected by adding 50 μL of fluoresceinamine solution (prepared with 3 μL conc. HCl (11.65 M)/1 mL fluoresceinamine solution) to each well to a final concentration of 0.1 mM (30). Assay plates were incubated with shaking at room temperature for 5 h. The fluorescence response from each well was analyzed at 485 nm (ex), 520 nm (em), and normalized to the mean fluorescence response of the negative controls ($[I - I_0]/I_0$).

Results

Identification of Iron-Coordinating Residues

Because our lab has extensive experience working with toluene dioxygenase (TDO) (27, 30), and because TDO has been one of the most widely used Rieske dioxygenases in the field of organic synthesis (16), this enzyme was selected as the template for mutagenesis in this study. To identify the residues that would be targeted for mutagenesis, the reported crystal structure of toluene dioxygenase was analyzed using the molecular visualization software ChimeraX (9, 13). This analysis revealed that the catalytic iron atom of toluene dioxygenase is coordinated by two histidine residues (HIS222 and HIS228) and by one aspartate residue (ASP376) (**Figure 1**). These residues were therefore determined to be the appropriate targets for mutagenesis in this study.

Production of Targeted Toluene Dioxygenase Variants

To test the hypothesis of this study, it was determined that each iron-coordinating residue of TDO would be mutated to three alternate residues capable of coordinating iron (aspartate, glutamate, and cysteine for native histidine residues; glutamate, cysteine, and histidine for the native aspartate residue) and to one residue that would eliminate iron-coordination at that

Figure 2

Visualization of the TDO active site with bound substrate (toluene, purple) (9).

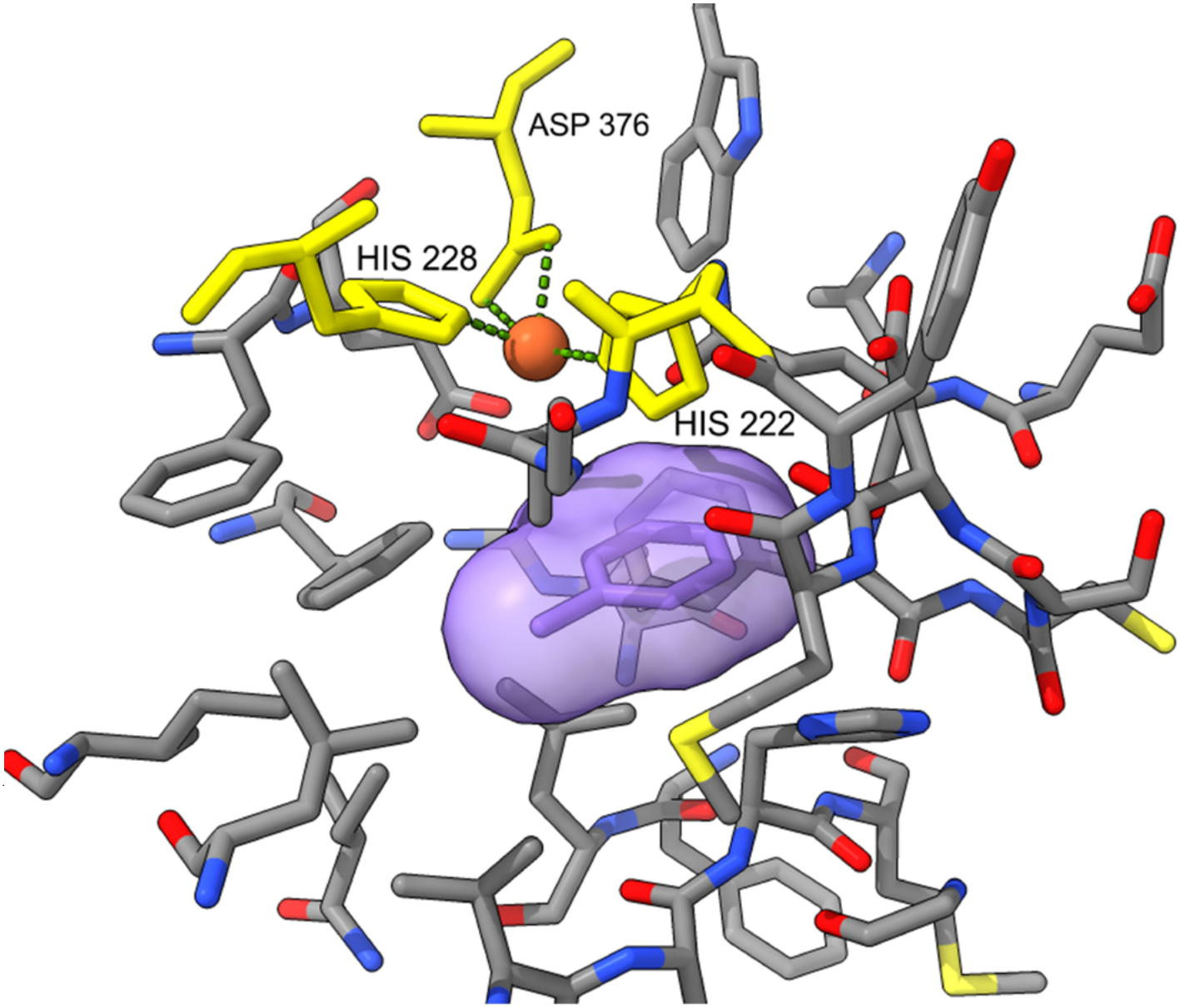

site (alanine). To generate the desired variants of toluene dioxygenase, targeted mutations were introduced through the PCR-based method of Liu and Naismith (24, 41). Mutagenic primers were designed according to this well-established protocol (**Table 1**), and the corresponding mutagenic PCR reactions were carried out as described. The successful introduction of the targeted mutations was confirmed through sequencing analysis performed by a third-party contractor. Representative aligned sequencing data is shown for the H222 mutants in **Figure 3**. Upon completion of this work, expression systems had been developed for twelve novel toluene dioxygenase variants with mutations introduced at the iron-coordinating residues (H222A, H222C, H222D, H222E, H228A, H228C, H228D, H228E, D376A, D376C, D376E, D376H).

Figure 3

Multiple sequence alignment of sequencing data from TDO variants with single active site mutations.

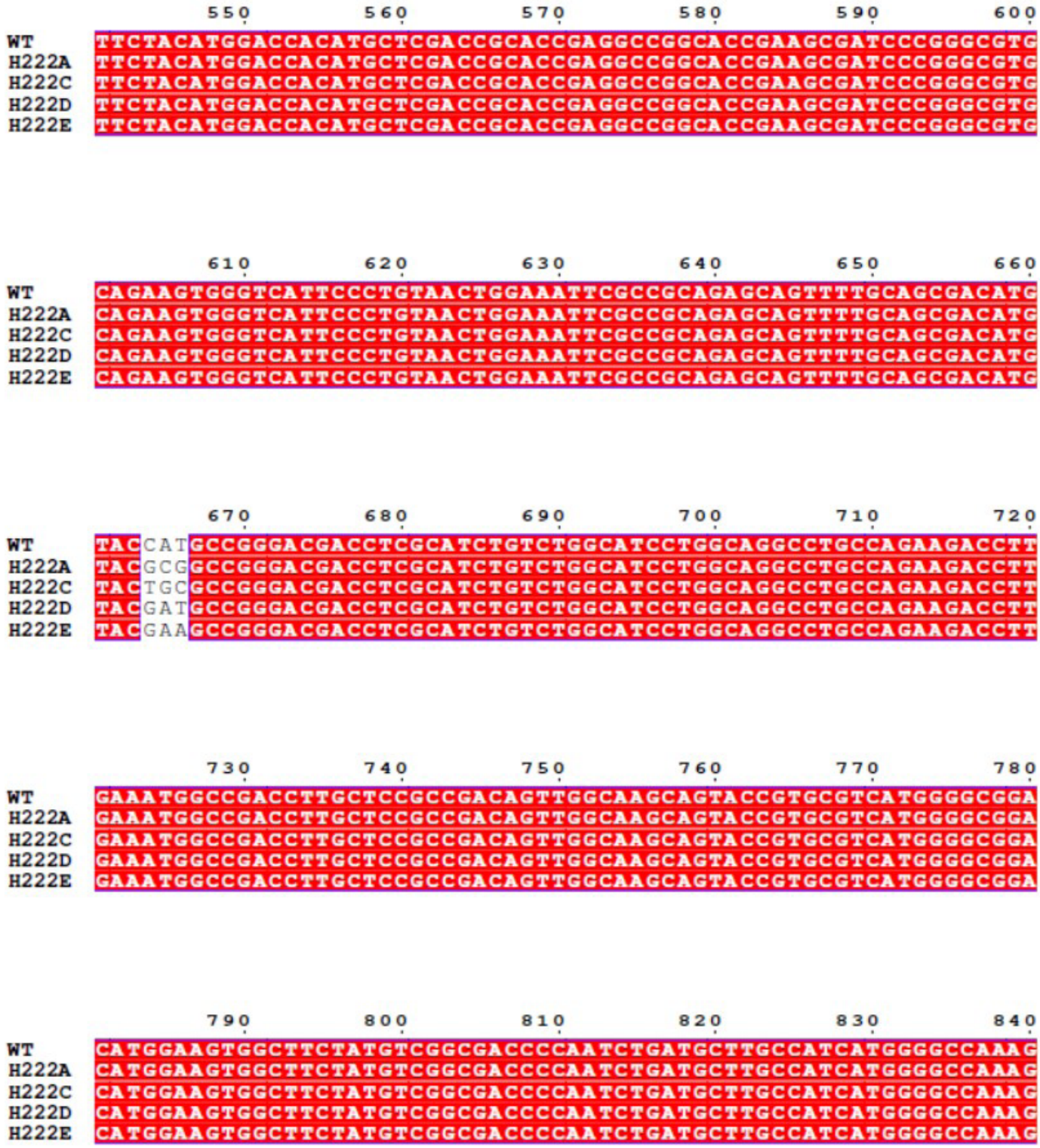

Figure 4

Coupled reactions employed by the fluorescence-based assay to detect and quantify the cis*-diol metabolites produced by active dioxygenases (30).*

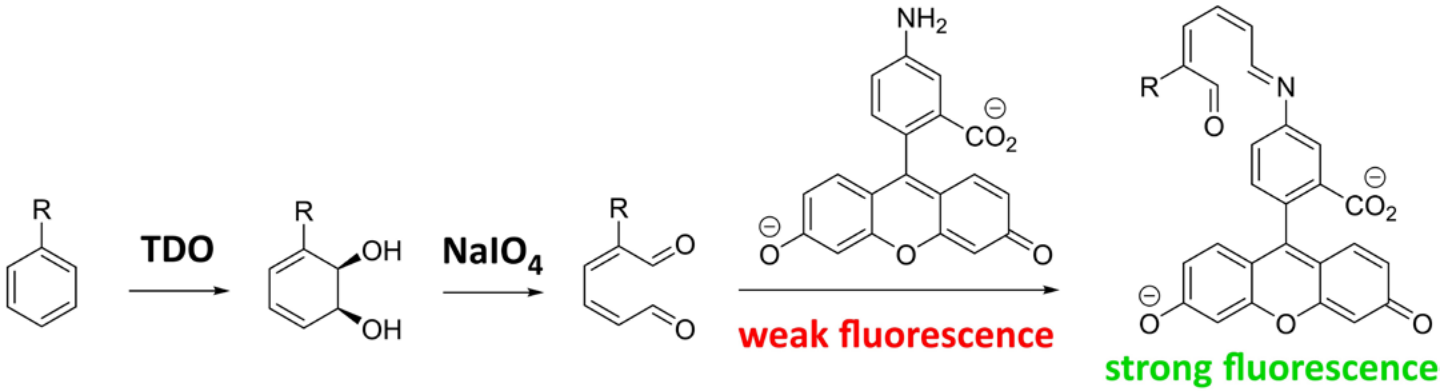

Screening of Toluene Dioxygenase Variants

To test the *cis*-dihydroxylation activity of the TDO variants produced in this study, a fluorescence-based assay that had previously been reported by our laboratory was applied (30). This assay, performed in 96-well plates, detects the presence of *cis*-diol metabolites produced by active dioxygenases in the bacterial growth media through the conversion of the *cis*-diol metabolites to a corresponding dialdehyde, and subsequent conjugation of the dialdehyde to a fluorescent probe (30) (**Figure 4**). In this way, the amount of fluorescence detected in each well provides information as to the amount of *cis*-diol metabolite produced by the enzyme variant present in the corresponding well.

As the possibility existed that the introduced mutations would cause the structure of the TDO active site to be altered, while retaining some *cis*-dihydroxylation activity, it was determined that the enzyme variants should be tested on a small library of diverse aromatic substrates (**Figure 5**). This would afford the opportunity to determine the effect of the introduced mutations on the enzyme's activity for a wide range of substrates, including those the native enzyme has high activity for, those the native enzyme has low activity for, and those the native enzyme has no activity for.

To test the *cis*-dihydroxylation activity of the designed TDO variants, vectors expressing each set of variants were separately transformed into *E. coli* (BL21 (DE3)) alongside vectors expressing the parent enzyme (pCP-02) and a negative control (pCP-01) (30). Six colonies expressing each variant were then inoculated into separate wells of a 96-well plate and cultured according to an optimized assay protocol (30), before being treated with the relevant aromatic substrate. Following an incubation period in the presence of the relevant substrate, the cells were removed, and the growth media was carried through the fluorescence-based assay protocol (**Figure 4**). Analysis of the resultant data from these assays revealed that all twelve of the designed TDO variants (H222A, H222C, H222D, H222E, H228A, H228C, H228D, H228E, D376A, D376C, D376E, D376H) lacked any activity for all eight substrates used in the screens (**Figure 6**). This included a

complete loss of activity for the native substrate (toluene), and other substrates for which the native enzyme possesses activity (benzyl alcohol, benzyl acetate, *n*-butyl benzene, *t*-butyl benzene, methyl benzoate) and no gain in activity for substrates that are not metabolized by the parent enzyme (benzyl acetamide and benzylamine) (**Figure 6**).

Discussion

To study the effect of mutating the iron-coordinating residues of Rieske dioxygenases on the activity of these enzymes, the first step was to select a member of this class of enzymes to act as the template for mutagenesis. Toluene dioxygenase (TDO) is a well-characterized member of the Rieske dioxygenase enzyme family, which is derived from the soil bacterium *Pseudomonas putida* F1 (42). Due to the historic importance of TDO in the production of valuable compounds (16), and because of our laboratory's experience working with this Rieske dioxygenase system (27, 30), TDO was chosen as the engineering scaffold for this study. Due to the structural similarity observed with many Rieske dioxygenases (2), the results of this study would be expected to be applicable across many members of this enzyme family.

The goals of this study were to investigate the effects of both altering and eliminating the iron-coordination of key residues in the active site of toluene dioxygenase. As TDO has been well characterized (9), the identification of the iron-coordinating residues of this enzyme (HIS222/HIS228/ASP376) using ChimeraX (13) was trivial (**Figure 2**). To effectively test the hypothesis of this study, it was determined

Figure 5

Aromatic substrates used to screen for cis*-dihydroxylation activity among the TDO mutants produced.*

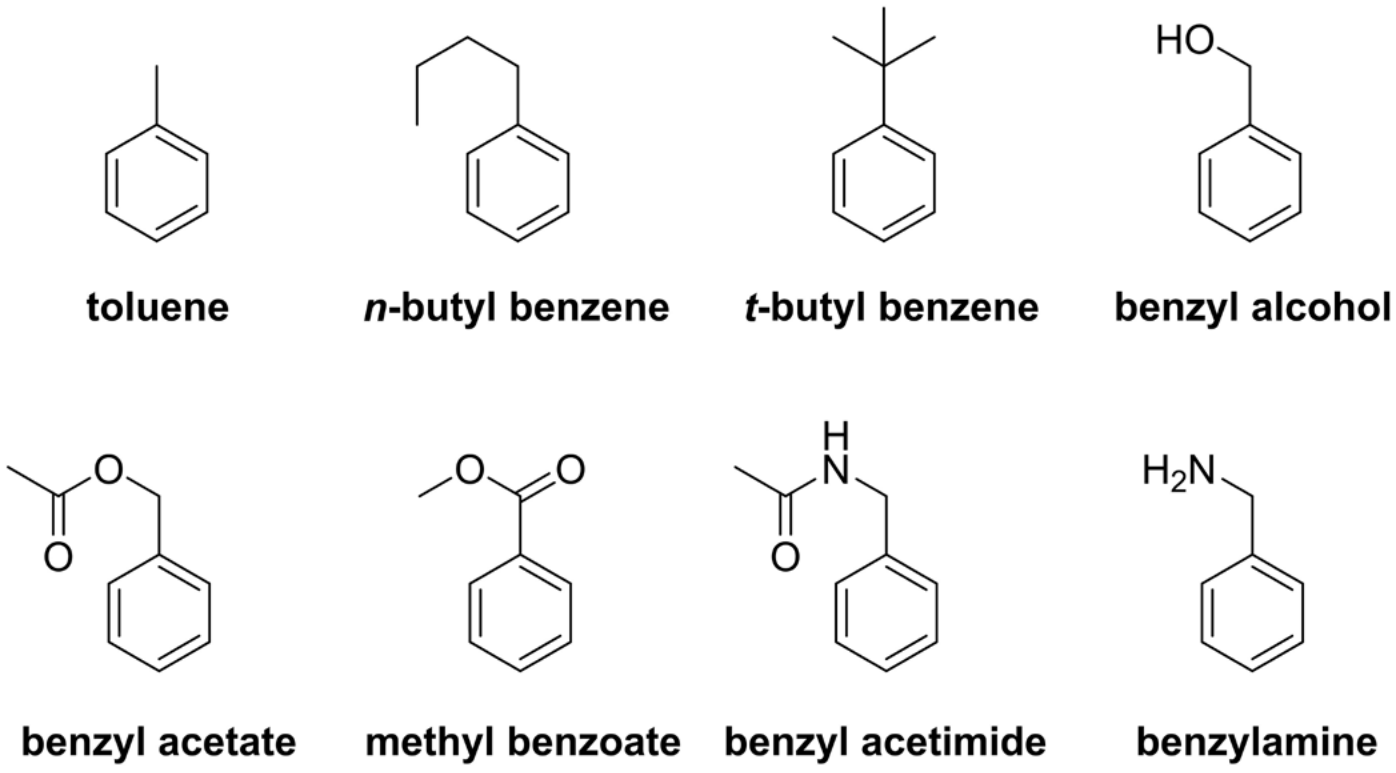

Figure 6

cis-*Dihydroxylation activity of H222 TDO variants (***A***), H228 TDO variants (***B***) and D376 TDO variants (***C***) for representative aromatic substrates* (n = *6*).

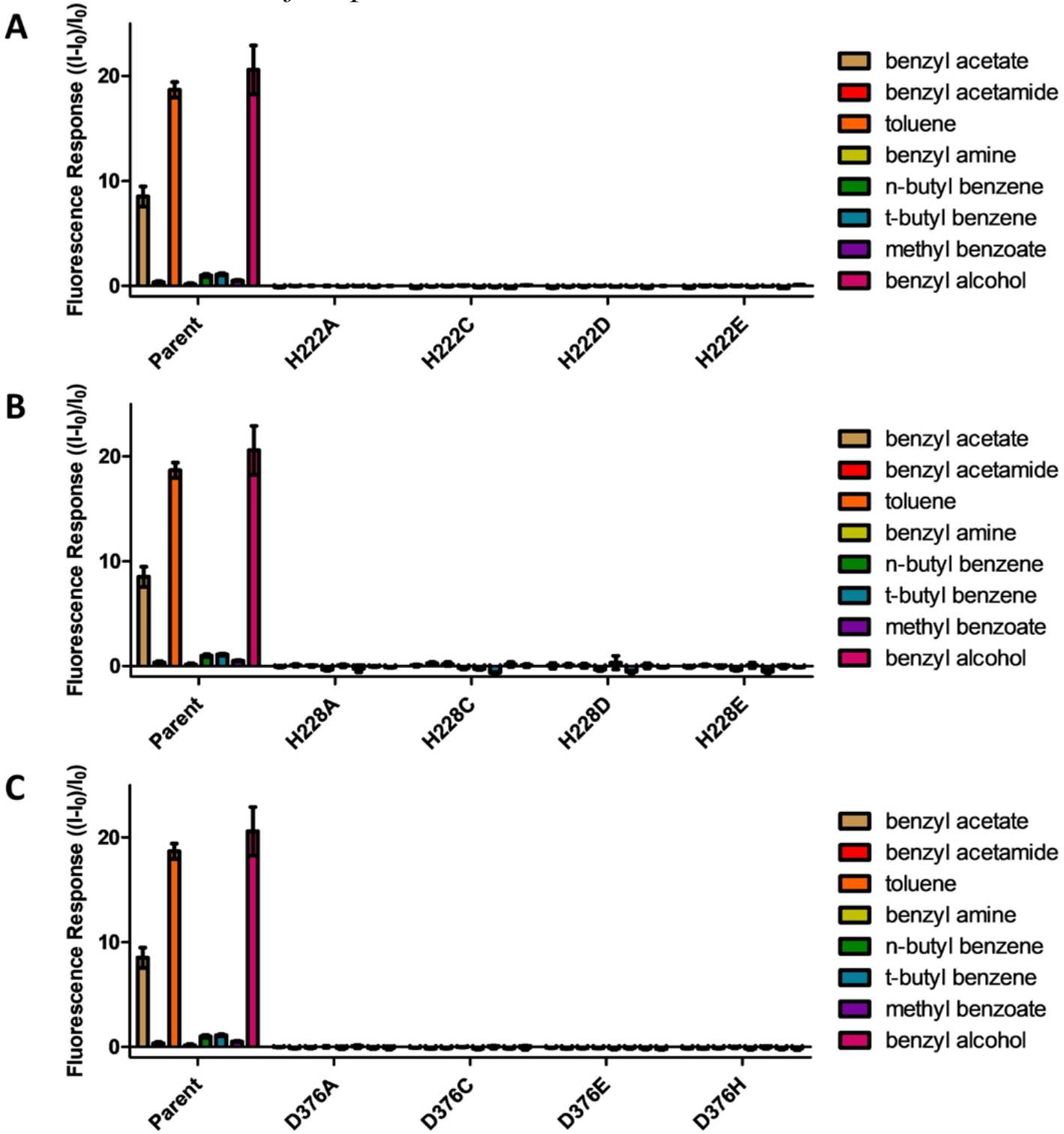

Note. Fluorescence response was normalized to the mean fluorescence response of the negative control (*E. coli* BL21 (DE3) pCP-01) ($[I - I_0]/I_0$) (21). Parent activity was determined from positive controls (*E. coli* BL21 (DE3) pCP-02), with the fluorescence response normalized to the negative control ($[I - I_0]/I_0$) (30).

that all three of the residues coordinating the catalytic iron would be mutated to three alternate residues capable of coordinating iron (aspartate, glutamate, and cysteine for native histidine residues; glutamate, cysteine, and histidine for the native aspartate residue) and to one residue that would eliminate iron-coordination at that site (alanine). This afforded the opportunity to evaluate the effects not only of eliminating iron coordination at specific sites, but also the potential beneficial effects of remodeling the active site and/or altering the electronics of the catalytic iron center by changing the iron coordinating residues while maintaining iron coordination.

Once the successful generation of the targeted TDO variants had been confirmed, the next step was to test the *cis*-dihydroxylation activity of these variants. As the possibility existed that the introduced mutations would cause the structure of the TDO active site to be altered, while retaining some *cis*-dihydroxylation activity, it was determined that the enzyme variants should be tested on a small library of diverse aromatic substrates. These aromatic substrates included the native substrate (toluene), one polar substrate for which the native enzyme possesses high activity (benzyl alcohol), one polar substrate for which the native enzyme possesses moderate activity (benzyl acetate), three polar substrates for which the native enzyme possess little or no activity (methyl benzoate, benzyl acetamide, and benzylamine), and two sterically bulky substrates for which the native enzyme possesses low activity (*n*-butyl benzene and *t*-butyl benzene) (**Figure 5**). By testing the activity of the designed mutants across these substrates, it would be possible to determine whether the introduced mutations had advantageous or detrimental effects in the *cis*-dihydroxylation of the native substrate, as well as in the *cis*-dihydroxylation of both sterically bulky and polar classes of substrates.

Upon testing the activity of each designed TDO mutant for all the designated substrates, it was revealed that none of the mutants designed in this study possessed activity for any of the diverse substrates selected (**Figure 6**). These results revealed the critical role played by the iron-coordinating residues of Rieske dioxygenases in their native state, as any alteration of these residues, either to other residues with the potential for iron-coordination or to residues incapable of coordinating iron, resulted in complete ablation of enzyme activity. Although the hypothesis that the mutations introduced in this study would significantly alter the activity and/or substrate scope of the enzyme was proven correct, these changes were shown not to be beneficial for enzyme activity. The loss of activity observed with mutations to non-coordinating alanine likely indicates that coordination by three residues is essential for iron to be bound to the active site of Rieske dioxygenases in a catalytically active state. The loss of activity observed with mutations to alternate iron-coordinating resides may indicate that these alterations result in a significant remodeling of the active site that prevents iron from binding in a catalytically active state. Alternately, these results may indicate that the active site iron of Rieske dioxygenases must specifically be bound by two histidine residues and one aspartate residue to effectively participate in the catalytic mechanism. Further studies, including enzyme structure elucidation/homology modeling,

docking analysis, and molecular dynamics simulations are required to precisely elucidate the cause of the loss of activity observed from these alterations to the iron-coordinating residues. These studies will be performed in due course.

Although this study did not succeed in producing novel TDO variants with improved or expanded activity, the results described will serve to guide future studies targeting the engineering of Rieske dioxygenases. With the increasing recognition of the need to employ more sustainable techniques in the chemical industry, and to remove harmful pollutants in contaminated environments, the field of enzyme engineering will continue to increase in importance. This is reflected in the fact that the engineering of Rieske dioxygenases to improve their utility either as green-chemical catalysts or as tools for the bioremediation of contaminated environments continues to be an active area of research (1, 3, 5, 20, 21, 26, 27, 33, 37, 38). Metagenomics research has shown that Rieske dioxygenases commonly evolve among soil bacteria (17), meaning that many unannotated Rieske dioxygenases remain to be studied in the context of enzyme engineering. As the field of microbiology continues to discover more diverse organisms and the powerful natural catalysts they produce, these new catalysts will provide valuable templates for the field of enzyme engineering. In this way, the natural ecological role of soil organisms can be harnessed and enhanced to create a safer and more sustainable future. This study, by demonstrating the importance of preserving key active site residues in the generation of Rieske dioxygenase mutant libraries in the pursuit of enzyme engineering, will inform and expedite these efforts.

Conclusions

Inspired by recent reports that have shown that the alteration of iron-coordinating residues in metalloenzymes can alter or even improve the activity of these enzymes in certain contexts (29, 40), the iron-coordinating residues of toluene dioxygenase (TDO) were comprehensively mutated in this study. These residues were mutated both to alternate residues that are capable of coordinating iron and to a residue that is incapable of iron coordination. Following the confirmation of successful mutagenesis, these new TDO variants were tested for their ability to catalyze the *cis*-dihydroxylation of a diverse group of potential aromatic substrates through a fluorescence-based assay system (30). The results of this study demonstrated the critical role played by the iron-coordinating residues of Rieske dioxygenases in their native state. These results revealed that any alteration of these residues, either to other residues with the potential for iron-coordination or to a residue incapable of coordinating iron, resulted in a complete loss of *cis*-dihydroxylation activity for any of the classes of substrates tested in this study. Although this study did not produce any Rieske dioxygenase variants with improved or altered *cis*-dihydroxylation activity, the findings of this study will serve to inform future engineering studies targeting these enzymes. Based on these results, it is clear that any attempts to engineer novel variants of Rieske dioxygenases should make every effort to preserve the iron-coordinating residues in their native state.

Acknowledgements

This material is based upon work supported by the National Science Foundation under Grant No. 2147098 (Research in Undergraduate Institutions) and by the Ball State University Junior Faculty ASPiRE grant program. This work was made possible in part by the Ball State University Provost Start-Up program.

Author Correspondence

Correspondence concerning this article should be addressed to: Jordan T. Froese, jtfroese@bsu.edu.

References

1. Ang, E. L., Obbard, J. P., & Zhao, H. M. (2009) Directed evolution of aniline dioxygenase for enhanced bioremediation of aromatic amines. Applied Microbiology and Biotechnology, 81, 1063-1070. https://doi.org/10.1007/s-00253-008-1710-0

2. Bagneris, C.; Cammack, R.; & Mason, J. R. (2005) Subtle Difference between Benzene and Toluene Dioxygenases of *Pseudomonas putida*. Applied and Environmental Microbiology, 71, 1570-1580. https://doi.org/10.1128/AEM.71.3.1570-1580.2005

3. Bernath-Levin, K., Shainsky, J., Sigawi, L., & Fishman, A. (2014) Directed evolution of nitrobenzene dioxygenase for the synthesis of the antioxidant hydroxytyrosol. Applied Microbiology and Biotechnology, 98, 4975-4985. https://doi.org/10.1007/s00253-013-5505-6

4. Bolden, A. L., Kwiatkowski, C. F., & Colborn, T. (2015) New Look at BTEX: Are Ambient Levels a Problem? Environmental Science and Technology, 49, 5261-5276. https://doi.org/10.1021/es505316f

5. Brimberry, M., Garcia, A. A., Liu, J., Tian, J., & Bridwell-Rabb, J. (2023) Engineering Rieske oxygenase activity one piece at a time. Current Opinion in Chemical Biology, 72, 102227. https://doi.org/10.1016/j.cbpa.2022.102227

6. Chang, H. K. & Zylstra, G. J. (1998) Novel organization of the genes for phthalate degradation from *Burkholderia cepacia* DBO1. Journal of Bacteriology, 180, 6529-6537. https://doi.org/10.1128/JB.180.24.6529-6537.1998

7. Cipolatti, E. P., Pinto, M. C. C., Henriques, R. O., Pinto, J. C. C., Castro, A. M., Freire, D. M. G., & Manoel, E. A. (2019) in Advances in Enzyme Technology (Eds.: Singh, R. S.; Singhania, R. R.; Pandey, A.; Larroche, C.) Amsterdam: Elsevier, p. 137-151.

8. Endoma, M. A., Bui, V. P., Hansen, J., Hudlicky, T. (2002) Medium-scale preparation of useful metabolites of aromatic compounds via whole-cell fermentation with recombinant organisms. Organic Process Research and Development, 6, 525-532. https://doi.org/10.1021/op020013s

9. Friemann, R., Lee, K., Brown, E. N., Gibson, D. T., Eklund, H., & Ramaswamy, S. (2009) Structures of the multicomponent Rieske non-heme iron toluene 2,3-dioxygenase enzyme system. Acta Crystallographica, D65, 24. https://doi.org/10.1107/S0907444908036524

10. Froese, J., Endoma-Arias, M.-A., Hudlicky, T. (2014) Processing of *o*-halobenzoates by toluene dioxygenase. The role of the alkoxy functionality in the regioselectivity of the enzymatic dihydroxylation reaction. Organic Process Research and Development, 18, 801–809. https://doi.org/10.1021/op400343c

11. a) Gally, C., Nestl, B. M., & Hauer, B. (2015) Engineering rieske non-heme iron oxygenases for the asymmetric dihydroxylation of alkenes. Angewandte Chemie, International Edition, 54, 12952-12956. https://doi.org/10.1002/anie.201506527; b) Halder, J. M., Nestl, B. M., & Hauer, B. (2018) Semirational engineering of the naphthalene dioxygenase from *Pseudomonas* sp. NCIB 9816-4 towards selective asymmetric dihydroxylation. ChemCatChem, 10, 178. https://doi.org/10.1002/cctc.201701262; c) Heinemann, P. M., Armbruster, D., & Hauer, B. (2021) Active-site loop variations adjust activity and selectivity of the cumene dioxygenase. Nature Communications, 12, 1095. https://doi.org/10.1038/s41467-021-21328-8; d) Wissner, J. L., Escobedo-Hinojosa, W., Vogel, A., & Hauer, B. (2021) An engineered toluene dioxygenase for a single step biocatalytical production of (-)-(1S,2R)-cis-1,2-dihydro-1,2-naphthalenediol. Journal of Biotechnology, 326, 37-39. https://doi.org/10.1016/j.jbiotec.2020.12.007; e) Wissner, J. L., Schelle, J. T., Escobedo-Hinojosa, W., Vogel, A., & Hauer, B. (2021) Semi-rational engineering of toluene dioxygenase from *Pseudomonas putida* F1 towards oxyfunctionalization of Bicyclic Aromatics. Advanced Synthesis and Catalysis, 363, 37, 4905-4914. https://doi.org/10.1002/adsc.202100296

12. Gibson, D. T., Koch, J. R., Schuld, C. L., & Kallio, R.E. (1968) Oxidative degradation of aromatic hydrocarbons by microorganisms. II. Metabolism of halogenated aromatic hydrocarbons. Biochemistry, 7, 3795-3802. https://doi.org/10.1021/bi00851a003

13. Goddard, T. D., Huang, C. C., Meng, E. C., Pettersen, E. F., Couch, G. S., Morris, J. H., & Ferrin, T. E. (2018) UCSF ChimeraX: Meeting modern challenges in visualization and analysis. Protein Science, 27, 14–25. https://doi.org/10.1002/pro.3235

14. Gómez-Gil, L., Kumar, P., Barriault, D., Bolin, J. T., Sylvestre, M., & Eltis, L. D. (2007) Characterization of biphenyl dioxygenase of *Pandoraea pnomenusa* B-356 as a potent polychlorinated biphenyl-degrading enzyme. Journal of Bacteriology, 189, 5705-5715. https://doi.org/10.1128/JB.01476-06

15. Gujral, S. S., Sheela, M. A., Khatri, S. K., & Singla, R. A. (2012) Focus & Review on the Advancement of Green Chemistry. Indo Global Journal of Pharmaceutical Sciences, 2, 397–408. https://doi.org/10.35652/IGJPS.2012.46

16. Hudlicky, T., & Reed, J. W. (2009) Celebrating 20 years of SYNLETT - Special account on the merits of biocatalysis and the impact of arene *cis*-dihydrodiols on enantioselective synthesis. Synlett, 5, 685-703. https://doi.org/10.1055/s-0028-1087946

17. Iwai, S., Chai, B., Sul, W. J., Cole, J. R., Hashsham, S. A., & Tiedje, J. M. (2010) Gene-targeted-metagenomics reveals extensive diversity of aromatic dioxygenase genes in the environment. The ISME Journal, 4, 279-285. https://doi.org/10.1038/ismej.2009.104

18. Karlsson, A., Parales, J. V., Parales, R. E., Gibson, D. T., Eklund, H., & Ramaswamy, S. (2003) Crystal structure of naphthalene dioxygenase: side-on binding of dioxygen to iron. Science, 299, 1039-1042. https://doi.org/10.1126/science.1078020

19. Kätelhöhn, A., Meys, R., Deutz, S., Suh, S., & Bardow, A. (2019) Climate change mitigation potential of carbon capture and utilization in the chemical industry. Proceedings of the National Academy of Science USA, 116, 11187-11194. https://doi.org/10.1073/pnas.1821029116

20. Kim, D., Yoo, M., Choi, K. Y., Kang, B. S., & Kim, E. (2013) Characterization and engineering of an o-xylene dioxygenase for biocatalytic applications. Bioresource Technology, 145, 123-127. https://doi.org/10.1016/j.biortech.2013.03.034

21. a) Kimura, N., Nishi, A., Goto, M., & Furukawa, K. (1997) Functional analyses of a variety of chimeric dioxygenases constructed from two biphenyl dioxygenases that are similar structurally but different functionally. Journal of Bacteriology, 179, 3936-3943. https://doi.org/10.1128/jb.179.12.3936-3943.1997; b) Kumamaru, T., Suenaga, H., Mitsuoka, M., Watanabe, T., Furukawa, K. (1998) Enhanced degradation of polychlorinated biphenyls by directed evolution of biphenyl dioxygenase. Nature Biotechnology, 16, 663-666. https://doi.org/10.1038/nbt0798-663

22. Lessner, D. J., Johnson, G. R., Parales, R. E., Spain, J. C., Gibson, D. T. (2002) Molecular characterization and substrate specificity of nitrobenzene dioxygenase from *Comamonas* sp. strain JS765. Applied and Environmental Microbiology, 68, 634-641. https://doi.org/10.1128/AEM.68.2.634-641.2002

23. Lewis, S. E. (2016) in Asymmetric Dearomatization Under Enzymatic Conditions (Ed. You, S.-L.), Chichester: Wiley, p. 279-346.

24. Liu, H., Naismith, J. H. (2008) An efficient one-step site-directed deletion, insertion, single and multiple-site plasmid mutagenesis protocol. BMC Biotechnology, 8, 91. https://doi.org/10.1186/1472-6750-8-91

25. Moretti, S., Armougom, F., Wallace, I. M., Higgins, D. G., Jongeneel, C. V., & Notredame, C. (2007) The M-Coffee web server: a meta-method for computing multiple sequence alignments by combining alternative alignment methods. Nucleic Acids Research, 35, W645-W648. https://doi.org/10.1093/nar/gkm333

26. Newman, L. M., Garcia, H., Hudlicky, T., & Selifonov, S. A. (2004) Directed evolution of the dioxygenase complex for the synthesis of furanone flavor compounds. Tetrahedron, 60, 729-734. https://doi.org/10.1016/j.tet.2003.10.105

27. Osifalujo, E. A., Preston-Herrera, C., Betts, P. C., Satterwhite, L. R., & Froese, J. T. (2022) Improving toluene dioxygenase activity for ester-functionalized substrates through enzyme engineering. ChemistrySelect, 7, e202200753. https://doi.org/10.1002/slct.202200753

28. Parales R.E., & Resnick S.M. (2007) in Biodegradation and Bioremediation. Soil Biology, Vol 2. (Eds. Singh, A.; Ward, O. P.) Berlin: Springer, p. 175-195.

29. Pott, M., Tinzl, M., Hayashi, T., Ota, Y., Dunkelmann, D., Mittl, P. R. E., & Hilvert, D. (2021) Noncanonical heme ligands steer carbene transfer reactivity in an artificial metalloenzyme. Angewandte Chemie International Edition, 27, 15063-15068. https://doi.org/10.1002/anie.202103437

30. Preston-Herrera, C., Jackson, A. S., Bachmann, B. O., & Froese, J. T. (2021) Development and Application of a High Throughput Assay System for the Detection of Rieske Dioxygenase Activity. Organic and Biomolecular Chemistry, 19, 775-784. https://doi.org/10.1039/D0OB02412K

31. Robert, X., & Gouet, P. (2014) Deciphering key features in protein structures with the new ENDscript server. Nucleic Acids Research, 42, W320-W324. https://doi.org/10.1093/nar/gku316

32. Saito, A., Iwabuchi, T., Harayama, S. (2000) A novel phenanthrene dioxygenase from Nocardioides sp. strain KP7: expression in *Escherichia coli*. Journal of Bacteriology, 182, 2134-2141. https://doi.org/10.1128/JB.182.8.2134-2141.2000

33. Sakamoto, T., Joern, J. M., Arisawa, A., & Arnold, F. H. (2001) Laboratory evolution of toluene dioxygenase to accept 4-picoline as a substrate. Applied and Environmental Microbiology, 67, 3882-3887. https://doi.org/10.1128/AEM.67.9.3882-3887.2001

34. Sharma, P., Kumar, M., Sharma, A., Arora, D., Patial, A., & Rana, M. (2020) An overview on green chemistry. World Journal of Pharmacy and Pharmaceutical Sciences, 8, 202-208. https://doi.org/10.20959/wjpps20195-13602

35. Sheldrake, G. N. (1992) in Chirality in Industry: the commercial manufacture and application of optically active compounds (Ed. A. N. Collins, G. N. Sheldrake, J. Crosby) Chichester: John Wiley & Sons Ltd, pp. 127–166.

36. Van Geem, K. M., Galvita, V. V., & Marin, G. B. (2019) Making chemicals with electricity. Science, 364, 734-735. https://doi.org/10.1126/science.aax5179

37. Vila, M. A., Umpierrez, D., Veiga, N., Seoane, G., Carrera, I., & Giordano, S. R. (2017) Site-Directed Mutagenesis Studies on the Toluene Dioxygenase Enzymatic System: Role of Phenylalanine 366, Threonine 365 and Isoleucine 324 in the Chemo-, Regio-, and Stereoselectivity. Advanced Synthesis and Catalysis, 359, 2149-2157. https://doi.org/10.1002/adsc.201700444

38. Wang, Y., Sun, C., Min, J., Li, B., Li, J., Chen, W., Kong, Y. & Hu, X. (2021) The engineered biphenyl dioxygenases enhanced the metabolism of dibenzofuran. International Biodeterioration and Biodegradation, 161, 105228. https://doi.org/10.1016/j.ibiod.2021.105228

39. Williams, P. A., & Sayers, J. R. (1994) The evolution of pathways for aromatic hydrocarbon oxidation in *Pseudomonas*. Biodegradation, 5, 195–217. https://doi.org/10.1007/BF00696460

40. Yang, Y., & Arnold, F. A. (2021) Navigating the unnatural reaction space: directed evolution of heme proteins for selective carbene and nitrene transfer. Accounts of Chemical Research, 5, 1209-1225. https://doi.org/10.1021/acs.accounts.0c00591

41. Zheng, L., Baumann, U., Reymond, J. L. (2004) An efficient one-step site-directed and site-saturation mutagenesis protocol. Nucleic Acids Research, 32, e115. https://doi.org/10.1093/nar/gnh110

42. Zylstra, G., & Gibson, D.T. (1989) Toluene degradation by *Pseudomonas putida* F1. Nucleotide sequence of the todC1C2BADE genes and their expression in *Escherichia coli*. Journal of Biological Chemistry, 264, 14940-14946. https://doi.org/10.1016/S0021-9258(18)63793-7

FINE FOCUS EDITORIAL BOARD